Studies on microtubule nucleation

during axon growth

Dissertation zur Erlangung des Doktorgrades
der Naturwissenschaften

an der Fakultät für Biologie

der Ludwig–Maximilians–Universität

München

Angefertigt am Max-Planck-Institut für Neurobiologie

in der Arbeitsgruppe 'Axonales Wachstum und Regeneration'

Vorgelegt von

Michael Stieß

München, 14. Oktober 2010

Erstgutachter: PD Dr. Frank Bradke

Zweitgutachter: Prof. Dr. Rainer Uhl

Tag der mündlichen Prüfung: 03. Dezember 2010

Ehrenwörtliche Versicherung:

Ich versichere hiermit ehrenwörtlich, dass ich die Dissertation mit dem Titel "Studies on microtubule nucleation during axon growth" selbständig und ohne unerlaubte Hilfe angefertigt habe. Ich habe mich dabei keiner anderen als der von mir ausdrücklich bezeichneten Hilfen und Quellen bedient.

Erklärung:

Hiermit erkläre ich, dass ich mich nicht anderweitig einer Doktorprüfung ohne Erfolg unterzogen habe. Die Dissertation wurde in ihrer jetzigen oder ähnlichen Form bei keiner anderen Hochschule eingereicht und hat noch keinen sonstigen Prüfungszwecken gedient.

München, den 14. Oktober 2010

Michael Stieß

The work presented in this thesis was performed in the laboratory of PD Dr. Frank Bradke, Independent Junior Research Group Axonal Growth and Regeneration, Max Planck Institute of Neurobiology, Martinsried, Germany.

The following articles have been published based on my thesis:

Stiess M, Bradke F. 2009. **Cytoskeleton in axon growth.** In: *Encyclopedia of Life Sciences (ELS).* Chichester: John Wiley & Sons, Ltd.

Stiess M, Maghelli N, Kapitein LC, Gomis-Ruth S, Wilsch-Brauninger M, Hoogenraad CC, Tolic-Norrelykke IM, Bradke F. 2010. **Axon extension occurs independently of centrosomal microtubule nucleation.** *Science* 327:704-707.

Stiess M, Bradke F. 2010. **Neuronal Polarity: The cytoskeleton leads the way.** *Developmental Neurobiology,* in press

Für meine Familie

Table of Contents

List of tables

List of figures

Abreviations

+TIP	Plus end tracking protein
ABP	Actin binding proteins
ADF	Actin depolymerizing factor
ADP	Adenosin-diphosphat
APC	Adenomatous polyposis coli protein
Arp2/3	Actin related protein
ATP	Adenosin-triphosphat
Cdc42	Cell division cycle 42
C-domain	Central domain
CLASP	Cytoplasmic linker associated protein
CLIP	Cytoplasmic linker protein
CNS	Central nervous system
CRMP2	Collapsin response mediator protein-2
CPAP	centrosomal P4.1-associated protein
DIV	Day in vitro
E17/18	Embryonic day 17/18
E. coli	Escherichia coli
EB	End binding protein
ECL	Enhanced chemiluminiscence
EDTA	Ethylenediamine tetraacetic acid
EGTA	Ethylene glycol tetraacetic acid

Ena/VASP	Ena (enabled)/Vasp (vasodilator stimulated phosphoprotein)
GAPDH	Glyceraldehyde 3-phosphate dehydrogenase
GCP	Gamma complex protein
γTuRC	γ-tubulin ring complex
GDP	Guaninediphosphate
GFP	Green fluorescent protein
GTP	Guanine-triphosphate
HEPES	4-(2-hydroxyethyl)-1-piperazineethanesulfonic acid
IQGAP1	IQ motif containing GTPase activating protein
LIS1	Lissencephaly-1 protein
MAP	Microtubule associated protein
MEM	Minimal essential medium
min	Minute(s)
MTOC	Microtubule organizing center
NEDD1	Neural precursor cell expressed, developmentally down-regulated 1
PAR	Partitioning defective
PBS	Phosphate buffered saline
P6	Postnatal day 6
PCM	Pericentriolar Material
P-domain	Peripheral domain
PFA	Paraformaldehyde
PIPES	Piperazin-N,N'-bis(2-ethansulfonsäure)
PI3K	Phosphatidylinositol 3-kinase
PTM	Posttranslational modification

Rac1	Ras related C3 botulinum toxin substrate 1
RhoA	Ras homolog gene family, member A
ROI	Region of interest
RT	Room temperature
s	Second
SCG10	Superior cervical ganglion-10 protein
SDS	Sodium dodecyl sulfate
SFV	Semliki Forest virus
T-domain/zone	Transitional domain/zone
TEMED	N,N,N',N'-Tetramethylethylenediamine
TIRF	Total internal reflection fluorescence
WASP	Wiskott-Aldrich syndrome protein
WAVE	WASP-family verprolin-homologous protein

1 <u>Summary</u>

Neurons are the signaling cells of the nervous system. To propagate signals, neurons elongate several neurites, which differentiate into a single axon and several dendrites during development. Among the factors that contribute to this differentiation process, the cytoskeleton and in particular the microtubules play a key role. For instance, the growth of the axon and the dendrites depends on dynamic microtubules and requires the formation of new microtubules. The centrosome is regarded as the primary source of microtubules in axonal and dendritic growth and has been proposed to direct axon formation. However, while microtubule nucleation from centrosomes enables efficient spindle-pole organization and cytokinesis during cell division, it is difficult to reconcile the distinct microtubule array in branching axons, dendrites and spines with such focal microtubule assembly. Thus, the exact role of the centrosome and centrosomal microtubule nucleation in axon growth is still unclear.

To address this question, my doctoral research focused on where microtubules are generated in developing neurons and what role centrosomal microtubule nucleation plays in axonal growth. Using rodent hippocampal neurons in culture as a model system, I found that the centrosome loses its function as a microtubule organizing center (MTOC) during neuronal development. The microtubule nucleating factor γ-tubulin was depleted from the centrosome. Consequently, after depolymerization with nocodazole, microtubules did not regrow at the centrosome at later stages of development. Nevertheless, acentrosomal microtubule nucleation still occurred. Furthermore, axonal growth was unchanged after the centrosome has lost its activity. Moreover, when the axon was lesioned in mature neurons, a new axon grew out in the absence of centrosomal γ-tubulin. As axons grow in mature neurons without a functional centrosome, I next asked the question of whether axon growth requires centrosomal micro-

tubule nucleation in earlier stages of development, when the centrosome still functions as a MTOC. With the use of a two-photon laser ablation setup, the centrosome was removed in neurons that just started to form an axon. Intriguingly, the neurons retained the ability to grow an axon when the centrosome had been ablated by a laser. Thus, loss of centrosomal microtubule nucleation is not a limiting factor for axon growth and regeneration.

My research implies that acentrosomal microtubule assembly is a key feature to establish the sophisticated cytoskeleton of neurons, which is the source for their complex morphology. While the centrosome is necessary for cell cycle progression and neurogenesis, neuronal differentiation requires sophisticated architectural changes that may be incompatible with a large microtubule network emanating from a focal point. Thus, acentrosomal microtubule nucleation may be a key feature during differentiation of neuronal, but also of non-neuronal cells. Dismantling the centrosome and decentralizing microtubule nucleation may be essential to enable axon branching, dendrite formation and spine generation.

2 <u>Introduction</u>

The human nervous system is a construction of billions of neurons, the signaling cells of the nervous system, and other cell types that together form one of the most complex networks in nature. To achieve directed signal propagation, neurons are highly polarized, i.e. they have two types of morphologically and functionally distinct processes; typically a single axon and several dendrites (**Figure 2-1**). The shorter and tapered dendrites receive information and relay it to the cell body for further processing and integration, whereas in contrast, the axon conducts the electrical signal as an action potential from the axonal hillock to the presynaptic terminals, which, in turn, form synapses with dendrites of other neurons.
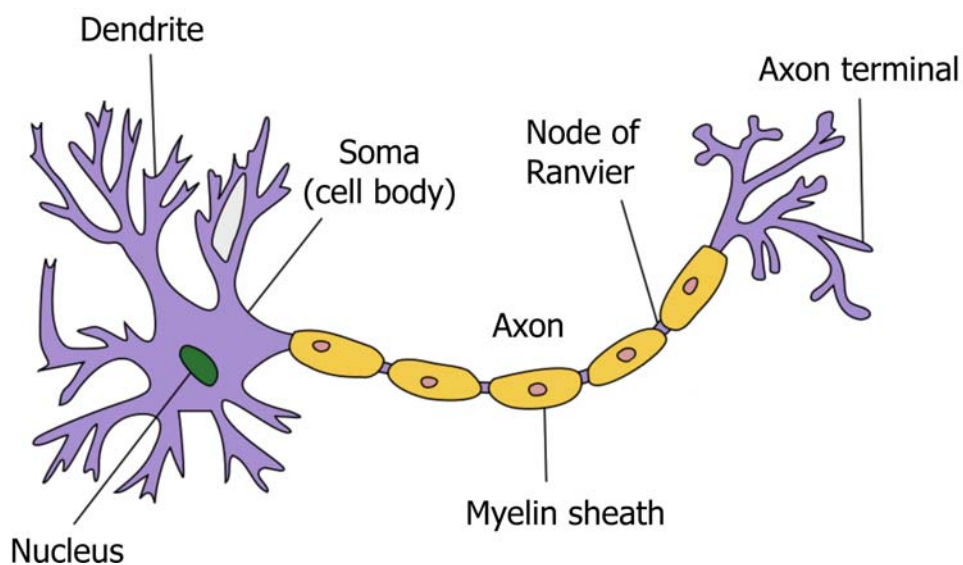
Figure 2-1: Schematic of a typical neuron.
The neuron is divided into the cell body and the extending processes, the single axon and several dendrites. The myelination of the axon enables rapid signal propagation (Figure by Quasar Jarosz at en.wikipedia).

Axons are microscopic in diameter (around 1μm), but extend to enormous lengths. For example, the human sciatic nerve can reach a length of more than one meter. In other organisms, such as giraffes and blue whales, axons can even exceed

lengths of five meters. To achieve such a growth in length, neurons have established sophisticated mechanisms to extend their processes. Axons grow to their target cells through efficient path finding strategies to wire the brain correctly. To this end, axons turn towards attractive cues and away from repulsive cues and form new branches. The cytoskeleton, in particular actin filaments and microtubules, plays a key role in these processes. It not only provides the construction material and backbone for axon elongation, but also controls the direction of growth. Furthermore, signaling cascades triggered by external guidance cues converge at the cytoskeleton. Thus, the cytoskeleton integrates external signals and neuron-intrinsic factors and is thereby the place where axon growth is established, controlled and directed.

2.1 The growth cone

The growth cone is the highly motile tip of the growing axon that controls the direction of axon growth. Ever since its first description by Ramón y Cajal as a conical structure "with amoeboid movements" and important for axon outgrowth (Ramon y Cajal, 1890), the growth cone has been under investigation, with increased intensity over the last 40 years. With the rise of modern cell biology, we began to understand the involvement of the cytoskeleton in axon growth and in particular, the unique organization of the growth cone cytoskeleton (Yamada et al., 1970; Yamada et al., 1971).

In cultured neurons, where axons grow on a two-dimensional substrate, the growth cone is a fan-like, flat structure that can be divided into three distinct domains (**Figure 2-2**)(Lowery and Van Vactor, 2009): Filopodia and lamellipodia, actin based structures, form the peripheral domain (P-domain). Filopodia are thin, finger-like membrane protrusions, which are surrounded by lamellipodia, flattened, veil-like

membrane extensions. The P-domain is the most dynamic structure of the growth cone. The central domain (C-domain) is a thicker region in the core of the growth cone. Microtubules are polymerized in this region and organelles and vesicles are transported along microtubules into the growth cone. The size of the C-domain depends on the growth mode of the axon: it is large when the growth cone is transiently pausing and thinner when the axon is rapidly extending. The transitional domain or transition zone (T-domain/T-zone) is a band at the interface of the actin-rich P- and the microtubule containing C-domain where actin filaments and microtubules interact.

Neurofilaments, the third neuronal cytoskeletal element, also exist in the C-domain of neurons. However, they seem not to be involved in axon growth and path finding, as mice with a genetic deletion of neurofilaments are viable and show typical neuronal connections (Eyer and Peterson, 1994).

Actin filaments and microtubules have different roles in axon growth. Actin filaments maintain the shape of the growth cone and are essential for proper axon guidance. In contrast, microtubules give structure to the axon shaft and are important for the elongation of the axon. Thus, growth cones without actin filaments can still elongate but in an undirected fashion (Marsh and Letourneau, 1984; Bradke and Dotti, 1999). Consequently, a dynamic interplay including structural and regulatory interactions between the two cytoskeletal systems is necessary to fulfill the complex task of directing axon growth to its appropriate target.
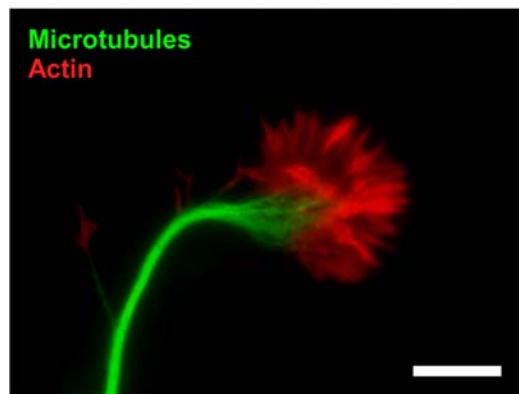
Figure 2-2: The growth cone.

(A) Growth cone of a hippocampal neuron. The actin cytoskeleton is visualized by fluorescently labelled phalloidin (red). Microtubules are stained with antibodies against tubulin (green). The peripheral domain of the growth cone shows the typical actin bundles while microtubules dominate the central domain of the growth cone and the axon shaft. Scale bar, 10 μm.
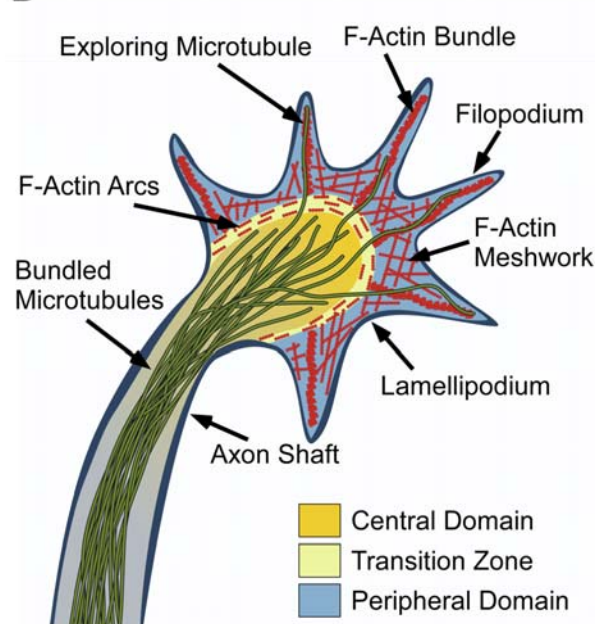
(B) Schematic diagram of a growth cone. The growth cone can be divided into three domains: The peripheral domain (P-domain) comprises the finger-like filopodia that are separated by membrane veils called lamellipodia. Filopodia are formed by F-actin bundles while lamellipodia are based on an F-actin meshwork. The central domain (C-domain) is filled with microtubules that enter the growth cone bundled from the axon shaft. Single, dynamic microtubules explore the peripheral domain. In between the P- and C-domain lies the transition zone (T-zone). Here, actin-myosin structures form F-actin arcs that surround the C-domain and are perpendicular to the F-actin bundles.

2.2 Axon elongation

Axon growth occurs by the conversion of the proximal site of the growth cone into a stable axon shaft, thereby enabling the advancement of the actual growth cone and the elongation of the axon shaft. Axon elongation itself can be seen as a repeated process of the three stages of growth cone maturation (**Figure 2-3**)(Goldberg and Burmeister, 1986). The first stage, termed protrusion, is characterized by the elonga-

tion of filopodia and lamellipodia. This is achieved by increased actin polymerization. Therefore, growth cone advance is directly correlated to the size and dynamics of filopodia and lamellipodia. In the next phase, called engorgement, dynamic microtubules invade the area into which the actin cytoskeleton has protruded; the membrane veils become enriched with vesicles and organelles, most likely by both Brownian motion and directed microtubule transport. In the final consolidation step, the proximal part of the growth cone adopts a cylindrical shape and becomes part of the axon shaft. Hereby, the actin polymerization and protrusion are repressed and microtubules bundle. Repeated rounds of these three steps lead to the elongation of the axon. Similarly, guided axon growth is a directed sequence of these three steps. During axon branching, these steps occur along the parental axon shaft. Importantly, after injury, neurons of the central nervous system cannot regrow because their microtubules are disassembled and disorganized at the tip (Erturk et al., 2007). This prevents the implementation of the consecutive steps that underlie axon growth.
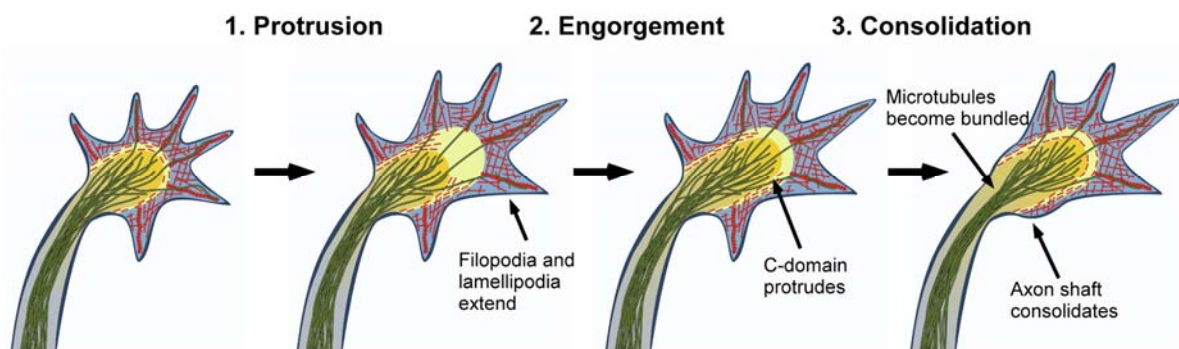
Figure 2-3: Stages of axon growth.

The process of axon growth can be divided into three different steps. 1. Protrusion: Actin filament polymerization is enhanced at the leading edge resulting in the extension of filopodia and lamellipodia and the clearance of actin from the corridor between the P- and C-domain. 2. Engorgement: Microtubules of the C-domain invade the free corridor towards the site of new growth. Through the forward movement of the C-domain, this region also becomes enriched with vesicles and organelles. 3. Consolidation: In the last step, microtubules get bundled and actin protrusion is repressed in the proximal part of the growth cone and thereby, the proximal part assumes cylindrical shape and is integrated into the axon shaft.

2.3 The role of the cytoskeleton in neuronal polarity

The cytoskeleton including actin filaments and microtubules plays not only an active role in axon elongation, but also in axon initiation and the establishment of neuronal polarity (Witte and Bradke, 2008; Hoogenraad and Bradke, 2009). Before an axon forms and elongates, the neuron is an unpolarized cell with several short, equal neurites. During development, the neuron acquires its highly polarized structure with typically one axon and several dendrites (Barnes and Polleux, 2009). It is proposed that negative and positive feedback loops regulate the breakage of neuronal symmetry by acting on cytoskeletal dynamics (Andersen and Bi, 2000). The breakage promotes growth of one of the former identical neurites, which will become the future axon (**Figure 2-4**). It was shown that the growth cone of the future axon shows enhanced actin dynamics, while the growth cones of the other neurites, the future dendrites, contain a more static and rigid actin cytoskeleton (Bradke and Dotti, 1999). Analog to axon growth, the dynamic actin network in the growth cone of the future axon allows dynamic microtubules to explore the growth cone and hence promotes the protrusion of the C-domain (engorgement) and finally axon growth. In the growth cones of the other neurites protrusion does not take place. The rigid actin network rather appears to function as barrier that hinders microtubules to explore the periphery of the growth cone. Thus, the actin filaments inhibit advance of the microtubule containing C-domain into the P-domain. Consequently, removal of this actin barrier by actin depolymerization allows microtubules to grow into the growth cone and non-growing neurites transform into growing axons (Bradke and Dotti, 1999).
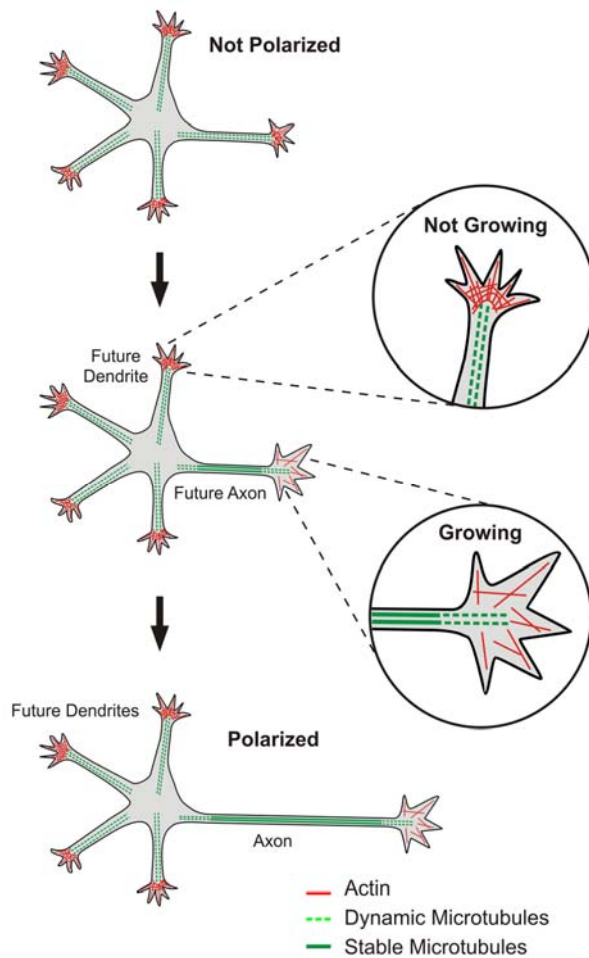
Figure 2-4: The role of the cytoskeleton in neuronal polarity.

At the beginning of neuronal development, a neuron has several equal processes. During neuronal polarization, intracellular signaling pathways change the cytoskeleton in one of these processes, the future axon. The actin cytoskeleton in the growth cone becomes more dynamic and thus, actin filaments do not function anymore as a barrier to protruding microtubules. Thus, the growth cone can advance and the axon forms. At the same time, microtubules are stabilized in the axon. These stable microtubules may serve as tracks for specific axonal transport and promote further axonal and somatodendritic segregation. In the non-growing processes, the actin filaments form a rigid barrier in the growth cone that prevents the protrusion of microtubules into the peripheral domain. Thus, this actin barrier inhibits the growth of the other processes, the future dendrites.

Neuronal polarization also involves the regulation of microtubule dynamics. To promote growth cone engorgement and consolidation, microtubules have to be stabilized. For that matter, microtubules in the future axon are more stable than in the other non-growing neurites. Moreover, the pharmacological stabilization of microtubules is sufficient to induce axon formation (Witte and Bradke, 2008). Thereby, the increased stability of microtubules does not only allow enhanced growth cone advance. Furthermore, through the stabilization of microtubules and axon-specific posttranslational modifications that are associated with increased stability, the future axon may also contain specific tracks for motor protein based transport of vesi-

cle cargoes (Bradke and Dotti, 1997; Baas, 1999; Nakata and Hirokawa, 2003; Jacobson et al., 2006; Reed et al., 2006; Konishi and Setou, 2009).

These polarization events are regulated by various signaling cascades including partitioning defective (PAR) proteins, phosphatidylinositol 3-kinase (PI3K) and similarly to the regulation of axon growth and guidance, the family of Rho GTPases (Arimura and Kaibuchi, 2007). They can be stimulated by extracellular signals (Barnes and Polleux, 2009). These pathways have in common that they converge on the actin and microtubule dynamics.

2.4 The actin cytoskeleton

Actin Filaments (F-actin) are helical polymers of globular actin monomers (G-actin) and measure approximately 7 nm in diameter (Pollard, 2007). The highest concentration of F-actin are found in the P- and T-domains of the growth cone and they are organized primarily into two types of arrays: polarized, bundled arrays found in the core of filopodia that also extend into the T-domain and meshwork-like arrays which constitute the bulk of lamellipodia in the P-domain (**Figure 2-2**). Furthermore, there are arc-like structures in the T-domain that surround the C-domain and are perpendicular to the F-actin bundles (Pollard and Borisy, 2003; Lowery and Van Vactor, 2009).

2.4.1 Actin filaments

Actin filaments have two structurally distinct terminals, termed barbed and pointed ends that result in an intrinsic polarity of the filaments. During polymerization, ATP-actin preferentially binds to the barbed end of the polymer. ATP-actin then hydrolyzes to ADP-Pi-actin and finally to ADP-actin. ADP-actin dissociates from the

pointed end and becomes recycled to ATP-actin; the hydrolysis cycle can then start again (**Figure 2-5**). These different stages of nucleotide hydrolysis occur along the filament resulting in different regions along the filament with ATP-actin close to the barbed end, ADP-Pi-actin in the middle and ADP-actin close to the pointed end. In the growth cone, barbed ends are located at the distal membrane and the pointed ends face the T-zone (Pak et al., 2008). Actin-polymerization at the distal membrane causes the filopodia and lamellipodia to extend. At the same time, the actin assembly creates a force that "pushes" the actin network backwards. This "retrograde flow" phenomenon is a steady state rearward movement of the actin network and thereby, also of the closely linked growth cone membrane (Suter and Forscher, 2000). Thus, the net protrusion of both filopodia and lamellipodia is regulated by modulating actin polymerization and retrograde flow. The retrograde flow is additionally supported by myosin II contraction in the T-domain (Medeiros et al., 2006). Myosin II is a molecular motor that generates forces on F-actin by means of ATP hydrolysis. Myosin II not only transports F-actin retrogradely to the T-domain, it also contracts the actin meshwork in the T-zone, which results in the formation of thick actin arcs. The increased contraction in the T-zone also induces severing and depolymerization of F-actin, which in turn supports actin treadmilling. It is thought that retrograde actin flow might negatively regulate axon outgrowth and hinder exploring microtubules from entering into the P-domain.

2.4.2 Actin binding proteins

The growth cone uses sophisticated mechanisms to control the actin cytoskeleton (Pak et al., 2008). The generation of the complex actin network in the growth cone occurs in two steps. First, new filaments are nucleated and assembled. Second, the growing F-actin has to be organized in a functional and dynamic network that allows the growth cone to direct axon growth in accordance to external and internal signals.

Both steps are driven by actin binding proteins (ABPs) and their regulators (**Figure 2-5**; for a comprehensive list of ABPs in growth cones: see (Dent and Gertler, 2003; Ishikawa and Kohama, 2007)).

A first group of ABPs promotes actin nucleation and polymerization. This increase in F-actin assembly is achieved by binding and/or sequestering G-actin, by nucleating F-actin, by capping the pointed end, by anticapping the barbed end or eventually by performing combinations of these mechanisms. Actin nucleator proteins include the Arp2/3 complex and formins. Barbed end anticapping proteins comprise the Ena/VASP family and pointed end capping proteins include tropomodulin (Ishikawa and Kohama, 2007; Kwiatkowski et al., 2007). A second group of ABPs regulates the depolymerization and severing of F-Actin in the T-zone and thereby refreshing the pool of available G-actin monomers. This group includes the severing proteins ADF/cofilin and Gelsolin (Lu et al., 1997; Garvalov et al., 2007). The third group of ABPs is involved in the higher order organization of F-actin by bundling, crosslinking or stabilizing F-actin and by anchoring F-actin to membrane adhesions or specific regions of the membrane. This group includes the bundling proteins fascin and filamin, as well as membrane anchoring proteins including cortactin, vinculin and spectrin (Ishikawa and Kohama, 2007).

These categories, however, are not exclusive and many of the ABPs function in several categories. The involved ABPs are well coordinated in space and time by their activation, their interaction as well as by their reciprocal competition. This results in a tight regulation of growth cone dynamics.
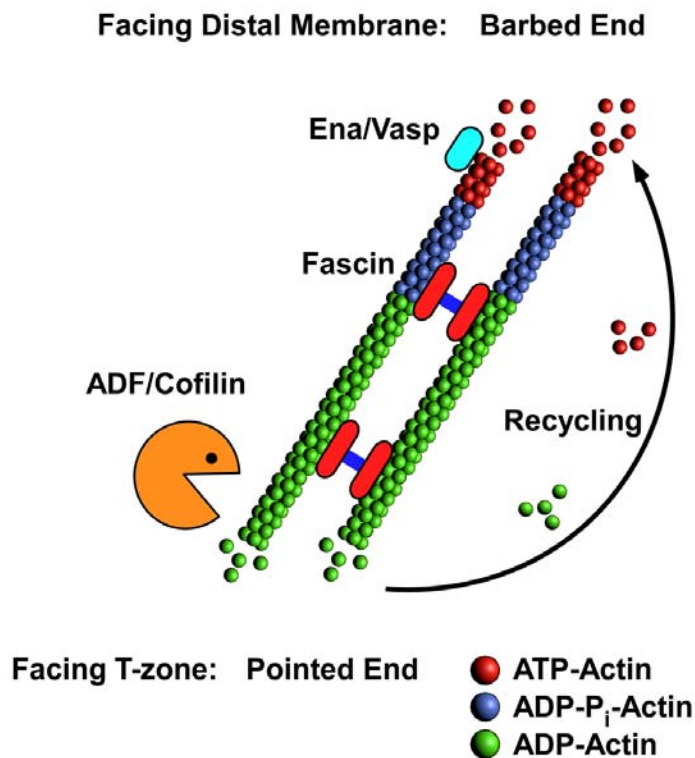
Figure 2-5: Dynamics of actin filaments.

Actin filaments grow by the addition of ATP-actin (red) to the barbed end which faces the distal membrane in the growth cone. After ATP-actin hydrolysis to ADP-Pi-actin (blue) and loss of inorganic phosphate, ADP-actin (green) becomes disassembled from the filament at the pointed end that faces the T-zone. Polymerization at the distal membrane and depolymerization in the T-zone leads to treadmilling of F-actin. ADP-actin becomes recycled to ATP-actin and can be used again for polymerization. Actin-binding proteins (ABPs) regulate these dynamics by either promoting polymerization like Ena/Vasp proteins or by severing and depolymerizing F-actin like ADF/cofilin. Furthermore, ABPs can organize the actin filaments into higher order structures, for example by bundling through proteins like fascin.

During development, axons grow through the embryonic environment and connect to their targets (Chilton, 2006). The cytoskeleton not only drives axon elongation, but also directs the growth along defined pathways to find the correct axonal targets. It is primarily the actin cytoskeleton that is involved in path finding. The actin cytoskeleton and the actin binding ABPs are downstream of the signaling pathways of guidance receptors. Therefore, they directly rearrange the actin cytoskeleton in the growth cone and turn the growth cone in response to guidance cues (Dent and Gertler, 2003). The guidance receptors on the growth cone sense attractive or repul-

sive cues, which provide the environmental directions. A plethora of signalling pathways downstream of these receptors translate the spatial information from the guidance cues to modulate the cytoskeleton dynamics in order to drive axon growth into the right direction. Beside kinases, phosphatases and calcium ions, the family of Rho GTPases, including RhoA, Rac1 and Cdc42, regulates the cytoskeleton downstream of most guidance receptors (Govek et al., 2005). The Rho-GTPases act on actin dynamics, but also affect microtubules (Watabe-Uchida et al., 2006).

2.5 Microtubules

Microtubules are the second cytoskeletal component in axon growth. They give structure to the axon shaft and are the driving force for axon elongation (Conde and Caceres, 2009).

2.5.1 Nucleation and polymerization of microtubules

Microtubules are polarized, tubular structures that are assembled into linear arrays in the axon. They are highly dynamic, yet rigid cylindrical polymers of α/β tubulin heterodimers with a diameter of about 25 nm. During polymerization the α/β tubulin heterodimers arrange into linear protofilaments that associate laterally to form the hollow microtubule cylinders. In most mammalian cells, microtubules form a tube of 13 protofilaments (**Figure 2-6**). Within a protofilament, the tubulin heterodimers associate in a head-to-tail fashion. This makes microtubules intrinsically polar, resulting in two, structurally and kinetically different ends: the highly dynamic plus-end and the less dynamic minus-end. The β-tubulin within the dimer is oriented toward the plus-end, and the α-tubulin subunit toward the minus-end (Desai and Mitchison, 1997; Howard and Hyman, 2003).

Microtubules are intrinsically dynamic, a feature termed dynamic instability. They undergo periods of growth and shrinkage at the microtubule plus-end. Dynamic instability allows microtubules to switch abruptly from growth to shrinkage (catastrophe) and from shrinkage to growth (rescue) (**Figure 2-6**) (Mitchison and Kirschner, 1984; Howard and Hyman, 2003).

The assembly and disassembly of microtubules are important for their generation but also their dynamic properties. The assembly of microtubules can be characterized by three steps: the first phase is defined by a thermodynamically unfavourable and therefore rate-limiting nucleation step. It is followed by rapid elongation of the polymer and finally by a steady-state phase. In the nucleation step small oligomers of α/β tubulin heterodimers form a nucleus. Once a stable oligomer of a certain size is reached, rapid polymerization of the microtubule occurs. During the steady state microtubules display the dynamic instability, when microtubules switch randomly at their plus-ends between "catastrophe" and "rescue" leading to their highly dynamic behaviour (Mitchison and Kirschner, 1984; Howard and Hyman, 2003).

To maintain the dynamic instability, microtubules consume energy by the hydrolysis of GTP. β-tubulin has a GTP-hydrolyzing activity that is strongly activated when the dimer is incorporated into the polymer. This hydrolyzing activity leads only to a small layer of tubulin dimers at the plus end that are bound to GTP, the so-called GTP cap (**Figure 2-6**). It stabilizes the plus-end, because GDP-bound microtubules are intrinsically more instable. If new polymerization is slower than the GTP hydrolysis, the plus-end becomes unstable and results in catastrophe (Mitchison and Kirschner, 1984; Howard and Hyman, 2003). The dynamic behaviour of the minus-ends is not of interest in vivo, because they are generally capped and thus stabilized (Dammermann et al., 2003). Because GTP hydrolysis is not necessary for micro-

tubule polymerization, the GTP hydrolysis is only important for the dynamic proper-

ties of microtubules.
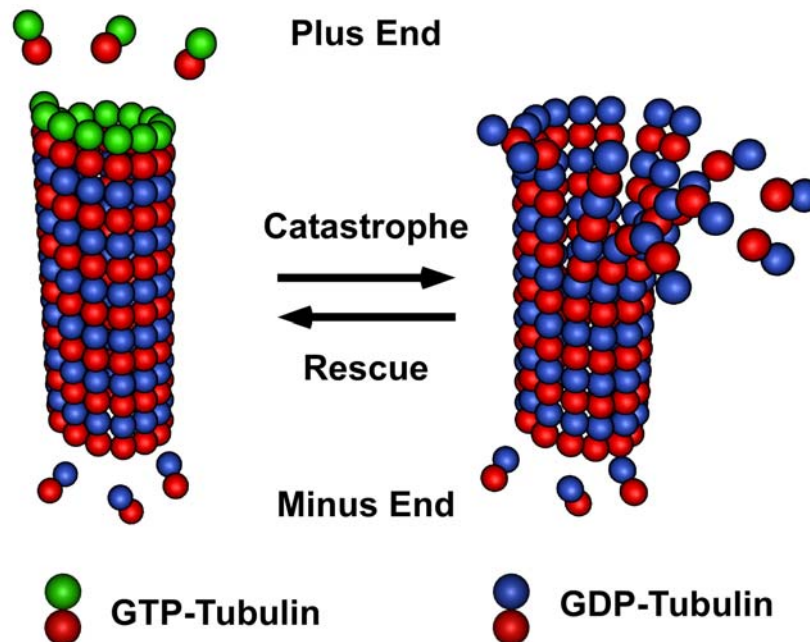
Figure 2-6: Dynamics of microtubules.

Microtubules are intrinsically dynamic. The polymers rapidly switch from a shrinking mode to a growing mode (rescue) or the reverse way (catastrophe). The Cap of GTP-bound tubulin at the plus-end stabilizes the microtubule. GDP-bound microtubules are intrinsically more instable and therefore, if new polymerization is slower than the GTP hydrolysis, the plus-end becomes unstable and results in catastrophe.

Microtubules polymerize spontaneously *in vitro* from high α/β tubulin con-

centrations. However, the intracellular monomer concentration seems too low for

spontaneous nucleation, although this possibility has not been excluded (Job et al.,

2003). Therefore, microtubule formation is assisted by specific structures called

microtubule organizing centres (MTOCs) (Luders and Stearns, 2007). MTOCs allow

the cell to control where and when to assemble microtubules. The conventional

MTOC in animal cells is the centrosome, an organelle next to the nucleus (see chap-

ter 2.5.5). Recently, also centrosome-independent and decentralized microtubule

formation has been identified in many organisms and cell types (Bartolini and Gundersen, 2006; Luders and Stearns, 2007).
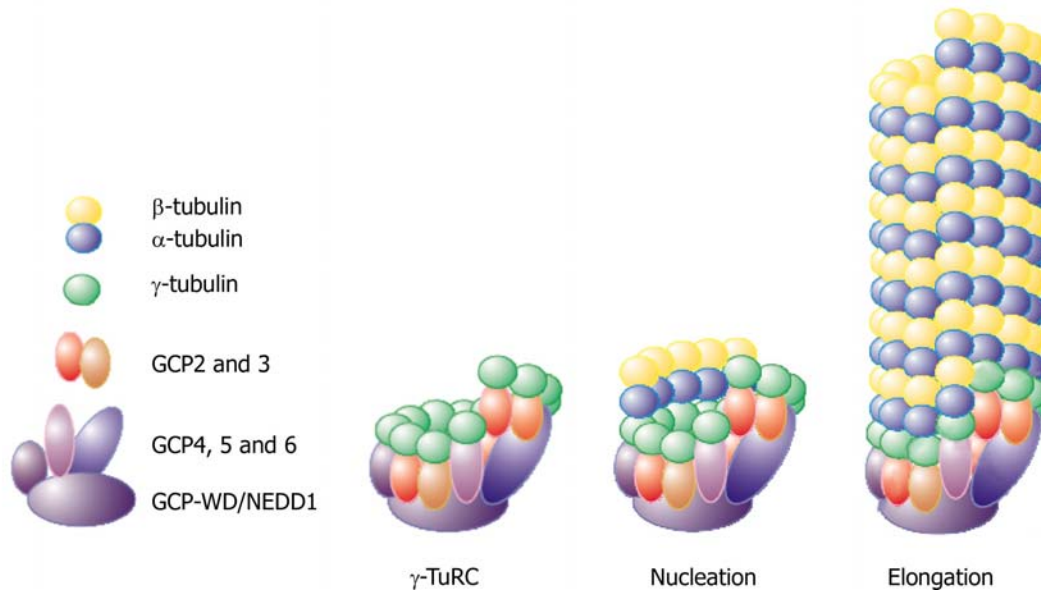
Figure 2-7: γTuRCs and microtubule nucleation.

The γTuRC consists of several γ-tubulin subunits, the GCPs 2 to 6 and GCP-WD/NEDD1, which anchors the γTuRC at the centrosome. According to the template model, the γTuRC mimics the end of a microtubule. Tubulin dimers bind to the γTuRC and a microtubule assembles (Figure modified from Job et al., 2003).

The key protein responsible for microtubule nucleation is thought to be γ-tubulin, a highly conserved protein that shares around 30% homology with α/β tubulin (Moritz and Agard, 2001). γ-tubulin is organized in large complexes that form an open ring structure, called the γ-tubulin ring complex (γTuRC; **Figure 2-7**). The γTuRC is composed of the gamma complex proteins (GCP) GCP 2-6 and γ-tubulin (GCP 1) (Raynaud-Messina and Merdes, 2007). Each of these GCPs is required for the assembly of the γTuRC (Verollet et al., 2006). Recently, NEDD1, which is therefore also called GCP-WD, was shown to be part of the γTuRC and to be responsible for the centrosomal targeting of the complex via its amino-terminal WD repeats (Haren et al., 2006; Luders et al., 2006). How γTuRCs nucleate microtubules is still

under debate, however the majority of evidence favours a template model, where the γTuRC essentially mimics the end of a microtubule and serves as a nucleation seed (Job et al., 2003). This view was supported by the γ-tubulin crystal structure, which showed lateral interactions between γ-tubulin subunits (Aldaz et al., 2005). Despite the data that support this model the definitive experimental evidence is still lacking.

2.5.2 Microtubule associated proteins (MAPs)

Microtubule dynamics are regulated by microtubule associated proteins (MAPs; **Figure 2-8**). There are different groups of MAPs that affect microtubule dynamics by different means. Structural MAPs stabilize microtubules and include the proteins MAP2 and tau. They bundle, stabilize and crosslink microtubules and can enhance microtubule growth by inhibiting catastrophe or by promoting rescue events. Their binding is regulated by posttranslational modifications (PTMs) or by phosphorylation of tubulin (Dehmelt and Halpain, 2004).

In the last years, plus-end tracking proteins (+TIPs) came to the fore as new specialized MAPs including Adenomatosis polyopsis coli (APC), Cytoplasmic linker proteins (CLIP-115 and CLIP-170), CLIP-associating proteins (CLASP1 and CLASP2) and End-binding proteins (EB1 and EB3). They specifically accumulate at the plus-ends of microtubules and regulate microtubule dynamics by stabilizing them. Stabilization is achieved by reducing the microtubule catastrophe rate or by promoting microtubule rescue. They are also proposed to link microtubules to F-actin by binding to ABPs (Akhmanova and Steinmetz, 2008).

Collapsin response mediator protein-2 (CRMP-2) acts in a different fashion than the MAPs mentioned so far. Instead of binding to the microtubule polymer, CRMP-2 binds free tubulin subunits and promotes microtubule assembly (Fukata et al., 2002). Furthermore, CRMP-2 is involved in the transport of free tubulin to the

distal part of the growing axon by binding to Kinesin-1 (Kimura et al., 2005). Its role is not only important for axon growth, but also for axon-dendrite specification. In both of its roles, CRMP-2 also affects actin dynamics by its involvement in kinesin-dependent transport of the WASP family and Verprolin-homologous proteins (WAVE)-complex, a regulator of actin polymerization, into the axon (Kawano et al., 2005).

Another group of MAPs acts as microtubule destabilizing proteins. Since dynamic microtubules are necessary for growth cone advance, they might counteract the structural MAPs in the growth cone, which stabilize microtubules and therefore reduce their dynamics. In neurons, stathmin and Superior cervical ganglion 10 protein (SCG10) increase the rate of microtubule catastrophes. Both proteins are highly expressed during neurite outgrowth. Furthermore, SCG10 localizes to the C-domain of the growth cone. Thus, they might regulate microtubule dynamics in the growing axon (Grenningloh et al., 2004).

Microtubule motors like kinesin or dynein also bind to microtubules, but do not directly affect their dynamics. Analog to myosin and actin, they generate forces on microtubules by means of ATP-hydrolysis. The motors transport the building material and single components to the growth cone that are required for axon growth. The intrinsic polarity of the microtubules specifies the direction of motor movement, since the motors can only move along the microtubule in one direction. Kinesin motor proteins move towards the plus-end and the dynein complex towards the minus end. Furthermore, the PTMs of the microtubules can determine the binding of motors. For example, kinesin-1 preferentially binds to the more stable, acetylated microtubules, which are localized in the axon (Reed et al., 2006; Witte et al., 2008). In addition, tyrosinated tubulins that are abundant in dendrites prevent kinesin-1 from

binding to microtubules (Konishi and Setou, 2009). By means of these directional controls, the molecular motors are a good checkpoint to regulate the transportation and hence, the final localization of specific cargos.
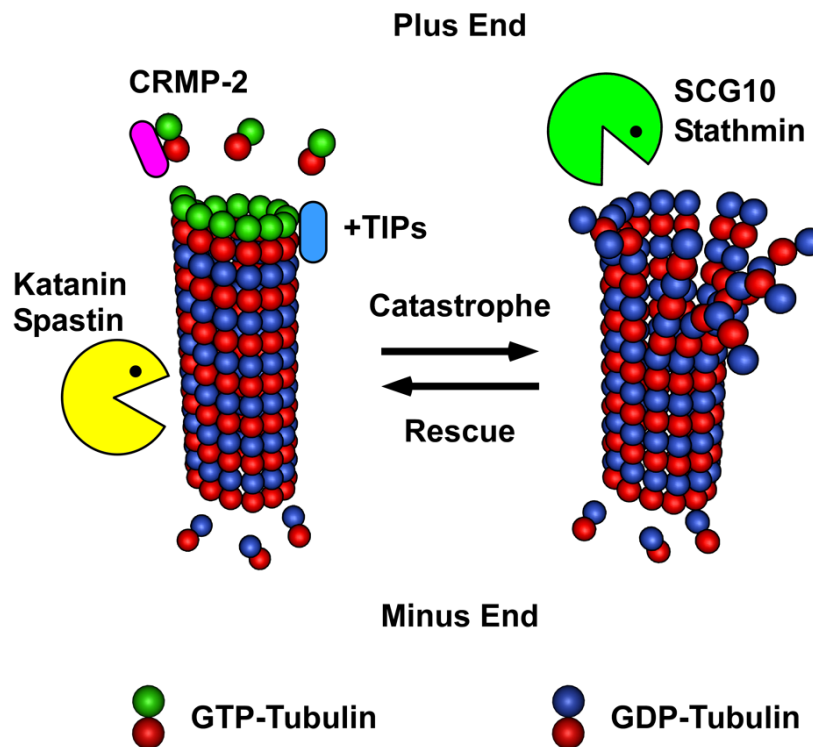
Figure 2-8: Microtubule associated proteins (MAPs) regulate microtubule dynamics.
CRMP-2 and plus-end tracking proteins (+TIPs) promote microtubule assembly. In contrast, SCG10 and stathmin destabilize microtubules. Furthermore, proteins like katanin or spastin sever microtubules and are therefore important in axon growth and branching.

Also important for axon growth and branching are microtubule severing proteins. Two microtubule severing proteins are found in neurons, katanin and spastin. Katanin is mainly responsible for axon growth and is localized to the centrosome where it releases microtubules, but is also present in growth cones and at branching points (Karabay et al., 2004). In contrast, spastin is primarily involved in microtubule reorganization at branching points (Yu et al., 2008).

In conclusion, microtubules and their dynamics are key for axon growth and are tightly regulated by a plethora of proteins during axon growth.

2.5.3 Microtubules in axon growth

Microtubules have a unique organization in neurons. In contrast to many somatic cells, neuronal microtubules are not anchored at the centrosome, but are abundant in the cytoplasm throughout the whole cell body and funnel into the processes (Baas, 1999). The microtubules reach lengths up to 100 microns within the axon shaft and are organized in regularly spaced, parallel arrays with their plus-ends distal to the cell body. In dendrites, microtubules are organized in anti-parallel arrays with microtubule plus-ends oriented towards as well as distal to the cell body (Conde and Caceres, 2009).

Microtubules are essential for axon growth (Yamada et al., 1970; Conde and Caceres, 2009). Upon entering the growth cone, microtubules splay out and are very dynamic. Within the growth cone they are mainly localized in the C-domain, but a subset of the microtubules also explores the P-domain by rapid extension and retraction into the domain (Lowery and Van Vactor, 2009). This dynamic exploration of the peripheral growth cone by microtubules is a key event in axon growth, guidance and branching. The transitions between catastrophe and rescue result in the dynamic exploration of the growth cone and a fast interconversion between splayed, looped and bundled arrays. These dynamics not only result in the extension of the axon, but are also an early step of path finding and branching. Hence, growth cone turning is abolished when microtubule dynamics are inhibited. Moreover, dynamic microtubules turn towards or away from extracellular attractants and repellents, respectively (Gordon-Weeks, 2004). Furthermore, microtubules steer the growth cone by their local stabilization at the desired site of growth and destabilization at the opposite site.

Consequently, by local application of the microtubule-stabilizing drug taxol, the stabilized microtubules grow and thereby steer the growth cone to the site of taxol application (Buck and Zheng, 2002). In contrast, after local application of the microtubule-depolymerizing drug nocodazole, the growth cone turns away from the site of application (Buck and Zheng, 2002). Guidance cues act in a similar way by regulating microtubule stability through their downstream pathways. Thereby, microtubules are instrumental and instructive for growth cone turning during path finding (Gordon-Weeks, 2004; Geraldo and Gordon-Weeks, 2009).

Although axon growth depends on microtubule polymerization (Tanaka et al., 1995), it is rather the formation of new microtubules than only the extension of existing microtubules that delivers the polymers necessary for axon extension (Yu and Baas, 1994). During the last decades it has been intensely debated how and where the microtubule arrays in axons are formed. First mentioned by Lasek (Lasek, 1986), the "polymer transport model" proposed that microtubules are nucleated at the centrosome, released from the centrosome through the microtubule severing protein katanin (Ahmad et al., 1998; Baas et al., 2005) and then transported along the axon by the motor protein dynein (**Figure 2-9A**)(Ahmad et al., 1998; Wang and Brown, 2002). In contrast, other groups reported that, if nothing else, growing microtubules are not transported in axons and most microtubules are stationary (Ma et al., 2004; Kim and Chang, 2006). Moreover, tubulin is transported into the axon and to the growth cone in its non-polymerized form (Terada et al., 2000; Kimura et al., 2005). The alternative hypothesis was therefore termed the "subunit transport model" that postulated that tubulin is transported into the processes in single subunits or oligomers that are then locally incorporated into the microtubules (**Figure 2-9B**)(Hirokawa et al., 1997). Indeed, local microtubule polymerization occurs in comparable rates throughout all neuronal compartments (Stepanova et al., 2003). Consistently, local inhibition

of microtubule assembly at the axon tip inhibits axonal growth whereas inhibition at the cell body does not have an effect on axon growth (Bamburg et al., 1986). To date, both models are under discussion, especially the aspect of microtubule transport into the axon, with different groups still presenting data for both models by the use of live cell imaging approaches (Wang and Brown, 2002; Ma et al., 2004; Kim and Chang, 2006). As the same experiments can be interpreted in different ways (Terada, 2003; Myers et al., 2006), finding the definitive answer is a complicated task.
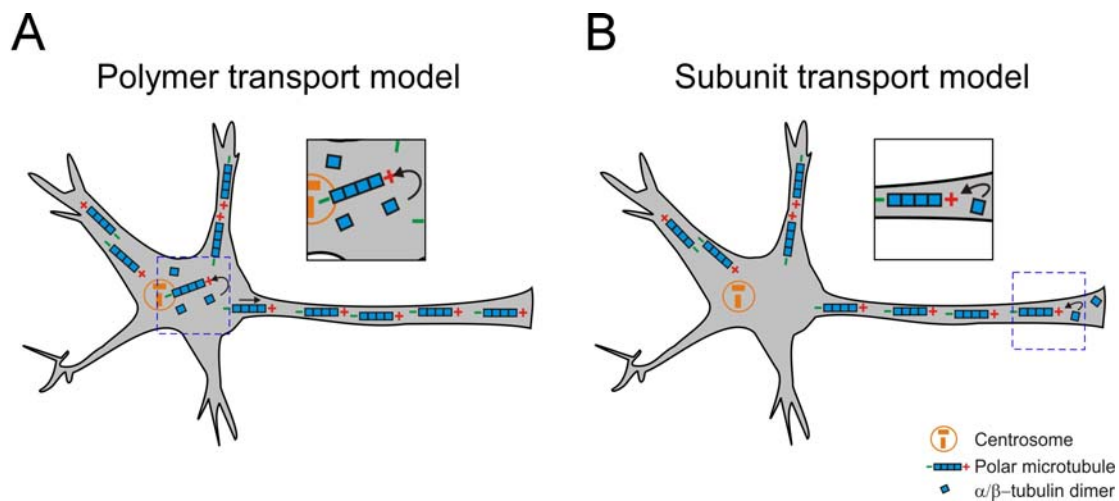
Figure 2-9: Microtubule generation during axonal growth.

(A) The polymer transport model: After their nucleation at the centrosome, microtubules are released and transported into the axon. **(B) The subunit transport model:** Tubulin subunits are transported into the axon and microtubules are assembled locally within the axon.

2.5.4 The centrosome

Due to their unique organization, it is still debated where neuronal microtubules are generated. In most animal cells, microtubules are nucleated and organized at the centrosome. Centrosomes were named by Theodor Boveri in the late 19th century on the basis of their central position in the cell. They are not only the main microtubule or-

ganizing centers (MTOC) in animal cells, they are also important regulators of cell-cycle progression (Doxsey, 2001) and serve as a template for the formation of the primary cilium (Bettencourt-Dias and Glover, 2007). Centrosomes are composed of two main structures: two cylinder-shaped centrioles and the amorphous pericentriolar material (PCM; **Figure 2-10**).
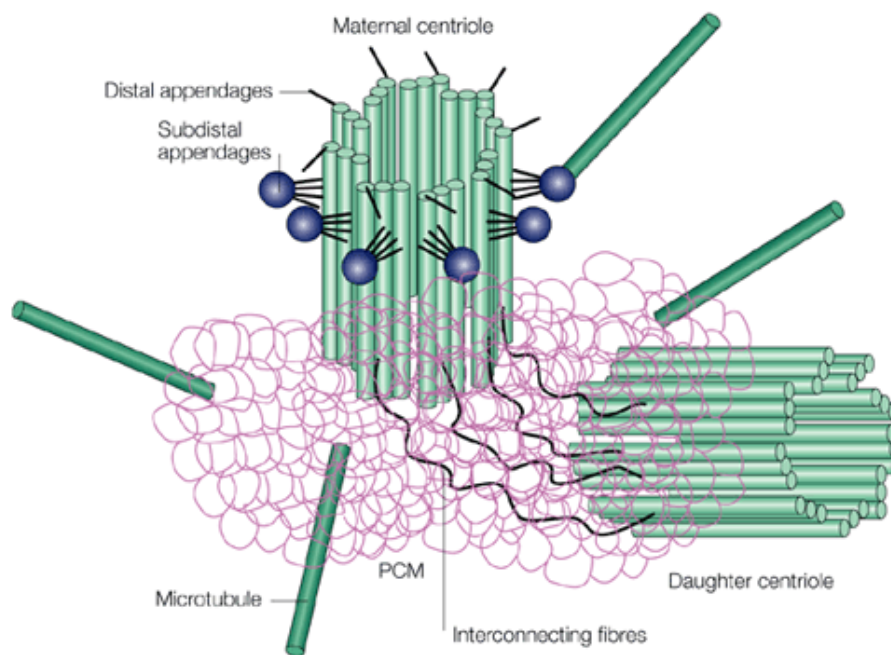
Figure 2-10: Centrosome structure.

A pair of centrioles is shown. Each centriole has pericentriolar material (PCM) that nucleates microtubules around the ends closest to one another. Only the maternal centriole has two sets of extra appendages, distal and subdistal; the latter seems to anchor microtubules. A series of interconnecting fibres, different from the PCM, links the closest ends of the two centrioles (Figure from Doxsey, 2001).

Centrioles are open-ended cylinders, comprised of nine sets of triplet microtubules linked together. The two centrioles are each around 500 nm in length and 200 nm in diameter. They are oriented perpendicular to one another and in close proximity at one end (proximal end). The older centriole has appendages at the distal

end and is called the mother centriole. This centriole forms the basal body, which is the base of the primary cilium, a sensory organelle that extends from the plasma membrane and that is also involved in developmental signalling of vertebrates (Singla and Reiter, 2006; Goetz and Anderson, 2010). Besides coordinating the formation of the primary cilium, the centrioles regulate the cell cycle and seem to organize the PCM (Doxsey, 2001; Bettencourt-Dias and Glover, 2007).

The PCM typically surrounds both centrioles and is the site of microtubule nucleation that is built up by an interconnected meshwork of fibers and protein aggregates forming a matrix or lattice. In total, the PCM consists of around 100 proteins, mainly with coiled-coiled domains (Andersen et al., 2003). This matrix provides a structural scaffold for the proteins that are important for microtubule nucleation, including γ-tubulin.

In vertebrate somatic cells, 80% of γ-tubulin is present in the cytoplasm, whereas only the residual 20% is associated with the centrosome (Moudjou et al., 1996). The cytoplasmic and centrosome-associated γTuRCs are related or even identical (Job et al., 2003). Multiple proteins seem to be involved in the recruitment of γ-tubulin to the centrosome and for the formation of the PCM itself. These proteins include pericentrin (Dictenberg et al., 1998; Zimmerman et al., 2004), AKAP450/CG-NAP (Takahashi et al., 2002) and NEDD1/GCP-WD (Haren et al., 2006; Luders et al., 2006). NEDD1 is considered as a part of the γTuRC. It anchors the complex in the PCM and therefore appears to be necessary for centrosomal targeting of γTuRCs, as shown by loss of function experiments (Haren et al., 2006; Luders et al., 2006). In dividing cells, fluctuation of γ-tubulin at the centrosome is a well known phenomenon and highly regulated by the cell cycle: at the onset of mitosis γ-tubulin is recruited to the centrosome, a process called centrosomal maturation

(Khodjakov and Rieder, 1999; Blagden and Glover, 2003). Later in cell cycle, during anaphase/telophase, the centrosome associated γ-tubulin decreases to its residual level. However, the knowledge about γ-tubulin recruitment to the centrosome is still very basic and the process is not completely understood.

2.5.5 The role of the centrosome in neuronal polarity

In most animal cells, the centrosome is the major microtubule nucleation site and it is also involved in polarity processes (Bornens, 2008). Thus, polarized microtubule nucleation at the centrosome could specifically support the outgrowth of one neurite, which subsequently would become the axon. Furthermore, the centrosome connects closely to the Golgi-apparatus (Sutterlin and Colanzi, 2010), which could allow polarized membrane traffic to the growing axon, a process that precedes axon formation (Bradke and Dotti, 1997). Consistently, the centrosome localizes to the site of axon outgrowth in cultured cerebellar granule cells (Zmuda and Rivas, 1998). Additionally, it has been proposed that the position of the centrosome determines the site of axon formation after the last round of precursor division of cultured hippocampal neurons (de Anda et al., 2005).

Interestingly, the knockdown of the polarity regulator LKB1 mispositioned the centrosome in migrating bipolar cortical neurons. In the case of an inverted position of the centrosome, the polarity of the neuron was also inverted, although in this case the centrosome position did not determine the axon, but dendrite formation (Asada et al., 2007). However, it is known that also other regulators of neuronal polarity like PI3K and Cdc42 can control the position of the centrosome (Etienne-Manneville and Hall, 2003; Siegrist and Doe, 2007). Therefore, it is unclear whether the centrosome directly controls polarity or whether it might just be a byproduct of the polarization

process itself (Arimura and Kaibuchi, 2007; Li and Gundersen, 2008; Witte and Bradke, 2008).

Supporting the latter, no correlation between centrosome position and the site of axon formation was found in cultured dorsal root ganglion neurons and hippocampal neurons, which did not polarize directly after the last cell division (Sharp et al., 1982; Dotti and Banker, 1991). This is also consistent with studies on zebrafish retinal ganglion neurons *in vivo*, which showed that the centrosome localizes opposite to the axon (Zolessi et al., 2006). Furthermore, Slit-mediated repolarization of developing interneurons of the olfactory bulb suggested that the centrosome does not determine the site of axon outgrowth, but may be necessary for process stabilization (Higginbotham et al., 2006)

2.6 Hippocampal neurons as model system for neuronal development and axonal growth

Many studies addressing the questions how a neuron develops and how axons grow are carried out in cell culture systems. Dissociated hippocampal neurons are the most widely used culture system for the examination of neuronal differentiation and polarization (Kaech and Banker, 2006). These neurons constitute a relatively homogenous neuronal culture, form extensive, synaptically coupled networks and resemble the neuronal morphology very well: they form only one axon, many dendrites and intercellular synapses in culture as well as *in vivo.* Furthermore, they develop in defined stages in a stereotypical fashion (Dotti et al., 1988; Craig and Banker, 1994).

Stage:	1	2	3	4	5
Characteristic feature:	Lamelli-podia	Minor Neurites	Axonal Outgrowth	Dendritic Outgrowth	Synapse Formation
Days in culture:	0.25	0.5	1.5	4	>7
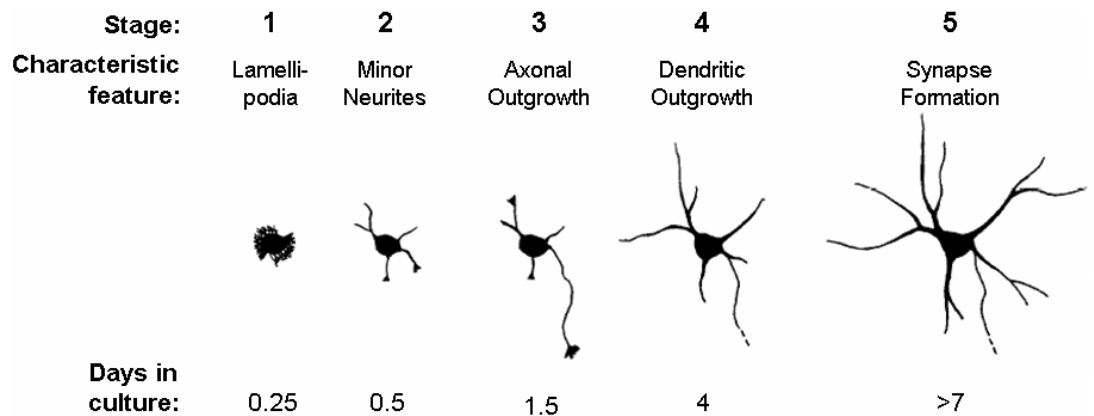
Figure 2-11: Developmental stages of hippocampal neurons in culture.
Figure from Dotti et al., 1988

Hippocampal neurons are dissected from embryonic mouse or rat hippocampi, dissociated and plated in growth medium. Shortly after, the cells attach and form lamellipodia around the cell body (stage 1). After 1 *day in vitro* (DIV) the lamellipodia condense and the cell forms several identical neurites that are 10-25 µm long (stage 2). Within the next 24 hours one of the neurites starts to grow very rapidly whereas the remaining neurites remain quiescent (stage 3). The growing neurite will later become the functional axon. Thus, at stage 3 the polarization process starts. After 4-6 DIV the other neurites grow (stage 4) and will later form the dendrites. Whereas the axon grows at an average rate of 70 µm/day, the dendrites grow at a slower rate of around 12 µm/day (Dotti et al., 1988). After 10 days in culture the axons and dendrites form synapses (stage 5).

2.7 Objectives of my research: Localization of microtubule nucleation during axon growth

During neuronal differentiation, the axon and the dendrites extend rapidly. This process requires microtubule polymerization and the generation of new microtubules (Yu and Baas, 1994; Tanaka et al., 1995). There is much controversy about where these microtubules are generated. The centrosome is regarded as the primary source of microtubules in axonal and dendritic growth (Baas, 1999; Higginbotham and Gleeson, 2007). It has been thought that they are nucleated and polymerized at the centrosome, released by the microtubule severing protein katanin and then transported into the axon by dynein (Polymer transport model; **Figure 2-9A**)(Wang and Brown, 2002; Baas et al., 2005). In contrast, it was shown that at least growing microtubules are not transported in axons (Ma et al., 2004). Moreover, various experiments showed the transport of non-polymerized tubulin into the axon (Terada et al., 2000; Kimura et al., 2005). Therefore, microtubules may also assemble locally from subunits or small oligomers within the axon (Subunit transport model; **Figure 2-9B**)(Hirokawa et al., 1997). Indeed, flies that lose centrosomes during development seem to develop a largely normal nervous system, where axon outgrowth appears not to be affected (Basto et al., 2006). Thus, the question where microtubules are generated in neurons is still unsolved.

To investigate this problem, I analyzed the centrosome and its microtubule nucleating activity in rodent hippocampal neurons during their development. In my thesis, I show that the centrosome lost its function as microtubule organizing center (MTOC) during neuronal development. Axons, however, still grew and regenerated through decentralized microtubule nucleation disconnected from the centrosome. Importantly, axons also extended after 2-photon laser ablation of the centrosome.

To summarize, I propose that decentralized microtubule assembly enables axon growth and regeneration and that it is instrumental to provide the different compartments of a neuron with a distinct cytoskeleton, the origin of the sophisticated morphology of neurons.

3 Results

3.1 Neuronal centrosomes lose their ability to nucleate microtubules during development

To define the role of the centrosome in microtubule nucleation during neuronal development, I determined where microtubules are nucleated at different developmental stages of rat hippocampal neurons.

To this end, cells were treated with nocodazole, a drug that depolymerizes microtubules. The centrosome was visualized by expressing a GFP tagged version of centrin-2, a centrosomal component, located in centrioles (Salisbury et al., 2002). After complete microtubule depolymerization with nocodazole (**Figure 3-1A and C**), the cells were then shortly washed in HBSS and then fixed after recovering in N2-medium at 37 °C for 90 s (2 days in vitro (DIV) neurons) or 3 min (12 DIV neurons). To visualize only polymerized microtubules without unpolymerized tubulin subunits, cells were simultaneously permeabilized and fixed using the PHEM-fixation (Witte et al., 2008). Microtubules were stained with an antibody against α-tubulin. Microtubule regrowth was analyzed in neurons that were just initiating an axon (2DIV) and in mature neurons (11-12 DIV). In young neurons (**Figure 3-1B**), microtubules regrew from the centrosome, consistent with previous results (Yu et al., 1993). After 90 s of recovery a microtubule aster or a focused microtubule spot at the centrosome was identified in 83 ± 5% of neurons that contained minor neurites and an axon (n > 200 cells). However, small microtubule seeds were also visible at acentrosomal sites. In mature neurons (**Figure 3-1D**), the recovery following nocodazole wash-out did not reveal such a focused repolymerization activity. In contrast, microtubules nucleated randomly throughout the whole cell, but did not emanate from the

centrosome ($n > 30$ cells). Newly formed microtubules appeared in mature neurons after around 2-3 minutes. This delay in comparison to the young neurons may be due to the possibility that acentrosomal microtubule nucleation is slower. Otherwise, the delay could be due to the higher nocodazole concentrations, which are necessary to depolymerize the more stable microtubules in the mature neurons.
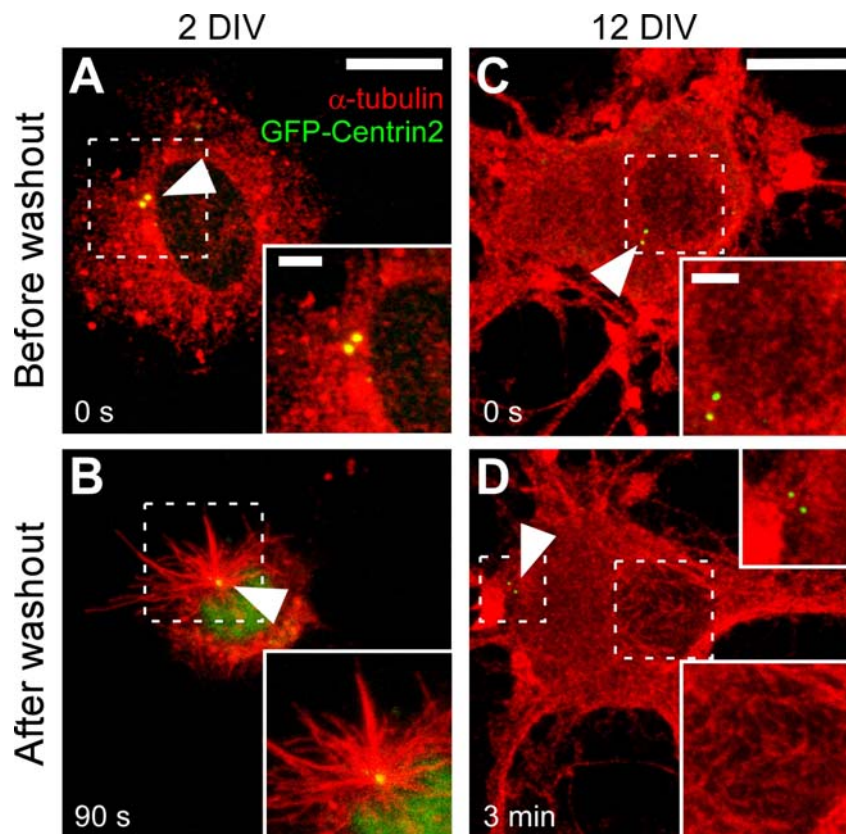
Figure 3-1: The centrosome loses its ability to nucleate microtubules during neuronal development.

(A and C) Microtubules (α-tubulin: red) are completely depolymerized using nocodazole. **(B)** After washout of nocodazole, microtubules regrow from the centrosome in young neurons (2 DIV). **(D)** In mature neurons (11 DIV), microtubules regrow from acentrosomal sites all over the cell body, but not from the centrosome. GFP-Centrin2 (green) marks the centrosome (arrowheads). Scale bar, 10 μm; inset, 2.5 μm.

We next tested wether microtubule dynamics are changed at different developmental stages. To this end, neurons were infected with the +TIP EB-3 fused to GFP,

treated with nocodazole and microtubule regrowth was imaged in real-time. EB3-GFP binds to the growing plus-end of microtubules, which enables the tracking of microtubule growth and is an established tool to analyze microtubule dynamics (Stepanova et al., 2003). These experiments were performed by Lukas Kapitein from the Erasmus Medical Center in Rotterdam, Netherlands. To express EB3-GFP in both young and differentiated neurons, Semliki Forest virus (SFV)-mediated gene delivery was used (Ehrengruber et al., 1999). Using total internal reflection fluorescence (TIRF) microscopy, microtubule nucleation following nocodazole wash-out was analyzed in young (2 DIV) and mature neurons (14 DIV). In young neurons, EB-3 comets emanated from the centrosome, but also emerged from acentrosomal regions (n = 11 cells; **Figure 3-2**). In contrast, in mature neurons, EB-3 comets did not emanate from a focal region but in an acentrosomal manner (n = 14 cells; **Figure 3-2**). Post hoc staining of the centrosomal marker pericentrin revealed the position of the centrosome, where no specific microtubule nucleation was observed (arrowhead, **Figure 3-2**).

Acentrosomal microtubule growth speed (67 ± 23 nm/s (mean ± s.d.); n = 83 comets) was indistinguishable from centrosomal microtubule growth speed (64 ± 24 nm/s; n = 85 comets) in young neurons, while the acentrosomal microtubule growth speed in mature neurons was slightly reduced (58 ± 15 nm/s; n = 435 comets). The observed microtubule growth speeds were significantly slower than previously published growth speeds (145 ± 8 nm/s (Grabham et al., 2007)). However, in contrast to our data, the published data are based on untreated neurons. As it was key for the experiment to assess the initial nucleation sites of microtubules, nocodazole wash-out experiments were performed. Due to remaining nocodazole after the rapid wash-out, microtubules might exhibit a lower rate of polymerization compared to untreated cells. This might also explain the slower speed of acentrosomal growth in mature neu-

rons compared to young neurons, as much higher nocodazole concentrations were used in the mature neurons.

In conclusion, these data indicate that the neuronal centrosome loses its potential to nucleate microtubules during development and that microtubules nucleate from acentrosomal sites in mature neurons. Interestingly, acentrosomal microtubule nucleation is also detectable in the younger neurons, even though centrosomal nucleation prevails.
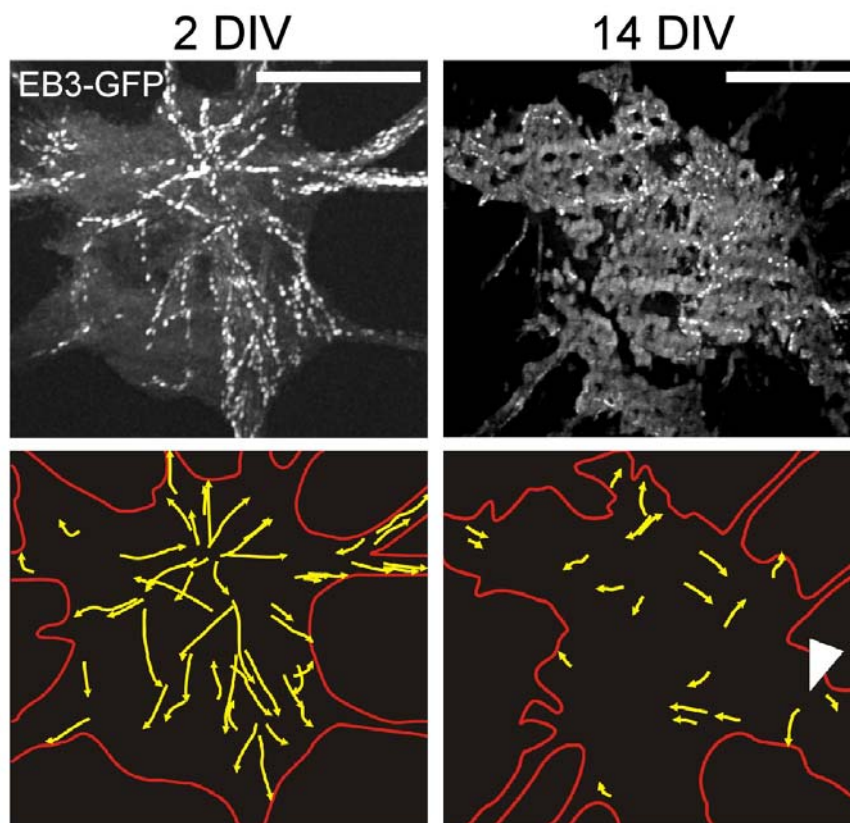
Figure 3-2: In young neurons, microtubules grow from a focal point, while in mature neurons EB3 comets emerge all over the cell body.

Maximum-projection of time-lapse recordings of EB3-GFP after nocodazole washout (time: 1 min 26 s). Comets predominantly grow radially from a central point in young neurons (2 DIV), but not in mature neurons (14 DIV). EB3-GFP tracks are indicated by yellow arrows. The arrowhead marks the centrosome in mature neuron (from post-hoc staining of endogenous pericentrin). Scale bar, 10 μm. Experiment performed by L. Kapitein, EMC Rotterdam, Netherlands.

3.2 The centrosome loses its role as MTOC during neuronal development

The next question was whether these changes in centrosomal activity during neuronal development can also be observed at the ultrastructural level of the centrosome. Due to the enormous amount of microtubules in neurons, the resolution of immunocytochemistry is too low to analyze centrosomal microtubules without depolymerization. Using electron microscopy does not only allow the analysis of the centrosome at an ultrastructural level, but can also give insight into microtubule organization at the centrosome without the need for pharmacological manipulation.

Electron microscopy revealed structural changes at the centrosome that correlate with the loss in centrosomal activity during neuronal development. In young neurons (2 DIV), microtubules emanated from centrioles in all analyzed neurons and formed an aster-like structure in 60% ± 5% of the cells, indicating considerable microtubule nucleation at the centrosome (n = 10 cells; **Figure 3-3A and B**). In contrast, only in 20% ± 4% of differentiated neurons (9 DIV) the centrioles or the pericentriolar region were linked to microtubules and no aster-like structures were found at this stage (n = 10 cells; **Figure 3-3A and B**). Although microtubules did not emerge from of the pericentriolar area, they were detectable in every mature neuron analyzed. Furthermore, one of the centrioles was often elongated in the mature neurons and surrounded by a membranous protuberance as it is characteristic of the primary cilium (**Figure 3-3A**, arrow). This finding indicates that during neuronal development the primary cilium extends from the basal body, a structure derived from the mother centriole of the neuronal centrosome (Pedersen et al., 2008). Whether the formation of the primary cilium can be accounted for the functional changes at the centrosome remains to be determined. Together, these differences between young and

mature neurons suggest a loss of microtubule nucleation and anchoring at the centrosome of differentiated neurons.
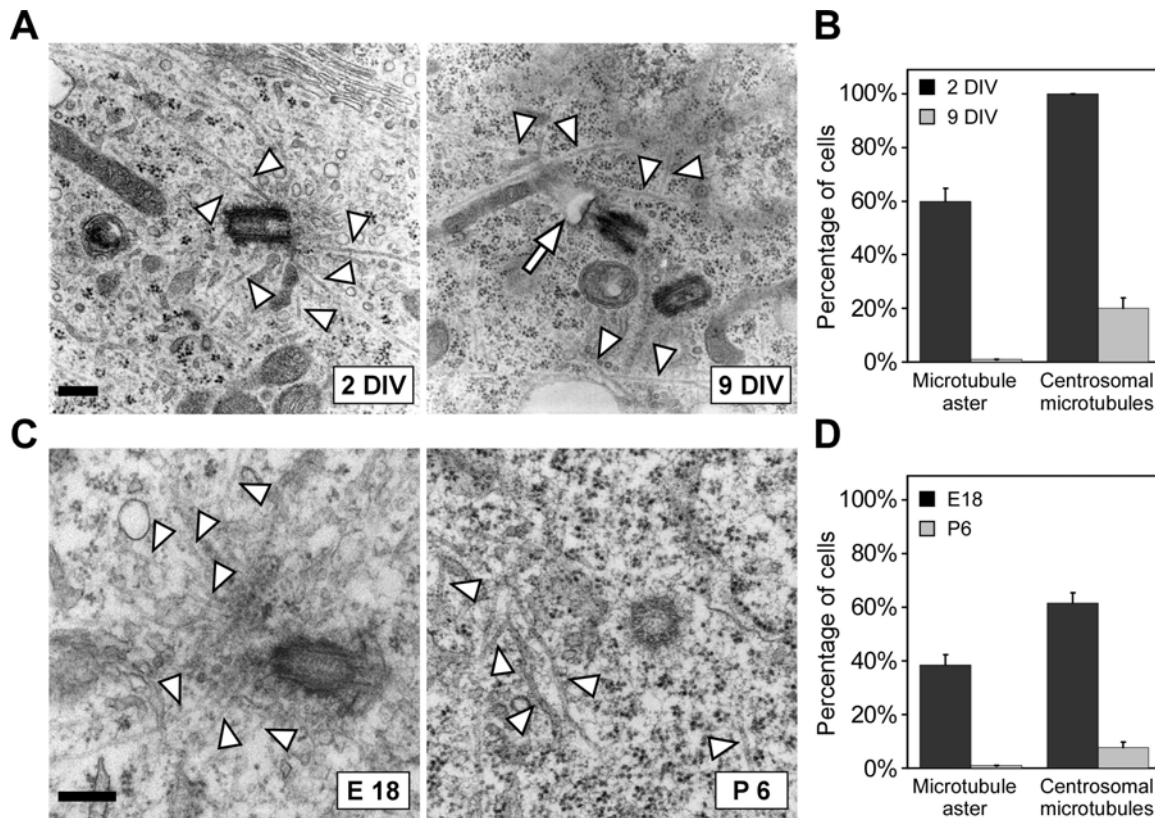
Figure 3-3: The centrosome loses its function as a microtubule organizing center (MTOC) during neuronal development.

Analysis of the neuronal centrosome by electron microscopy: Microtubules emerge from the pericentriolar area in young rat hippocampal neurons (2 DIV, **A**) and the neuronal centrosomes of E18 hippocampi **(C)**, but not in mature neurons (9 DIV, **A**) and P6 hippocampi **(C)**. Arrowheads indicate microtubules. Arrow indicates membrane protrusion of primary cilium. Scale bars, 250 nm. **(B and D)** Quantification of microtubule organization at the neuronal centrosome in 2 DIV and 9 DIV neurons (n = 10 cells each, B) as well as in E18 and P6 hippocampi (n = 13 cells each, **D**). Error bars, s.e.m. of a binominal distribution.

Since these changes of the centrosome were only observed in dissociated neurons the next step was to determine whether these centrosomal changes occur in a similar manner *in vivo*. Therefore, centrosomes in pyramidal neurons of the hippocampus at embryonic day 18 (E18) were compared with centrosomes of neurons at postnatal day 6 (P6)(*n* = 13 cells each; **Figure 3-3C and D**) with the age difference

approximately resembling the age difference in the cell culture experiments. I found that 62% ± 4% of the analyzed centrosomes in the pyramidal layer in E18 hippocampi showed microtubules that emerged out of the pericentriolar area (**Figure 3-3C and D**). Specific aster-like microtubules emerged from the centrioles in 38% ± 4% of the analyzed centrosomes. In P6 hippocampi, microtubules rarely emerged from centrosomes (8% ± 2%) and aster-like organized microtubules were not observed (**Figure 3-3C and D**). Thus, the neuronal centrosome loses its function as MTOC also during development *in vivo*.

In line with the microtubule regrowth experiments, the ultrastructural data show that the centrosome loses its function as MTOC during neuronal development. This is not only the case for dissociated neurons in culture, but also for hippocampal neurons *in vivo*.

3.3 γ-tubulin is depleted from the centrosome during neuronal development

How are these structural and functional changes of the neuronal centrosome reflected at the molecular level? To address this question, I determined whether γ-tubulin changes its intracellular localization during neuronal development. γ-tubulin, is one of the key proteins in microtubule nucleation (Wiese and Zheng, 2006), localizes to the centrosome and is essential for axon outgrowth (Ahmad et al., 1994). To this end, I analyzed cells by immunocytochemistry, where axon growth was just initiated (1 DIV; stage 3), already polarized cells with a growing axon and growing dendrites (4/5 DIV; stage 4) as well as mature neurons that formed synapses (11/12 DIV; stage 5) (Dotti et al., 1988). Centrosomes were localized by co-staining against pericentrin, another component of the pericentriolar material (PCM) (**Figure 3-4A**).

At 1 DIV, γ-tubulin localized to the centrosome in all neurons and showed an intensive centrosomal staining (ratio of centrosomal / cytoplasm fluorescence intensity: 2.16 ± 0.05; $n = 44$ cells; **Figure 3-4A and C**). At 4/5 DIV, when not only the axons but also dendrites grow, centrosomal γ-tubulin was detectable in $97\% \pm 2\%$ of the neurons (**Figure 3-4A and C**). However, the intensity of the γ-tubulin staining at the centrosome was reduced by 52% (ratio of centrosomal / cytoplasm fluorescence intensity: 1.55 ± 0.03, $n = 49$ cells; **Figure 3-4A and C**). After 11/12 DIV, centrosomal γ-tubulin was only detectable in $42\% \pm 10\%$ of mature neurons (**Figure 3-4A and C**) and the intensity was even reduced by 81% (ratio of centrosomal / cytoplasm fluorescence intensity: 1.22 ± 0.02, $n = 43$ cells; **Figure 3-4A and C**).

The γ-tubulin depletion seems to come along with a general reduction of PCM around the centrioles, because the PCM component pericentrin also decreased at the centrosome by 30% from 1 DIV (ratio of centrosomal / cytoplasm fluorescence intensity: 2.52 ± 0.04; $n = 47$ cells; **Figure 3-4A and C**) to 4/5 DIV (ratio of centrosomal / cytoplasm fluorescence intensity: 2.06 ± 0.03; $n = 59$ cells). At 11/12 DIV centrosomal pericentrin was still visible in all cells, but the staining was reduced by 49% (ratio of centrosomal / cytoplasm fluorescence intensity: 1.78 ± 0.03; $n = 52$ cells). As seen in the electron microscopy images, the centrioles remained in the cells (**Figure 3-4B**). Consistently, the centriolar component centrin remained relatively constant (ratio of centrosomal / cytoplasm fluorescence intensity at 1DIV: 1.65 ± 0.03; at 4/5 DIV: 1.54 ± 0.04; at 11/12 DIV: 1.52 ± 0.03; $n = 83/56/27$ cells; **Figure 3-4B and C**).
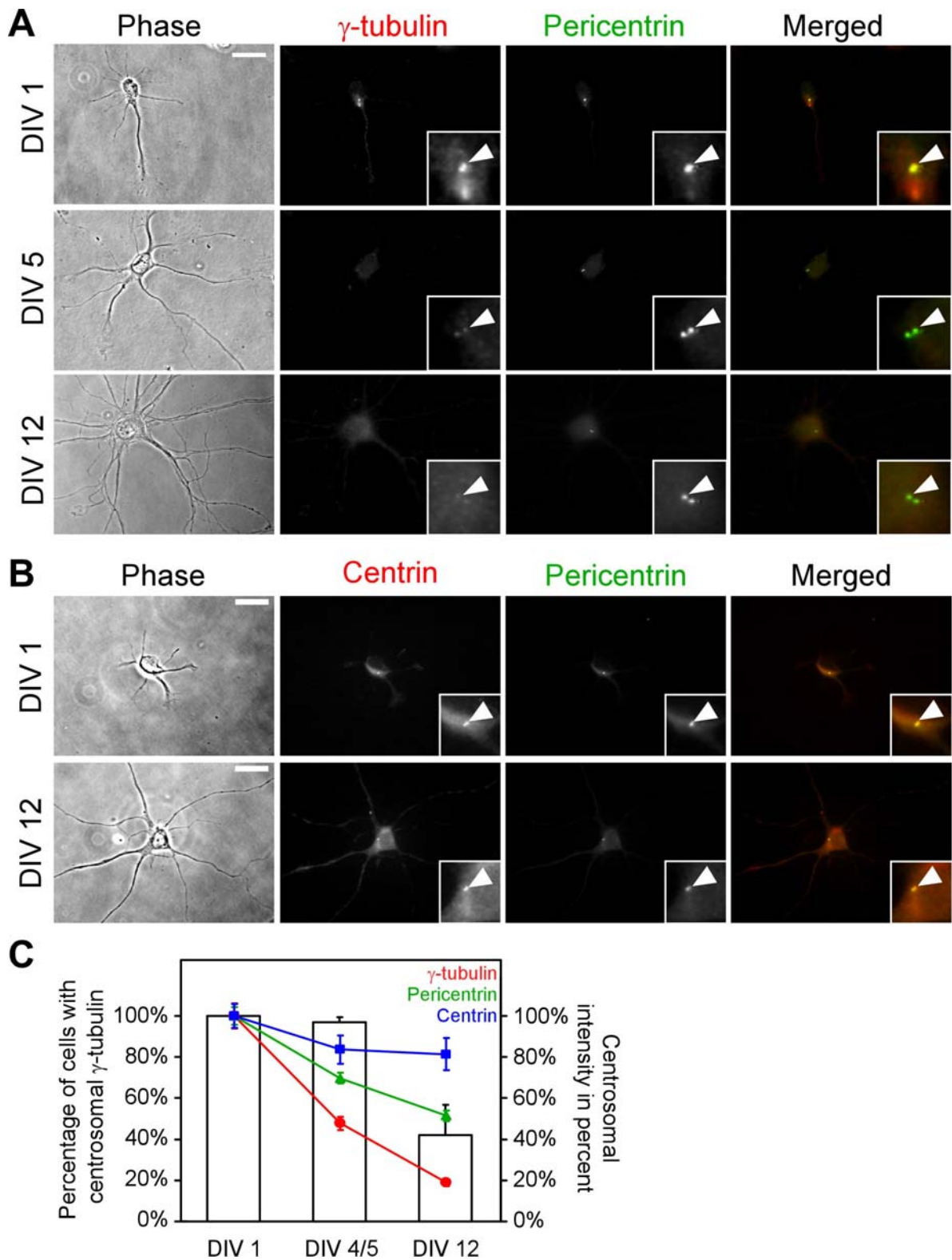
Figure 3-4: The pericentriolar material (PCM) proteins γ-tubulin and pericentrin are depleted from the neuronal centrosome during development, but the centriolar protein centrin remains.

(A) Rat hippocampal neurons at 1, 5 and 12 DIV were stained for γ-tubulin (red) and pericentrin (green). Centrosomes are indicated by arrowheads. Scale bar, 20 μm. **(B)** Rat hippocampal neurons at 1 and 12 DIV were stained for centrin (red) and pericentrin (green). Centrosomes are indicated by arrowheads. Scale bar, 20 μm. **(C)** Lines indicate the intensity ratio of centrosomal and cytoplasmic γ-tubulin (red), pericentrin (green) and centrin (blue) staining normalized to their 1 DIV signal (n = 27-83 cells per data point). Results are means ± s.e.m.

In conclusion, the microtubule nucleator γ-tubulin is depleted from the centrosome during neuronal differentiation. This might be a general feature of CNS neurons, because a similar depletion of centrosomal γ-tubulin was also reported for cortical and thalamic neurons (Leask et al., 1997). Since γ-tubulin is the key molecule in microtubule nucleation, the loss of centrosomal nucleation activity as seen in the regrowth experiments may therefore be caused by the centrosomal γ-tubulin depletion.

3.4 γ-tubulin is still present in differentiated neurons, but cannot be recruited to the centrosome

The immunofluorescence experiments clearly showed that γ-tubulin is depleted from the centrosome during neuronal development. This observation raises the question, whether γ-tubulin is only delocalized from the centrosome, but still present in the differentiated neurons or if the observed depletion of centrosomal γ-tubulin is caused by a reduction of the total γ-tubulin protein levels. To address this question the amount of γ-tubulin in whole cell extracts of neurons at different developmental stages were examined by western blotting. The western blot revealed that γ-tubulin is still present in differentiated neurons (9 DIV; **Figure 3-5A**). However, γ-tubulin protein levels are reduced compared to earlier stages of development (1 and 4 DIV; **Figure 3-5A**).

Figure 3-5: γ-tubulin is still present in mature neurons.

(A) Western blot of total cell lysates of rat hippocampal neurons at different developmental stages. Antibodies are used as indicated. For each point in time the equivalent protein amount was loaded. **(B)** Western blot of axon and soma preparation of neurons at 8 DIV. Antibodies are used as indicated. Of note, the nuclear marker histone H3 is not found in the axonal preparations.

These results suggest that γ-tubulin is still present in mature neurons despite its centrosomal depletion. However, immunofluorescence could not reveal where γ-tubulin might have relocalized to due to the high background staining in mature neurons (**Figure 3-4A**). Therefore, neurons were plated on a filter with a laminin coated bottom side, which attracted axons to grow through the filter. The pore size of the filter was 3 μm and thus only allowed axons to cross the filter whereas the somato-dendritic compartment remained on the other side. After 8 days of growth, neurons were fixed and either the cell bodies including dendrites on the upper side or the axons on the lower side of the filter were removed. The remaining cell bodies or axons were lysed and collected for western blot analysis. The purity of the axonal extracts was confirmed by the lack of the nuclear marker histone H3, indicating cell soma-free axonal extracts. With the western blot analysis I detected γ-tubulin in the axons of mature neurons (**Figure 3-5B**), which is contrary to previous immuno electron microscopy studies on sympathetic neurons that did not detect γ-tubulin in the axon (Baas and Joshi, 1992). This finding suggests delocalization of γ-tubulin from the centrosome into the growing axon, where it may act as a local microtubule nucleator.

It is difficult to conclude from the western blot experiment (**Figure 3-5A**), whether the depletion of centrosomal γ-tubulin is caused by the observed general reduction of γ-tubulin protein levels. If this was the case, overexpression of γ-tubulin would rescue the centrosomal depletion. Alternatively, the depletion could be due to impaired targeting of γ-tubulin to the centrosome of mature neurons and thus, overexpression of γ-tubulin would not affect the depletion of centrosomal γ-tubulin. To this end, I ectopically expressed a GFP-tagged form of γ-tubulin in neurons. In young neurons (1 DIV), GFP-γ-tubulin colocalized with the centrosome marker centrin in all cells (n = 258 cells; **Figure 3-6**). Interestingly, the overexpression of γ-tubulin in-

terfered with the development of the neurons and the cells died after a few days *in vitro*. Transfection in mature neurons (8 DIV) did not lead to obvious effects. In contrast to the young neurons, no specific recruitment of GFP-γ-tubulin to the centrosome was observed in the differentiated neurons (10 DIV) (**Figure 3-6**).

These observations suggest that mature neurons cannot recruit γ-tubulin to the centrosomes, probably as a consequence of changes in the centrosomal composition. Whether excess targeting of overexpressed γ-tubulin to the centrosome in the young neurons caused impaired development and neuronal cell death after γ-tubulin overexpression remains unclear. In mature neurons that were unable to target γ-tubulin to the centrosome, such cell death was not apparent after overexpression. These findings indicate that γ-tubulin levels and perhaps also its localization have to be tightly regulated during neuronal development.
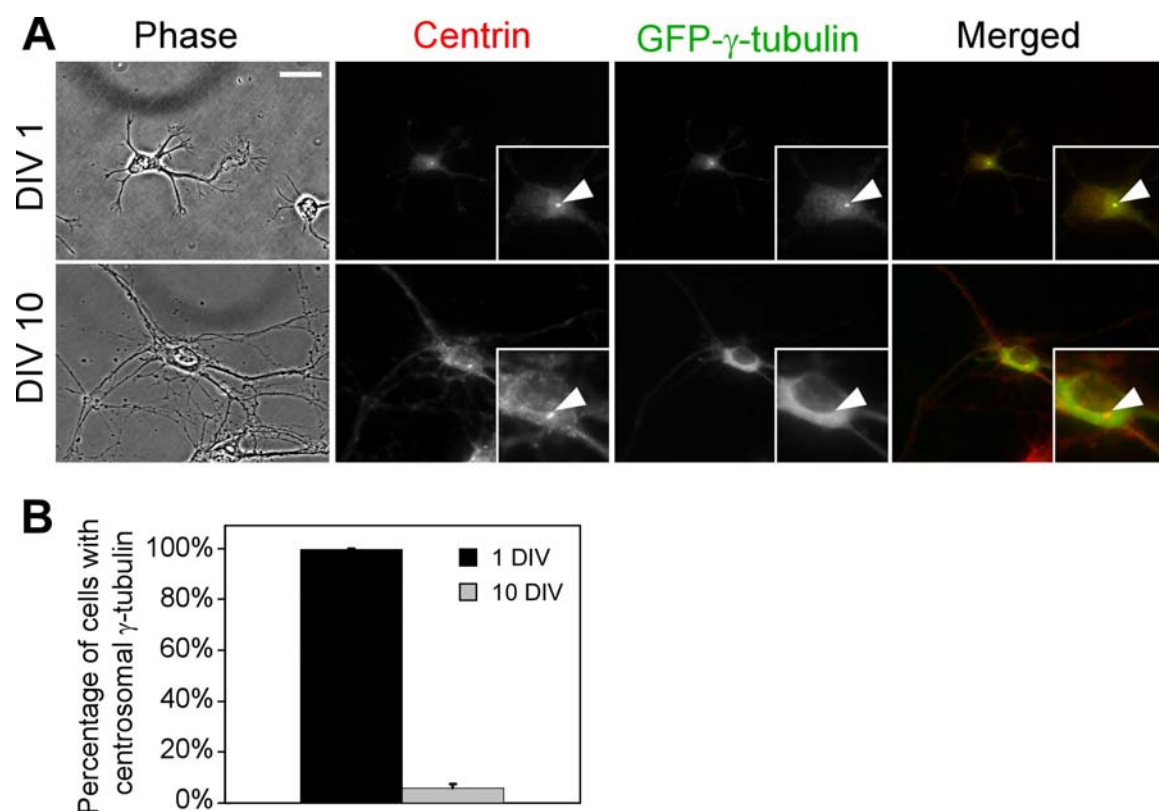
Figure 3-6: GFP-γ-tubulin is not recruited to the centrosome in mature neurons.

(A) Neurons at 1 and 10 DIV transfected with GFP-γ-tubulin (green). Arrowheads mark centrosomes identified by Centrin staining (red). Scale bar, 20 μm. **(B)** Quantification of centrosomal localization of GFP-γ-tubulin in 1 DIV (n = 258 cells) and 10 DIV neurons (n = 121 cells). Results are shown as mean ± s.e.m.

3.5 Regulation of centrosomal γ-tubulin targeting in neurons

The previous data suggest that during neuronal development the centrosome changes in a way, which disables centrosomal γ-tubulin targeting. Regulation of centrosomal γ-tubulin targeting is highly regulated at the on- and off-set of mitosis, a process called centrosome maturation (Khodjakov and Rieder, 1999; Blagden and Glover, 2003). Analysis of the localization and expression of several known centrosomal proteins, involved in centrosome regulation during mitosis identified two proteins: centrosomal protein 4.1-associated protein (CPAP) and NEDD1/GCP-WD. Both proteins showed a similar reduction in protein expression and a similar centrosomal depletion during neuronal development as γ-tubulin and could be therefore involved in the regulation of centrosomal γ-tubulin targeting in neurons.

Indeed, I found that in parallel to the depletion of γ-tubulin from the centrosome, the expression of CPAP was strongly reduced during development (**Figure 3-7**). The downregulation of total CPAP protein levels occurred simultaneously with the loss of centrosomal CPAP (**Figure 3-8**): All young neurons (1 DIV) showed centrosomal staining of CPAP (ratio of centrosomal / cytoplasm fluorescence intensity: 1.54 ± 0.04; n = 50 cells; **Figure 3-8**). At 4/5 DIV, most cells had a visible centrosomal staining of CPAP (92% ± 6%), but the intensity was reduced by 57% (ratio of centrosomal / cytoplasm fluorescence intensity: 1.23 ± 0.03; n = 63 cells; **Figure 3-8**). After 11/12 DIV, less than half of the cells (46% ± 21%) showed centrosomal CPAP staining with a barely detectable centrosomal signal (ratio of centrosomal / cytoplasm fluorescence intensity: 1.21 ± 0.03; n = 60 cells; **Figure 3-8**).
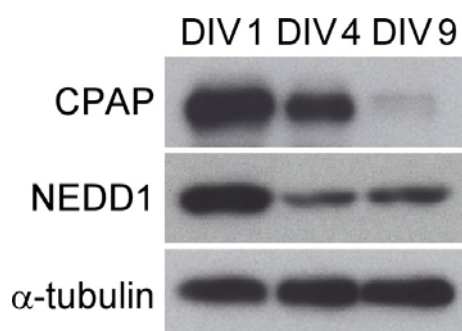
Figure 3-7: Potential γ-tubulin recruiting factors are downregulated during neuronal development.

Western blot of total cell lysates of rat hippocampal neurons at different developmental stages. Antibodies are used as indicated. For each point in time the equivalent protein amount was loaded.

Studies showed that CPAP is involved in centriole duplication, but also in microtubule nucleation (Hung et al., 2000; Tang et al., 2009). Furthermore, its putative homologue in C. elegans SAS-4 controls the amount of pericentriolar material (PCM) (Kirkham et al., 2003). The downregulation of the centriolar protein CPAP in hippocampal neurons might therefore indicate changes at the centrioles that come along with the loss of PCM including γ-tubulin.
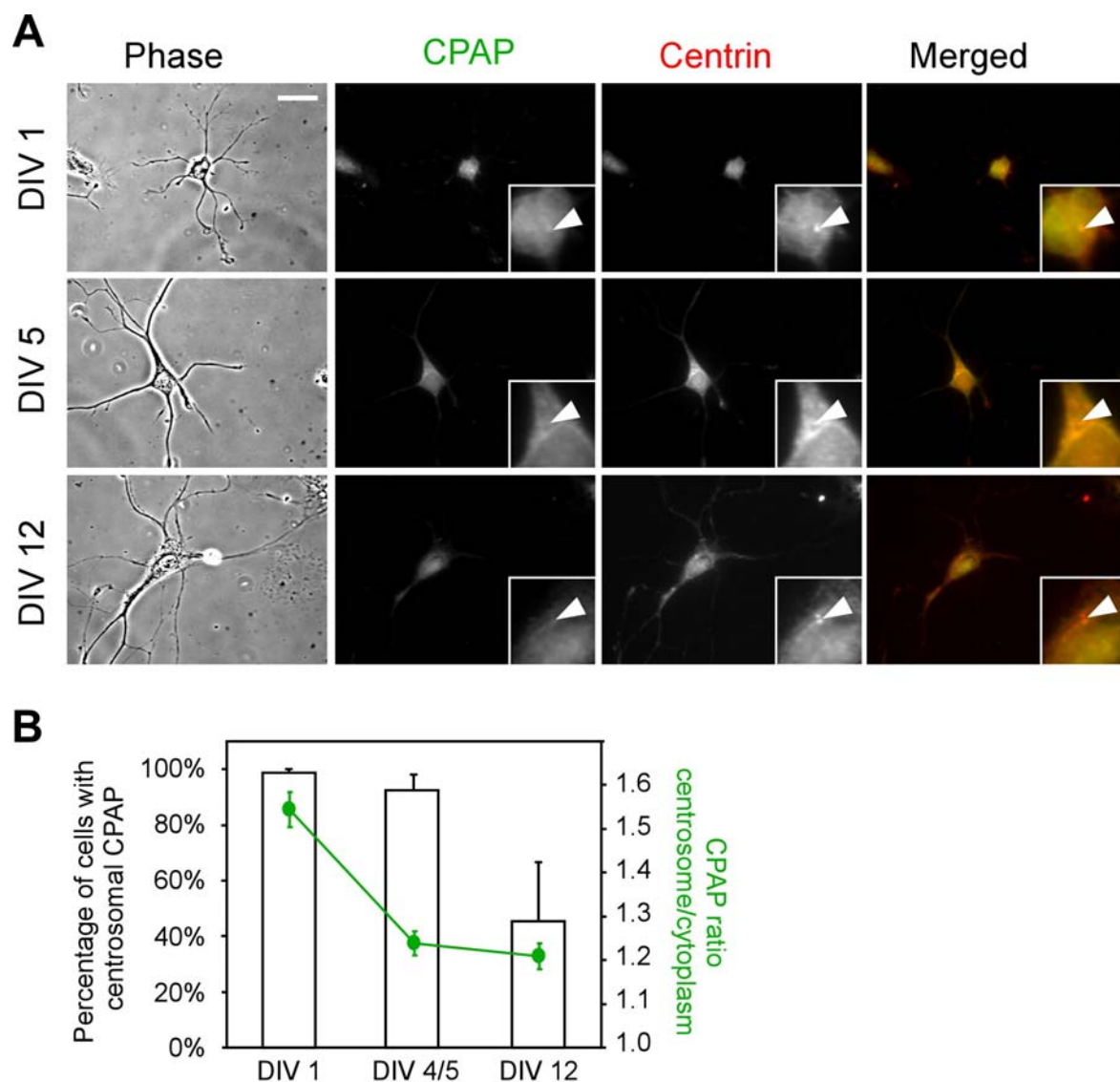
Figure 3-8: CPAP is depleted from the neuronal centrosome during development.

(A) Rat hippocampal neurons at 1, 4/5 and 11/12 DIV were stained for CPAP (green) and Centrin (red). Centrosomes are indicated by arrowheads. Scale bar, 20 μm. **(B)** Bars represent the percentage of neurons (1, 4/5 and 12 DIV) with centrosomal CPAP (n > 300 cells per data point). The green line indicates the intensity ratio of centrosomal and cytoplasmic CPAP staining (n > 50 cells per data point). Results are shown as mean ± s.e.m.

The γ-tubulin targeting factor NEDD1/GCP-WD was also downregulated during development (**Figure 3-7**). NEDD1 is a part of the γ-TuRC and targets the γ-TuRC to the PCM (Haren et al., 2006; Luders et al., 2006). However, even though NEDD1 and γ-tubulin were still present in mature neurons (**Figure 3-7**), NEDD1 is not able to target γ-tubulin to the centrosome. The downregulation of NEDD1 expression was accompanied by the loss of centrosomal NEDD1 (**Figure 3-9**). At 1 DIV, I found NEDD1 at the centrosome of all neurons with a strong signal (ratio of centrosomal / cytoplasm fluorescence intensity: 1.83 ± 0.03; $n = 41$ cells; **Figure 3-9**). At 4/5 DIV, the centrosome of most neurons (89% ± 6%) had a visible centrosomal staining of NEDD1, but the intensity was decreased by 48% (ratio of centrosomal / cytoplasm fluorescence intensity: 1.43 ± 0.02; $n = 41$ cells; **Figure 3-9**). After 11/12 DIV, NEDD1 was only detectable in around half of the neurons (51% ± 12%) with a very low signal (ratio of centrosomal / cytoplasm fluorescence intensity: 1.28 ± 0.03; $n = 41$ cells; **Figure 3-9**).

Together with the depletion of the PCM components γ-tubulin and pericentrin, the depletion of the PCM protein NEDD1 suggests that the delocalization of γ-tubulin is due to a general reduction of PCM. In turn, the reduction might be caused by structural changes of the centrioles, as indicated by the CPAP depletion and the electron microscopy images.
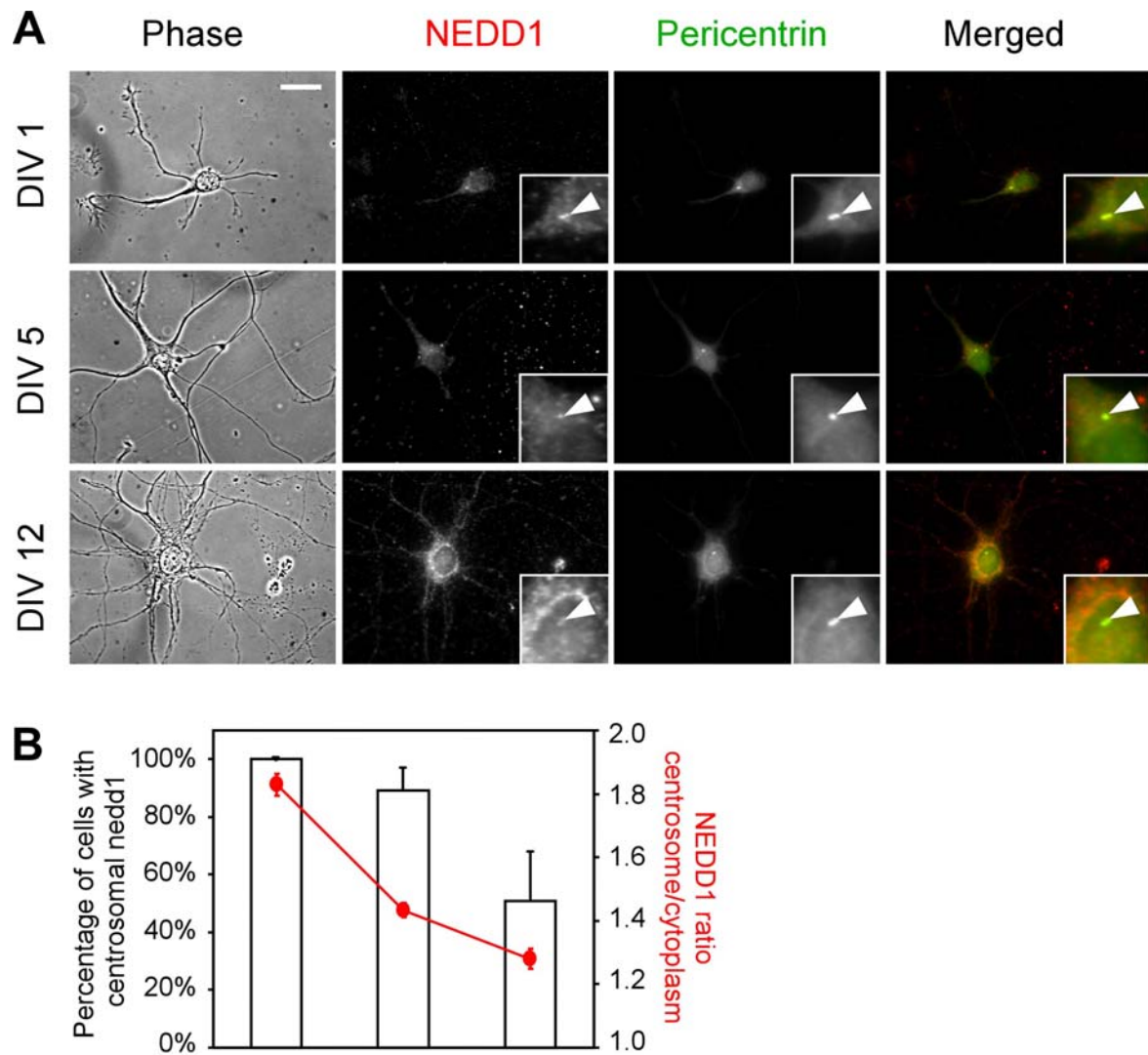
Figure 3-9: NEDD1 is depleted from the neuronal centrosome during development.

(A) Rat hippocampal neurons at 1, 5 and 12 DIV were stained for NEDD1 (red) and pericentrin (green). Centrosomes are indicated by arrowheads. Scale bar, 20 μm. **(B)** Bars represent the percentage of neurons (1, 4/5 and 12 DIV) with centrosomal NEDD1 (n > 200 cells per data point). The red line indicates the intensity ratio of centrosomal and cytoplasmic NEDD1 staining (n > 41 cells per data point). Results are shown as mean ± s.e.m.

3.6 Axons of mature neurons extend in the absence of centrosomal microtubule nucleation

Axon growth depends on microtubule polymerization (Tanaka et al., 1995). However, the average length of microtubules does not increase during axon growth, whereas the microtubule number increases extensively (Yu and Baas, 1994). In most cell types, microtubules are nucleated at the centrosome. Thus, the question whether axon growth is affected when the centrosome is depleted of γ-tubulin and has lost its function as a MTOC was investigated. To this end, the length of the longest axon branch was measured over two weeks.

To measure axon length, neurons from a GFP-labeled mouse were used. These GFP-positive neurons were grown in a background of non-fluorescent neurons from wildtype animals resulting in a culture with single GFP-labeled neurons (Gomis-Ruth et al., 2008). This approach allowed the observation of axon growth in single neurons fully integrated into neuronal networks. Axons grew at a constant rate throughout all developmental stages, even after centrosomal microtubule nucleation ceased (**Figure 3-10**). On average, axons grew 131 ± 39 µm/day (2 DIV - 4 DIV) when γ-tubulin was present at the centrosome, and 178 ± 55 µm/day (9 DIV - 13 DIV) when the centrosome was inactive (**Figure 3-10**). Since the axon was also branching, the total axon growth rate even increased with time. Thus, although mature neurons have lost their ability to nucleate microtubules at the centrosome, this does not restrain their potential to extend the existing axon.
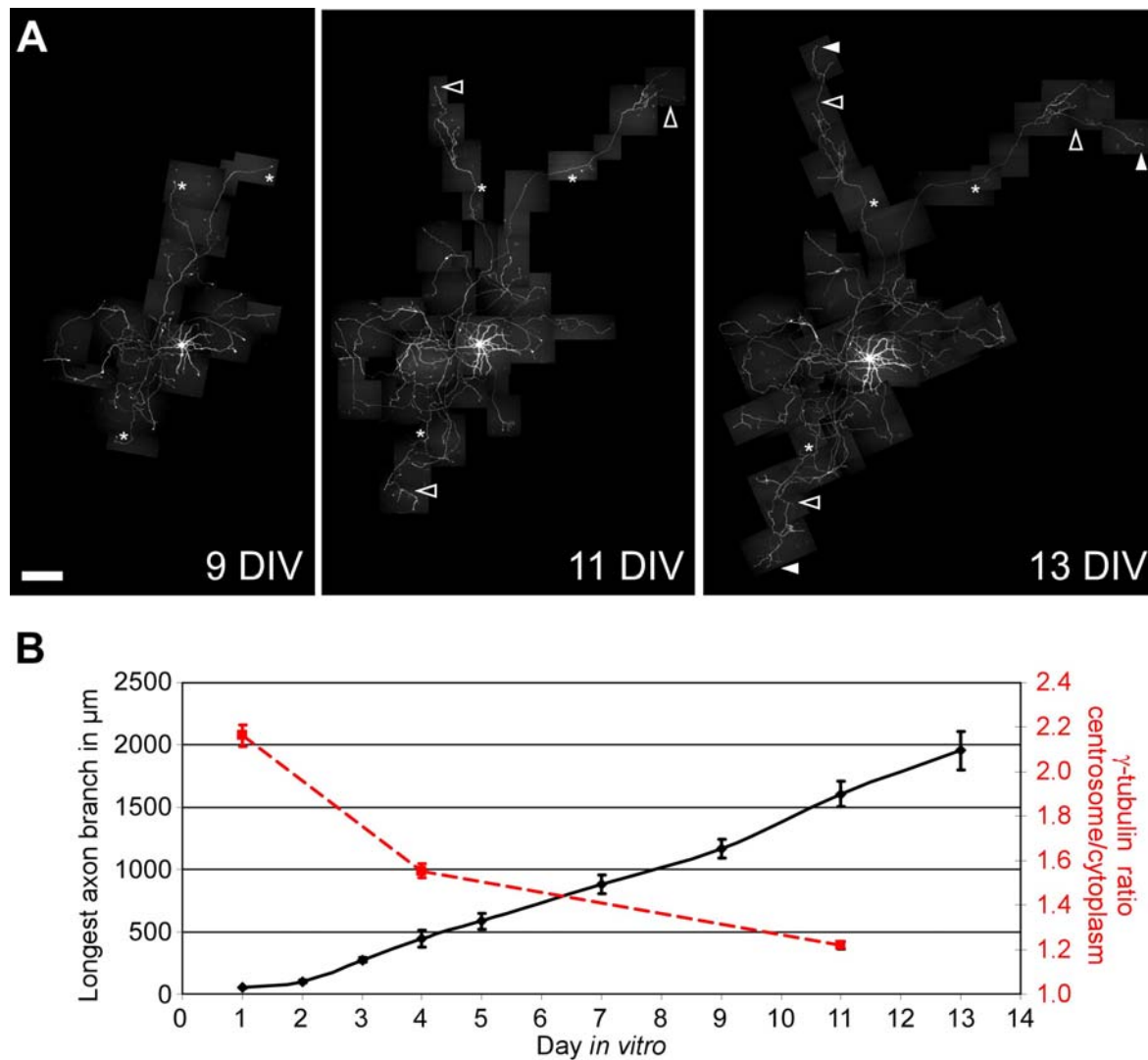
Figure 3-10: Axon growth is not affected when the centrosome has lost its ability to nucleate microtubules.

(A) The axon of a GFP labeled mouse hippocampal neuron grows from 9 DIV (asterisk) to 11 DIV (empty arrowheads) and 13 DIV (arrowheads). Scale bar, 200 μm. **(B)** Growth of longest axon branch over time (black line, n = 18 to 52 cells per data point) and intensity ratio of centrosomal and cytoplasmic γ-tubulin staining (dashed line; from Figure 3-4). Results are mean ± s.e.m

3.7 Axons regenerate in the absence of centrosomal microtubule nucleation

As shown above, the extension of axons of mature neurons is independent of centrosomal microtubule nucleation. However, this extension could still be based on the rearrangement of existing microtubules. Thus, the question arose, whether it is possi-

ble that the centrosome contributes to axon growth when the axon is cut and a large amount of microtubules is removed. Upon lesioning the axon, hippocampal neurons show different regenerative responses independent of their degree of polarization (Dotti and Banker, 1987; Goslin and Banker, 1989; Bradke and Dotti, 2000; Gomis-Ruth et al., 2008). The neurons regrow their axon when the axon is cut distally; lesioning the axon close to the cell body (<35 µm) causing axon outgrowth from an existing dendrite (Gomis-Ruth et al., 2008). Remarkably, although a large amount of microtubules are removed by cutting the axon and axon regeneration requires new microtubule polymerization (Moskowitz and Oblinger, 1995), regenerative growth rates are comparable in young and mature neurons (Gomis-Ruth et al., 2008).

Therefore, I tested whether axon regeneration after axotomy occurs in mature neurons in the absence of centrosomal microtubule nucleation. Alternatively, axotomy may rejuvenate mature neurons and reactivate their centrosome. To this end, the axon of neurons integrated in neuronal networks (>10 DIV) were cut using a micro-needle (**Figure 3-11**). Axotomy was performed together with Susana Gomis-Rüth from our laboratory. Proximal axotomy caused the dendrites to elongate and to be become new axons (**Figure 3-11C**, arrows with T [transformation]), whereas distal axotomy lead to axon regrowth (Gomis-Ruth et al., 2008). After cutting the axon of 8-17 DIV neurons, we examined one day later if a new axon had grown from the same process (axon regrowth) or a new axon initiated from a dendrite (identity change). In case the neurons regenerated, either axon regrowth or identity change, the cell was fixed and centrosomal γ-tubulin was analyzed by immunocytochemistry.

Before axotomy
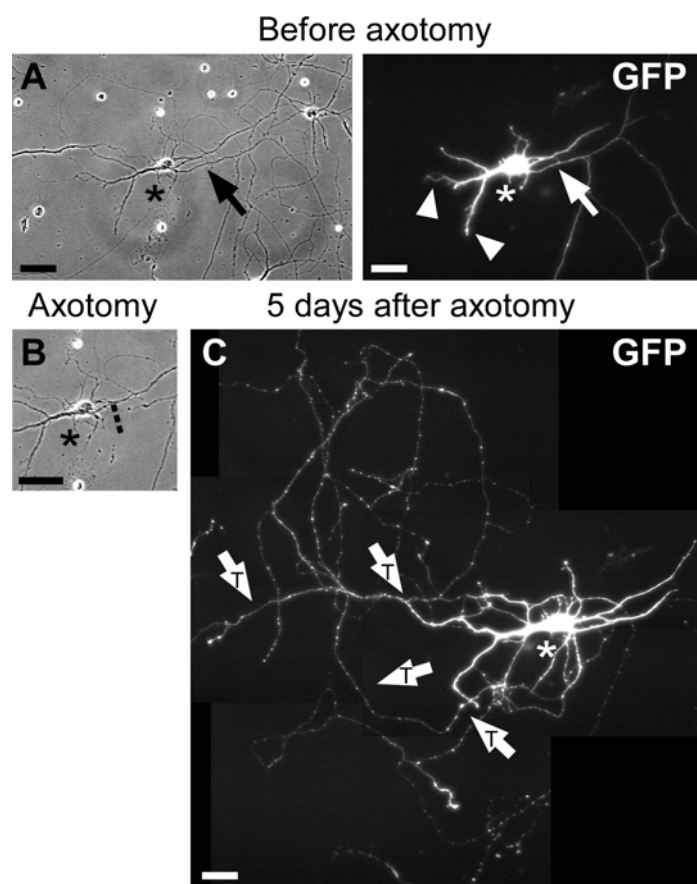
Figure 3-11: Axotomy close to the cell body leads to the transformation of a dendrite into an axon.

(A) The axon (arrow) of a GFP-positive cell (asterisk; 14 DIV) was cut close to the cell body (**B**, dashed line). **(C)** Former dendrites of the same neuron (indicated by arrowhead in **A**) elongated 5 days after axotomy to form an axon (arrows with T [transformation]). Scale bars, 50 μm.

The intensity of centrosomal γ-tubulin staining was measured in lesioned neurons showing axon regeneration (ratio of centrosomal / cytoplasm fluorescence intensity: 1.19 ± 0.03; n = 20 cells; **Figure 3-12**) and in unlesioned neurons on the same coverslip (ratio of centrosomal / cytoplasm fluorescence intensity: 1.19 ± 0.01; n = 244 cells; **Figure 3-12**). No recruitment of centrosomal γ-tubulin was observed in axotomized neurons undergoing dendritic-axonal transformation or axonal regrowth. Centrosomal γ-tubulin remained at low levels similar to that seen in unlesioned cells and was not comparable to the strong signal seen in young neurons (1 DIV; ratio of centrosomal / cytoplasm fluorescence intensity: 1.79 ± 0.03; n = 60 cells; **Figure 3-12B**). Thus, axons regenerate independently of centrosomal microtubule nucleation in mature neurons.
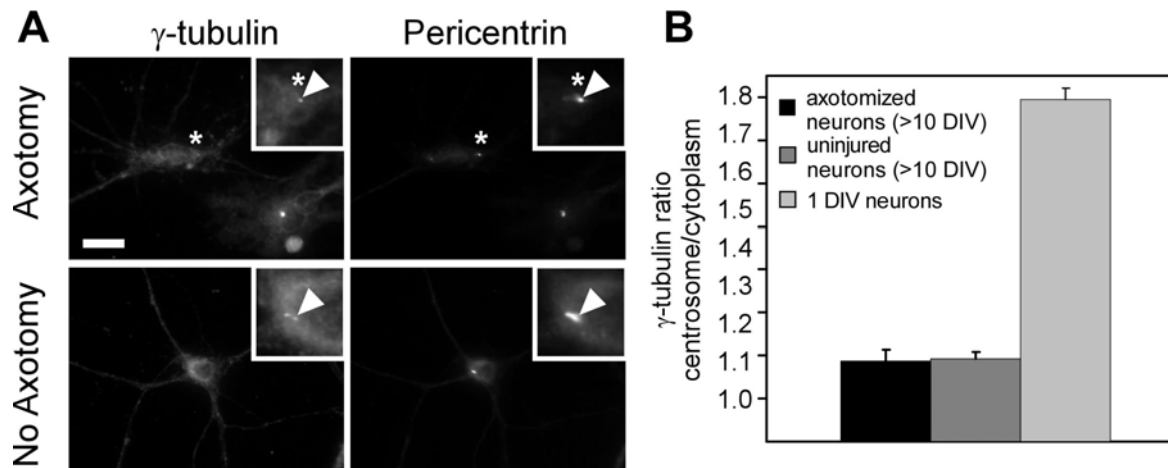
Figure 3-12: γ-tubulin is not recruited to the centrosome during axon regeneration.

(A) Mouse hippocampal neuron 24 hours after axotomy at 14 DIV and uninjured control neuron from the same coverslip. Arrowheads indicate the centrosome stained by γ-tubulin and pericentrin antibodies. Scale bar, 20 μm. **(B)** Quantification of intensity ratio of centrosomal and cytoplasmic γ-tubulin in axotomized (*n* = 20 cells), non-axotomized (*n* = 244 cells), and young neurons (1 DIV, *n* = 60 cells). Results are means ± s.e.m.

3.8 Axon growth in young neurons does not require centrosomal microtubule nucleation

As axons grow and regenerate in mature neurons without a functional centrosome, I asked whether axon growth requires centrosomal microtubule nucleation in earlier stages of development, when the centrosome still functions as a MTOC. Therefore, we physically ablated the centrosome by laser microsurgery in young neurons (2 DIV), which possess a functional centrosome. Laser ablation of the centrosome is an established technique that had been successfully performed in non-neuronal cells (Khodjakov et al., 2000; Efimov et al., 2007; Loncarek et al., 2008). For my project, I collaborated with Nicola Maghelli from the Max Planck Institute of Cell Biology and Genetics in Dresden, who developed a two-photon laser ablation setup, which can precisely ablate sub-micrometer structures inside living cells (Maghelli and Tolic-Nørrelykke, 2008). The destruction was achieved by increasing the power of the laser while scanning the beam over a user-defined region of interest (ROI). The two cen-

trioles of the centrosome were visualized by transfecting the neurons with centrin2-GFP. By drawing a circular ROI around the two centrioles, the site of ablation was defined. First, we determined the laser power in the sample plane and the exposure time that was necessary to successfully ablate the centrosome. The difficulty was to find the window, in which the laser power was high enough to destroy the centrosome, but not too high to fatally damage the neurons.

To validate successful centrosome ablation, I used the following approaches. First, I stained the ablated neurons for the presence of centrosomal components by using immunocytochemistry. I found that neither γ-tubulin nor Pericentrin were present at the centrosome of ablated neurons, both directly after ablation and also 24 hours later (**Figure 3-13A**). Moreover, laser ablation not only removed the PCM, but
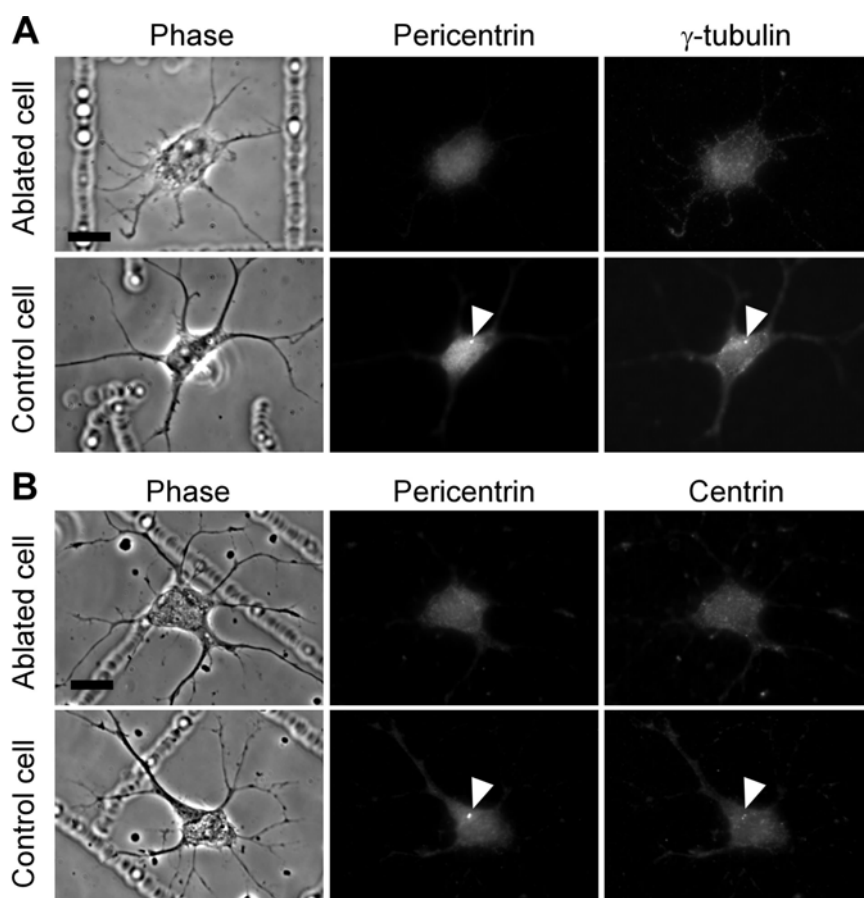
Figure 3-13: Laser ablation destroys the centrioles and disrupts the pericentriolar material (PCM).

After laser ablation of the centrosome, the neuron (2 DIV) was stained for the pericentriolar proteins Pericentrin **(A and B)**, γ-tubulin **(A)** and the centriolar protein centrin **(B)**. The centrosomes of non-ablated control neurons (2 DIV) are indicated by arrowheads. Scale bar, 10 μm

also the centrioles as shown by staining against centrin (**Figure 3-13B**).

Second, laser ablated neurons were analyzed with serial section electron microscopy, performed by Michaela Wilsch-Bräuninger (MPI-CBG, Dresden). The serial sectioning enabled the analysis of the whole neuron for its centrioles. In control neurons, the centrioles were detected in the 70 nm thin sections and similar to **Figure 3-3**, microtubules grew out of the pericentriolar area. In ablated neurons, the micrographs confirmed the expected physical destruction of the centrosome (**Figure 3-14**). However, occasional centriolar fragments were visible in the micrographs, which still might have been able to nucleate microtubules (**Figure 3-14**). Therefore, microtubule nucleation in centrosome ablated neurons was analyzed and subsequent nocodazole washout experiments were performed. In centrosome ablated neurons, only acentrosomal microtubule regrowth occurred after nocodazole washout (n = 19; **Figure 3-15B**).

Finally, microtubule regrowth in living neurons was imaged after nocodazole washout. Neurons were cotransfected with both GFP-centrin2 to visualize the centrosome for ablation and with the microtubule plus-end tracking (+TIP) protein EB3-GFP to visualize growing microtubules. In cells, where microtubules were depolymerized with nocodazole, the centrosome was ablated at the two-photon setup. Afterwards, the cells were transferred to a spinning disc confocal microscope and microtubule regrowth was observed in real-time after nocodazole washout. In non-ablated control neurons, microtubule regrowth from the centrosome was observed using GFP-centrin2 for the visualization of the centrosome (**Figure 3-15E**). After laser ablation, no centrosomal but only acentrosomal microtubule nucleation occurred (**Figure 3-15D**).
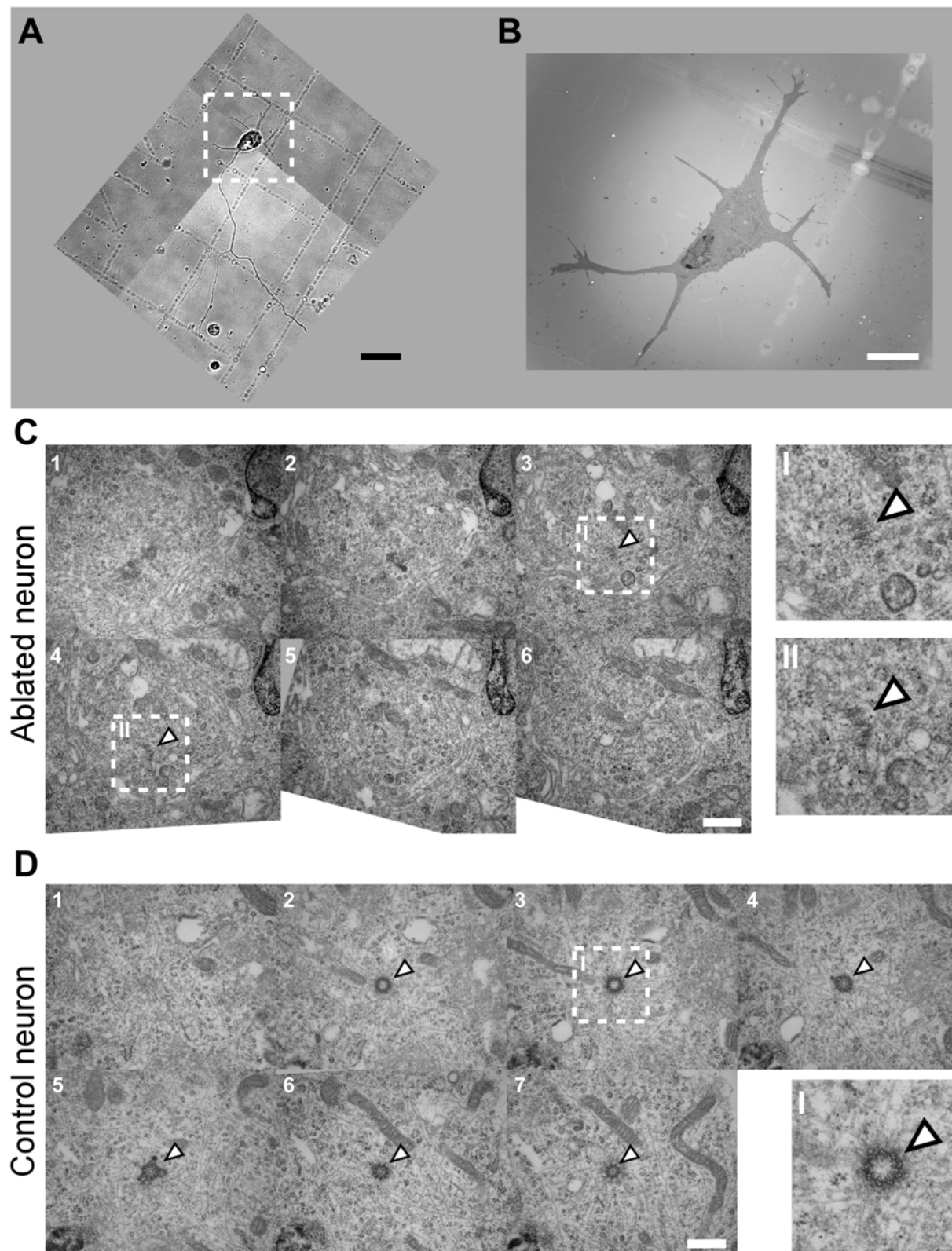
Figure 3-14: Laser ablation destroys the centrosome.

(A) Rat hippocampal neuron (2 DIV) before laser ablation. Scale bar, 25 μm. **(B)** Electron microscope picture of the neuron from A after centrosome ablation. Scale bar, 10 μm. **(C)** Serial sections of the ablated neuron. Image details I and II show centriolar fragments at a higher magnification (arrowheads). Scale bar, 500 nm. **(D)** Serial sections of a control neuron. Arrowheads indicate the centriole. Note the microtubules emerging from the centriole. Scale bar, 500 nm. Pictures taken by Michaela Wilsch-Bräuninger, MPI-CBG, Dresden.
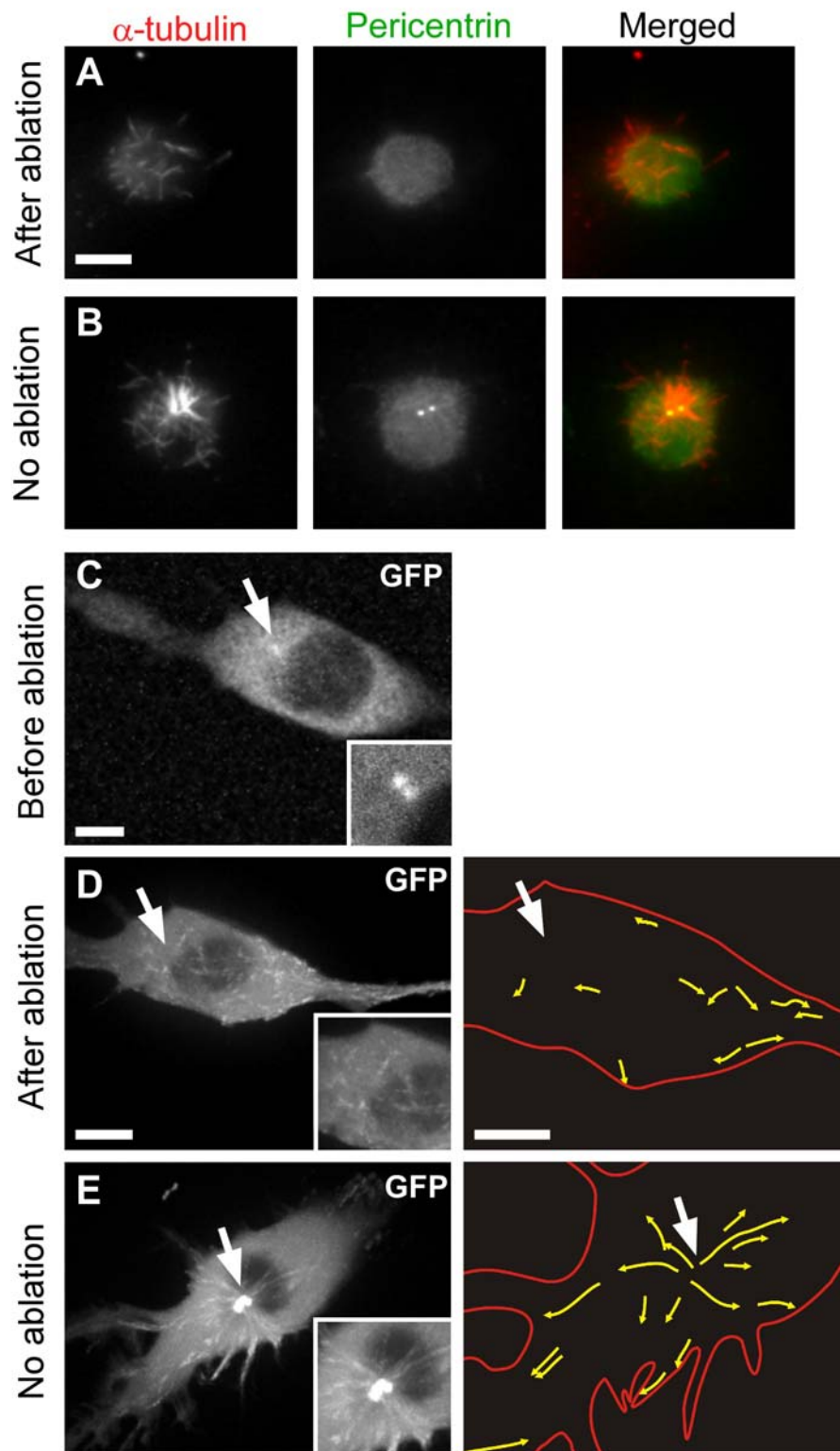
Figure 3-15: Microtubules regrow acentrosomally after laser ablation of the centrosome.

(A) After washout of nocodazole, microtubules (α-tubulin: red) regrow from acentrosomal sites in ablated neurons (2 DIV). Scale bar, 10 μm. **(B)** Microtubules regrow from the centrosome in control cells. Pericentrin (green) marks the centrosome. **(A)** Centrosome indicated by centrin2-GFP (arrow) before laser ablation in a 2 DIV neuron. Scale bar, 5 μm. **(B and C)** Maximum-projection of time-lapse recordings of GFP-EB3 after nocodazole washout. GFP-EB3 tracks are indicated by yellow arrows. **(B)** In the ablated neuron, comets grow from acentrosomal sites. Arrow marks position of centrosome before ablation. **(C)** GFP-EB3 comets predominantly grow radially from the centrosome (arrow) in a control neuron (2 DIV). Scale bars, 5 μm.

In conclusion, using these different approaches, I showed that the laser parameters employed allowed successful centrosome ablation. Therefore, I could address the actual question, whether axons of young neurons are able to grow without a centrosome. To this end, the centrosomes in neurons that just started to form an axon (2 DIV) were ablated. Ablation killed approximately half of the neurons. In the surviving neurons, axon growth was followed during the subsequent 24 hours after ablation (**Figure 3-16**). To prove successful ablation and to exclude formation of a new centrosome, all cells were analyzed for the absence of centrosomal γ-tubulin and pericentrin staining at the end of the experiment (**Figure 3-13A**). 8 hours after ablation, axons extended 38 ± 6 μm on average (*n* = 40 cells) similar to untreated control neurons (34 ± 7 μm; *n* = 52 cells). Also 24 hours after the removal of the centrosome, axon growth of ablated and control cells was indistinguishable (P = 0.81, two-tailed t-test). The axon of centrosome ablated neurons grew 115 ± 17 μm on average (*n* = 12 cells), similarly to control neurons (121 ± 16 μm; *n* = 26 cells). Thus, also young neurons can extend their axon without a centrosome.

Together with the previous data, the presented results showed that axons can grow independently of centrosomal microtubule nucleation. Thus, acentrosomal microtubule assembly creates the new microtubules necessary for normal axon growth in young and mature neurons as well as during axon regeneration or new axon formation from a dendrite after axotomy
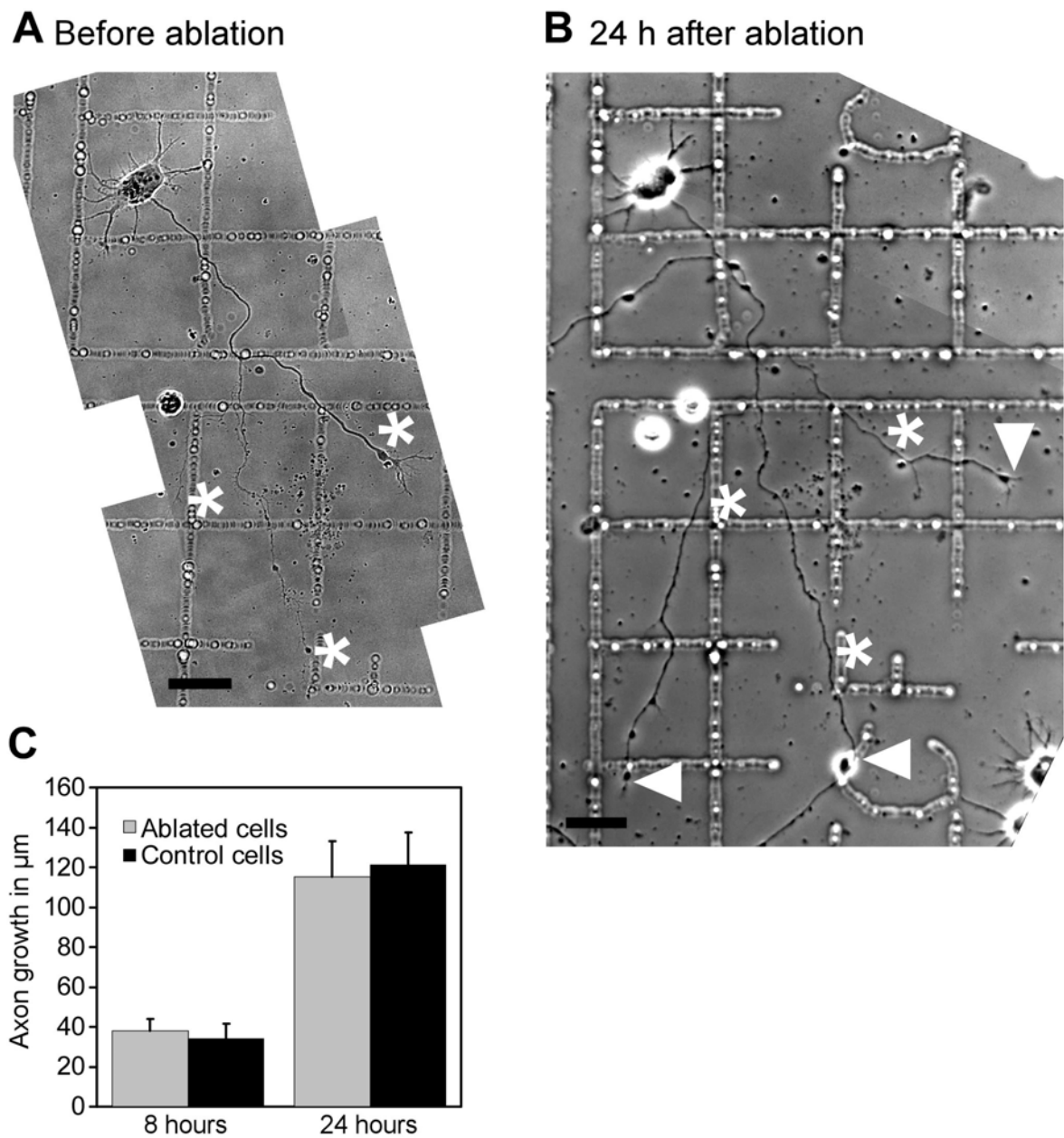
Figure 3-16: Laser ablation in young neurons does not affect axon growth.

(A) Asterisks mark axon endings of a rat hippocampal neuron (2 DIV) before laser ablation. **(B)** Axon growth 24 h after ablation of the centrosome (arrowheads). Successful ablation was proven by immunostaining against centrosomal components after the experiments (**Figure 3-13A**). Scale bars, 25 μm. **(C)** Axons grow similarly 8 h and 24 h after ablation compared to axons of control cells (n = 12 to 52 cells). Results are shown as mean ± s.e.m.

.

4 <u>Discussion</u>

Microtubules are essential for axon growth by giving structure to the axon shaft and driving axon extension (Lowery and Van Vactor, 2009). To extend the axon, neurons have to generate new microtubules and unlike most animal cells that are known to form microtubules at the centrosome it is still unclear how and where new microtubules are generated in neurons. It has been proposed that neuronal microtubules are nucleated at the centrosome, and then transported as polymer into the axon (Wang and Brown, 2002; Baas et al., 2005). Nevertheless, it was also shown that growing microtubules are not transported in axons (Ma et al., 2004; Kim and Chang, 2006). Moreover, various experiments showed the transport of nonpolymerized tubulin into the axon (Terada et al., 2000; Kimura et al., 2005), suggesting local, decentralized microtubule assembly. In summary, while the debate heavily focused on microtubule transport, very little is known about where microtubules are actually formed. The goal of this study was therefore to address this problem from a different perspective and to investigate where microtubules are generated in neurons during axon growth.

My data show that the centrosome loses its function as microtubule organizing center during development of rodent hippocampal neurons. The microtubule nucleating factor γ-tubulin was depleted from the centrosome and after depolymerization with nocodazole, microtubules did not regrow at the centrosome at later stages of development. Nevertheless, axonal growth was unchanged after the centrosome had lost its activity. Moreover, when the axon was lesioned in fully mature neurons, a new axon grew out in the absence of centrosomal γ-tubulin. Finally, developing neurons kept their ability to extend the axon when the centrosome had been ablated by a laser.

In summary, I present evidence that axon growth and regeneration occur independently of microtubule nucleation at the centrosome, and consequently, when the axon is initiated, decentralized microtubule assembly arranges the cytoskeleton, which is the source of the sophisticated neuronal morphology. Therefore, I propose that acentrosomal microtubule nucleation may be a key feature during differentiation of neuronal, but also of non-neuronal cells.

4.1 Decentralization - The generation of neuronal microtubule arrays

In contrast to most somatic cells, few microtubules are attached to the centrosome in neurons. Instead, the vast majority of microtubules is free in the cytoplasm where they tend to coalesce into bundles that "funnel" into the axon and dendrites (Baas, 1999). Even though the microtubules are not attached to the centrosome, they lie in precisely oriented positions in the cytoplasm and the processes. Therefore, it is difficult to reconcile the distinct microtubule array in neurons with such focal microtubule assembly at the centrosome as it is seen in many cells and as it is also proposed for neurons (Baas et al., 2005).

In this work, I show that during neuronal development, microtubule formation becomes decentralized: in young neurons, centrosomal as well as acentrosomal microtubule nucleation could be detected. Later in development, centrosomal microtubule nucleation ceased in mature neurons, and only acentrosomal microtubule nucleation is visible. Intriguingly, in these mature neurons, axon growth was unaffected compared to younger neurons with a functional centrosome. Moreover, mature neurons rapidly regenerated an axon when the original axon was lesioned without reactivating the centrosome as a MTOC. Thus, these axons regenerated through acentro-

somal, decentralized microtubule assembly and were not limited by centrosomal microtubule nucleation. My results therefore suggest that axon growth depends on acentrosomal microtubule assembly, at least in the later stages of development.

This finding raised the question whether centrosomal microtubule nucleation is necessary for axon growth in young neurons, in which the centrosome is still active. To answer this question, we destructed the centrosome using a 2-photon laser ablation approach (Maghelli and Tolic-Nørrelykke, 2008) and analyzed axon growth afterwards. Centrosome ablated young neurons showed axon growth patterns and speeds indistinguishable from control neurons, arguing that centrosomal microtubule nucleation is dispensable for axon extension also in young neurons.

However, one could argue that enough microtubules were already present in the centrosome-ablated young neurons or in the axotomized mature neurons to support extension of the growing axon. Several arguments speak against this assumption. The microtubule regrowth experiments in the centrosome-ablated neurons showed that these cells were still able to nucleate new microtubules without a centrosome. The same is true for mature neurons that were used for the axotomy experiments. Although I cannot completely exclude that axon extension in the young neurons after centrosome ablation relies on the transport and redistribution of already existing microtubules, this argument can be disproved for the growth of a new axon after axotomy. It was previously shown that after proximal axotomies, about 50% of the neurons formed multiple axons, when the original axon had been cut closer than 35 μm to the cell body (Gomis-Ruth et al., 2008). These new axons reach a total length of more than 5 mm per neuron, which is a length for which the existing microtubules would not be sufficient (Baas and Ahmad, 1993). Hence, my data do not support the hypothesis that only microtubules already present in the short axon stump could enable

long-distance regeneration. This is further supported by the fact that axon growth is accompanied by an increase of microtubule polymer number (Yu and Baas, 1994). As the regeneration occurs without centrosomal microtubule nucleation, the new microtubules have to form in an acentrosomal manner.

Taken together, my data show that axon growth occurs independently of centrosomal microtubule nucleation. In contrast to the prevailing view that the centrosome is the primary source of neuronal microtubules (Baas et al., 2005; Higginbotham and Gleeson, 2007; Conde and Caceres, 2009), I found that the generation of new microtubules becomes decentralized. This is an important finding since microtubules shape the sophisticated morphology of neurons, which is the base for neuronal function. Different mechanisms of decentralized microtubule assembly could therefore be involved in the formation and plasticity of axon branches, dendritic trees and dendritic spines (Jaworski et al., 2009).

My results also put a new perspective on the discussion about the polymer and subunit transport models. Most microtubules in the axon are stationary and only a very small subset of short microtubules is transported (Brown, 2003). Since I showed that axons extend without a functional centrosome, there is also no new supply of new polymers from the cell body. Therefore, it seems that the transport of microtubule polymers from the cell body to the axon might be negligible for axon growth. Alternatively, the transport of short microtubules into the axon might be also used for delivering tubulin subunits, when the short microtubules disassemble in the axon after the transport. Therefore, the subunit transport model seems to describe the actual situation in the growing axon much better than the polymer transport model. Motor proteins together with microtubule bundling proteins, however, might play an important role in establishing the uniform polarity of microtubules in axons. For instance,

the minus-end oriented motor dynein was proposed to sort out disoriented microtubules from the axon causing the uniform microtubule polarity in axons (Zheng et al., 2008). The oriented assembly of microtubules within the axon could be an alternative to form uniform microtubule arrays.

4.2 Acentrosomal microtubule generation during axon growth

The presented data show that a mechanism different than centrosomal microtubule nucleation is responsible for the formation of new microtubules during axon growth. How then are microtubules generated if not at the centrosome? There are several possibilities and most probably it is a combination of some or all that contribute to the establishment of new axonal microtubule arrays that are necessary to elongate the axon. In the following, I will discuss potential mechanisms.

Microtubule severing proteins including katanin and spastin could play a role in the generation of new microtubules (**Figure 4-1**). Inhibition of the microtubule severing protein katanin severely compromises axon growth (Karabay et al., 2004). Considering that axons can extend without centrosomal microtubule nucleation, my data indicate that this effect of katanin inhibition might be based on the formation of many short microtubules in the axon. As described for the formation of the meiotic spindle in *C. elegans*, locally severed microtubules could serve as new seeds for microtubule growth and thereby, increase microtubule polymer number and mass (Roll-Mecak and Vale, 2006). Consistently, katanin is present along the axon, especially close to the growth cone (Yu et al., 2005) and is enriched at the tip of axons and dendrites at later developmental stages, when the centrosome becomes deactivated (Yu et al., 2005). Additionally, short microtubules are found in growth cones and newly developing axonal branches (Kalil et al., 2000). In contrast to katanin, the microtubule

severing protein spastin localizes to axonal branch sites and seems to be important for axon branching as branching is strongly reduced by depleting spastin (Yu et al., 2008). Thus, severing microtubules in the axon could play an important role in re-modeling microtubule arrays, as it could potentially provide new microtubules for polymerization and enable the severed fragments to enter axon branches. In line with this hypothesis, injection of the protease trypsin into axons led to strong microtubule severing and extensive axon branching close to the injection site (Ziv and Spira, 1998).

A question that remains open in general and in particular in neurons is which mechanisms and proteins stabilize the newly formed microtubule minus ends after polymer breakage (Dammermann et al., 2003). The elucidation of these processes should provide more insight into the organization and regulation of acentrosomal microtubule arrays with free minus ends as found in neurons (Schaefer et al., 2002), but also in many other cells like in the lamellae of migrating epithelial cells (Waterman-Storer and Salmon, 1997; Gupton et al., 2002). As I found γ-tubulin in the growing axon, it could be a key candidate for minus-end stabilization. In epithelial cells for example, ninein and nezha are known to organize and anchor microtubules in an acentrosomal array (Dammermann et al., 2003; Lechler and Fuchs, 2007; Meng et al., 2008). In fact, ninein was found to localize to dendrites during neuronal development (Ohama and Hayashi, 2009), and could therefore stabilize the minus ends of dendritic microtubules.

Another possibility of generating new microtubules is acentrosomal nucleation within the growing axon. I found that γ-tubulin becomes depleted from the centrosome over time, but was present in axons of mature neurons. Localized in the axon, γ-tubulin could serve as a local microtubule nucleator (**Figure 4-1**). However, it is still

unclear how acentrosomal nucleation in axons would be organized on a molecular level. For some degree, the observed regrowth might be also caused by spontaneous self-assembly due to the high tubulin concentrations after depolymerization, as it is also seen in vitro (Johnson and Borisy, 1977). Nevertheless, acentrosomal micro-tubule nucleation by γ-tubulin has been found in many organisms from fission yeast and plant cells up to differentiated mammalian cells (Bartolini and Gundersen, 2006; Luders and Stearns, 2007).

In plant cells, for example, microtubules are present in a well organized array at the cell cortex, despite the absence of a MTOC (Wasteneys and Ambrose, 2009). Cytosolic γ-tubulin binds to existing microtubules and nucleates new microtubules as branches analog to the Arp2/3 complex in actin nucleation (Murata et al., 2005). A similar phenomenon was observed in interphase cells of fission yeast, where γ-tubulin complexes are transported along existing microtubules. During the transport, these complexes nucleate microtubules in an anti-parallel manner (Janson et al., 2005). Acentrosomal nucleation is also found in mitotic spindles of human cells. Analog to the fission yeast interphase array, new microtubules are nucleated from existing spin-dle microtubules by γ-tubulin/augmin complexes (Uehara et al., 2009), which seems to be a general mechanism for spindle assembly (Goshima and Kimura, 2010). Addi-tionally, nucleation of spindle microtubules also takes place near chromatins, inde-pendently of the centrosome (Gadde and Heald, 2004). Recently, it was also shown that the +TIP CLASP in concert with γ-tubulin nucleates acentrosomal microtubules at the trans-Golgi-network (Efimov et al., 2007).

As my data suggested for neurons, many different cell types feature different mechanisms to nucleate new microtubules independent of a functional centrosome (Bartolini and Gundersen, 2006; Luders and Stearns, 2007). These mechanisms are

important and, intriguingly, they take over after removal of the centrosome by laser ablation in mammalian fibroblasts (Khodjakov et al., 2000), or in plant cells and animal oocytes that naturally lack centrosomes (Szollosi et al., 1972; Dumont et al., 2007; Wasteneys and Ambrose, 2009).
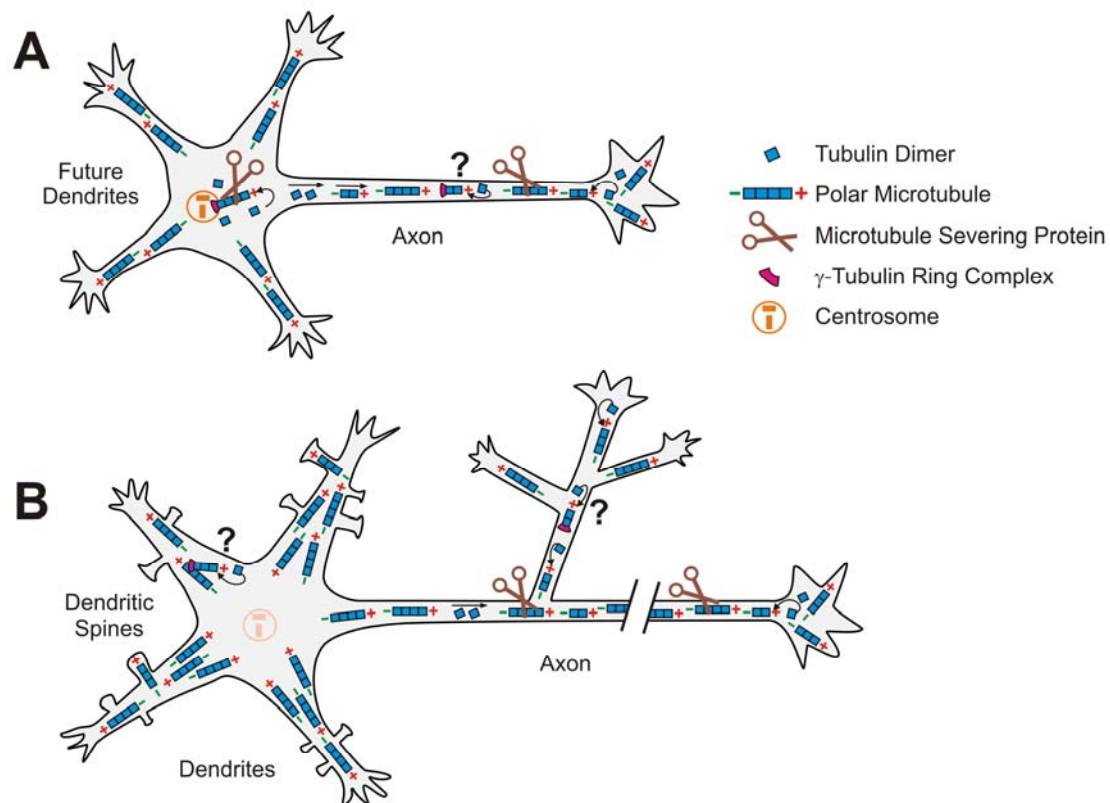
Figure 4-1: Decentralization - generation of microtubules during neuronal development.

(A) During axon specification, microtubules are uniformly polar in all processes, with their plus-end distal to the cell body. Microtubules are nucleated at the centrosome and released by the microtubule severing protein katanin. Short microtubules are transported within the axon, but also tubulin dimers are transported into the axon for microtubule assembly. Whether new microtubules are nucleated in the growing axon, remains speculative. However, new microtubules are formed by the severing of existing microtubules.

(B) In later stages of development, microtubules are uniformly oriented with their plus-end distal in the axon and in the distal dendrite. In the proximal dendrites, microtubules are oriented in both directions with either the plus- or minus-end distal. Moreover, microtubules also invade dendritic spines. During development, the centrosome loses its ability to nucleate microtubules and acentrosomal microtubule assembly takes over. New microtubule fragments are formed through severing by katanin and spastin. Furthermore, acentrosomal microtubule nucleation could play a role in axon growth and branching. Another speculation is that the bipolar microtubule arrays in proximal dendrites are established by microtubule nucleation on existing microtubules.

4.3 Establishment of a distinct microtubule array in dendrites

In addition to investigating the role of microtubules in axon growth, my data also have an implication for the establishment of microtubule arrays in dendrites. In contrast to axons, where microtubules are uniformly oriented with the plus-end distal, dendritic microtubules are oriented in both directions in the proximal part of the dendrite (Baas et al., 1988; Stepanova et al., 2003). Recently, it was shown that bidirectional dynein-driven transport on bipolar microtubules in dendrites provides a potential mechanism for selective transport into dendrites (Kapitein et al., 2010).

Until now, it was proposed that this bipolar array is established by transporting microtubule polymers either with their plus- or minus-end distally into the dendrite through different motors (Baas, 1999). In this work, I show that the centrosome becomes disabled in cultured hippocampal neurons after 4 to 5 DIV, the time when dendrites start to grow and develop their morphological characteristics including the mixed polarity of microtubules. Therefore, my data indicate that acentrosomal microtubule assembly may also be involved in the establishment of the bipolar microtubule arrays of dendrites, as the polymer transport model would require new polymers from a functional centrosome. Since the centrosome ceases microtubule nucleation during development, different mechanisms have to take over to generate the distinct microtubule array of dendrites.

A potential mechanism in dendrites may be that bipolar microtubule arrays are established by acentrosomal microtubule nucleation through γ-tubulin on existing microtubules (**Figure 4-1B**). As explained above, this mechanism functions for the generation of bipolar microtubule arrays in fission yeast (Janson et al., 2005), in the mitotic spindle (Goshima and Kimura, 2010), and for the generation of cortical microtubules in plant cells (Murata et al., 2005). Moreover, it was shown in fission

yeast, that cells can dynamically organize the acentrosomal nucleated microtubules into bipolar arrays by combining motor and bundling proteins (Janson et al., 2007). Consistent with this idea, crosslinkers like MAP-2 or NuMa (Ferhat et al., 1998) and motors like CHO1/MKLP1 or Eg5 (Ferhat et al., 1998; Ferhat et al., 1998) are also present in dendrites and could similarly contribute to establish these networks. In line with this hypothesis, the depletion of the crosslinker MAP-2 or the motor CHO1/MKLP1 severely disturbs dendritic morphogenesis (Yu et al., 2000; Harada et al., 2002). The axonal exclusion of these proteins may also explain why only in dendrites microtubules are oriented with a mixed polarity.

Furthermore, it was reported that centrosomal proteins relocalize from the centrosome into dendrites during neuronal development, which might allow local microtubule nucleation (Ferreira et al., 1993; Ohama and Hayashi, 2009). As mentioned above, one place that enables acentrosomal microtubule nucleation is the membrane of the Golgi apparatus (Efimov et al., 2007). Golgi outposts are located in dendrites and are necessary for the branching and development of dendrites (Horton and Ehlers, 2003; Horton et al., 2005; Ye et al., 2007). Whether acentrosomal microtubule nucleation at these Golgi outposts plays a role for dendritic development and the generation of the bipolar microtubule array remains to be determined.

In summary, it is still unclear how a minor neurite develops into a complex dendrite with all its branches and spines. The bipolar microtubule arrays in dendrites are necessary for dendritic morphology and trafficking (Sharp et al., 1996; Kapitein et al., 2010). My data indicate that the dendritic microtubules are established in an acentrosomal manner. Further analysis of how the dendritic microtubule arrays are established will help to understand dendritic development.

4.4 Decentralization as a mechanism for cell differentiation

The centrosome is an important organelle during the cell cycle. It is necessary for cell cycle progression, it is an important signaling hub and it forms the base of the primary cilium (Doxsey, 2001). Recently, it was also shown that the centrosome plays an important role in neurogenesis, specifying cell fate during asymmetric cell division of neuronal progenitors (Wang et al., 2009).

Here, I have found that the centrosome loses its function as a microtubule organizing center during neuronal development and becomes dispensable for axon extension and regeneration. Parallel to the loss of centrosomal nucleation activity of neurons, I found γ-tubulin relocalizing from the centrosome to the axons of differentiated neurons. In fact, this loss of γ-tubulin from the centrosome appears to contribute to the neuronal differentiation process in general, as it is found also in other CNS neurons including cortical and thalamic neurons (Leask et al., 1997). Furthermore, also other components of the pericentriolar material (PCM) redistribute from the centrosome to dendrites in mouse CNS neurons (Ferreira et al., 1993; Ohama and Hayashi, 2009).

These observations raise the question why the centrosome becomes deactivated during neuronal development, while it is necessary for cell cycle regulation and neurogenesis. There are probably two main reasons. First, the postmitotic neurons have left the cell cycle and therefore key regulators of the cell cycle have to be reorganized. Second, as neuronal differentiation requires sophisticated architectural changes, this remodeling may be incompatible with a large microtubule network emanating from a focal point. Therefore, deactivation of a focal microtubule organizer and acentrosomal microtubule nucleation may be key features during differentiation of neuronal but also of non-neuronal cells (Bartolini and Gundersen, 2006; Luders and Stearns,

2007). For example, during skeletal muscle differentiation, centrosomal proteins are redistributed from the centrosome to the nuclear membrane and the cytoplasm where they form new sites of microtubule nucleation (Bugnard et al., 2005). Similarly, microtubule regrowth from specific sites is also observed at the plasma membrane of polarized epithelia (Reilein et al., 2005), melanosomes in pigment cells (Malikov et al., 2004) as well as in osteoblasts (Mulari et al., 2003) and epithelial Sertoli cells (Vogl et al., 1995). Similar to my data, the decentralization of microtubule assembly comes along with acentrosomal distribution of PCM components, including pericentrin, ninein or γ-tubulin. Taken together, dismantling the centrosome and decentralizing microtubule generation, as it is observed in other differentiating cells, may be essential to enable late neuronal differentiation, including axon branching, dendrite formation and spine generation (Jaworski et al., 2009).

How the observed depletion of centrosomal γ-tubulin and the associated inactivation of the centrosome is regulated remains so far unknown. During the cell cycle the amount of PCM and centrosome function are tightly controlled by cell cycle proteins (Khodjakov and Rieder, 1999; Blagden and Glover, 2003). In the last years, the concept evolved that many of these cell cycle proteins have also essential functions in post-mitotic neurons (Becker and Bonni, 2005; Herrup and Yang, 2007). Simultaneously, it was proposed that after their last mitosis, postmitotic neurons must constantly suppress their cell cycle to avoid cell death (Herrup and Yang, 2007). Proteins that are controlling the mitotic exit including the anaphase promoting complex/cyclosome (APC/C) (Sullivan and Morgan, 2007) are active in postmitotic neurons and play a crucial role in the activation of neuron-specific gene expression, axon growth and dendrite development (Yang et al., 2010). As the same proteins regulate fluctuation of γ-tubulin levels at the centrosome during mitosis and cell cycle exit,

similar pathways could be involved in the deactivation of the neuronal centrosome as well as cell cycle suppression. Interestingly, it was recently found that the centrosomes of newborn neurons and their progenitor cells differ in their composition and that this difference is required for their neuronal cell fate (Wang et al., 2009). Thus, dismantling the centrosome, as one of the key regulators of the cell cycle (Doxsey et al., 2005), may be essential to maintain the neuronal cell cycle arrest and to avoid neurodegeneration.

Although I found that the PCM became disprupted and the centrosome lost its microtubule nucleating activity, the centrioles remained in the neuron. As the electron microscopy images indicate, one centriole, the mother centriole, changed its morphology during development and formed the basal body, the base for the primary cilium. The primary cilium is a cellular protrusion that develops in the interphase/G_0 phase of many cells including neurons (Pedersen et al., 2008). The formation of the primary cilium is regarded as one of the most important functions of the centrosome: it is necessary for survival (Basto et al., 2006) and its dysfunction underlies various human disorders (ciliopathies), including mental retardation or possibly even autism and schizophrenia (Fliegauf et al., 2007; Lancaster and Gleeson, 2009). The primary cilium is seen as a complex signaling hub sensing its environment and is involved in inter- and intracellular signaling, including Sonic hedgehog (Shh) and Wingless (Wnt) pathways (Singla and Reiter, 2006).

As it is now known that most CNS neurons contain primary cilia, *in vivo* as well as *in vitro* (Berbari et al., 2007; Bishop et al., 2007), it could be that the observed loss of PCM and microtubule nucleating activity at the centrosome are necessary requirements for the proper formation and function of the primary cilium in neurons. The exact function, however, of neuronal primary cilia is still unknown. A recent

study showed that the somatostatin receptor type 3, which is only found at the primary cilium, is critical for recognition memory (Einstein et al., 2010). Therefore, it seems that the neuronal cilium represents a novel nonsynaptic compartment involved in a special form of learning and memory. Furthermore, the primary cilium seems also to be involved in axonal and dendritic development. For instance, defects in axon guidance were observed in ciliopathies (Lee and Gleeson, 2009). Whether these defects are linked to disturbed Wnt-APC signaling, which is involved in axon guidance and occurs at the primary cilium, remains speculative at the moment (Purro et al., 2008). Additionally, the histone deacetylase HDAC6 that regulates primary cilium morphogenesis (Pugacheva et al., 2007) controls also ubiquitin signaling at the centrosome, a pathway that drives dendrite differentiation (Kim et al., 2009).

Taken together, the primary cilium seems to be an important signaling hub for neuronal development as well as neuronal function. Therefore, the occurring changes at the centrosome during neuronal development might also play a role for proper cilium formation and function in neurons.

4.5 The centrosome and neuronal polarization

In many cell types, the centrosome is involved int the establishment of cell polarity. It can determine cell polarity either by organizing the microtubule network and the Golgi apparatus in an asymmetric manner or by its function as a signaling hub (Cowan and Hyman, 2004; Bornens, 2008). Some studies also suggested that the position of the centrosome determines the site of axon outgrowth and thus, neuronal polarity (Zmuda and Rivas, 1998; de Anda et al., 2005). Other studies, however, did not find such a correlation (Sharp et al., 1982; Dotti and Banker, 1991; Zolessi et al., 2006). Furthermore, it was proposed that the observed correlation of centrosome po-

sition and axon outgrowth might have only been an epiphenomenon of the polarization itself (Arimura and Kaibuchi, 2007). Taken together, the role of the centrosome and centrosomal microtubule nucleation in neuronal polarization is still controversial (Arimura and Kaibuchi, 2007; Higginbotham and Gleeson, 2007; Witte and Bradke, 2008).

As I focused on the extension of already initiated axons and the regeneration of severed axons, my work can only provide indications about the role of the centrosome in initial neuronal polarization including axon initiation. I found that after proximal axotomies, new axons formed from dendrites in mature neurons, in which the centrosome had already lost its ability to nucleate microtubules. These results show that a new axon can initiate and grow independently of centrosomal microtubule organization. Therefore, this formation of new axons suggests that the centrosome might be also dispensable for axon initiation. Following the position of the centrosome after axotomy and during the subsequent regeneration may give further insight in this process, whether other functions of the centrosome might determine the site of axon outgrowth. Nevertheless, a study with flies that lose their centrosomes during development further substantiates the view that the centrosome is not necessary for axon initiation. The neuronal organization of these flies without centrosomes was unperturbed and the direction of axon outgrowth was not affected (Basto et al., 2006). However, when precisely these flies lose their centrosomes during development is under debate, since they still have functional centrosomes during early embryogenesis (Gonzalez, 2008).

In conclusion, next to axon extension, also axon initiation might be possible without centrosomal microtubule nucleation. Further ablation studies have to prove whether centrosomal microtubule nucleation is necessary for the initial formation of

the axon. These studies might then elucidate the causal relation between the centrosome (position) and axon formation both *in vitro* and *in vivo*.

4.6 Implications for axonal regeneration after injury

My results also have implications for the regenerative behavior of neurons in the absence of a microtubule-nucleating centrosome. If microtubules would only assemble at the centrosome, it would be impossible to generate new microtubules in lesioned mature neurons. Therefore, all approaches to induce regeneration of injured neurons would be doomed to failure. This apparently is not the case as regeneration also occurs in mature neurons (Gomis-Ruth et al., 2008). In my thesis, I could now show that axons regenerate through acentrosomal microtubule assembly and are not limited by centrosomal microtubule nucleation. Importantly, it was shown that inhibitory components of the central nervous system myelin inhibit local microtubule assembly in axons (Mimura et al., 2006). Together with my findings, this implies that affecting local microtubule assembly may be beneficial for successful nerve regeneration after injury. As modest stabilization of microtubules by Taxol helps injured axons to regenerate, it indicates that increasing decentralized microtubule assembly is a promising path to improve axonal regeneration after spinal cord injury (Erturk et al., 2007).

4.7 Concluding remarks

In summary, here I present the direct evidence that centrosomal microtubule nucleation is not necessary for axonal growth. These results reopen a discussion that was stuck for many years, namely how the microtubule arrays of axons and dendrites are formed. These microtubule arrays are required for neuronal polarization, neuronal

morphology and the correct trafficking of dendritic and axonal proteins (Conde and Caceres, 2009; Kapitein et al., 2010) and thus, are key for neuronal function. In conclusion, my data suggest that acentrosomal microtubule generation plays a key role during axon growth and neuronal differentiation. Future studies will need to reveal the molecular mechanisms regulating this process. It will be exciting to see whether the molecules that are involved in acentrosomal microtubule nucleation in other species and cell types are evolutionary conserved and also regulate acentrosomal microtubule nucleation in neurons. Furthermore, it remains unclear how these changes in microtubule generation from centrosomal to acentrosomal nucleation are organized. To this end, the use of cryo electron microscopy and tomography might help to elucidate how new microtubules are generated within axons and dendrites (Hoenger and McIntosh, 2009). Potential nucleation events and sites might be visible as well as the particular organization of the microtubule arrays. Additionally, the regulation of the cell cycle exit in postmitotic neurons as well as the formation and function of the primary cilium in neurons will be interesting topics of future research.

5 **Materials and Methods**

5.1 Materials

5.1.1 Chemicals

Chemicals were analytical grade or the best commercially available.

Table 5-1: Chemicals

Chemicals	Supplier
α-Chymotrypsine	Sigma
Acetone	Merck
Agarose	Biomol
Ammonium Persulfate (APS)	Sigma
Ammonium chloride	Merck
Apo-transferrin, human	Sigma
Aprotinine	USB Corporation
β-Mercaptoethanol	Roth
Borax (Sodium borat)	Sigma
Boric acid	Merck
Bovine serum albuminum, powder	Sigma
Calcium Chloride (CaCl$_2$)	Merck
DMRIEC reagent	Invitrogen
Dimethyl sulfoxide (DMSO)	Roth
EDTA (ethylene diamine tetraacetic acid)	Sigma
EGTA (ethylene glycol tetraacetic acid)	Sigma
Ethanol absolute	Sigma
Fetal bovine serum	Invitrogen
Fish gelatine	Sigma
Gelmount mounting medium	Sigma
D(+)Glucose monohydrate	Merck
L-Glutamine 200mM	Invitrogen
Glutaraldehyde (25% solution)	Serva
Glycerol	Roth
Hank's balanced salt solution (HBSS) with Calcium and Magnesium	Invitrogen
HEPES (N-2-Hydroxyethylpiperazine-N'-2-ethane sulfonic acid)	Biomol
Horse serum	Sigma

Hydrochloric acid (HCl; 1M)	Merck
Insulin	Sigma
Laminin (0.5mg/mL)	Roche
Magnesium chloride hexahydrate (MgCl$_2$*6H$_2$O)	Merck
Methanol	Merck
Minimal essential Medium (MEM) 10x	Invitrogen
MEM essential amino acids 50x	Invitrogen
MEM non-essential amino acids 100x	Invitrogen
Milk powder	Heirler Cenovis
Nitric acid (HNO$_3$; ≥65%)	Roth
Nocodazole	Sigma
Ovalbumin (albumin from chicken egg white)	Sigma
Paraffin	Merck
Paraformaldehyde	Merck
PIPES (1,4-Piperazinediethanesulfonic acid)	Sigma
Poly-L-lysine hydrobromide	Sigma
Potassium Chloride (KCl)	Merck
Potassium dihydrogen phosphate (KH$_2$PO$_4$)	Roth
Progesteron	Sigma
Putrescine-dihydrochloride	Sigma
Pyruvate (pyruvic acid)	Sigma
Sodium dodecylsulfate (SDS)	Merck
Disodium hydrogen phosphate (Na$_2$HPO$_4$)	Roth
Selenium-dioxide	Sigma
Sodium Chloride (NaCl)	Merck
Sodiumhydrogencarbonate (NaHCO3)	Merck
Sodium hydroxide	Merck
Sucrose	Merck
TEMED	Sigma
Tris(hydroxymethyl)-aminomethane	Merck
Tris base	Sigma
Triton X(TX)-100	Roth
Trypsin-EDTA (1x, 0.05 % Trypsin, 0.53 mM EDTA*4Na)	Invitrogen
Tryptone	Roth
Tween 20 (Polyoxyethylene (20) sorbitan monolaurate)	Sigma
Yeast extract	Roth

5.1.2 Buffers and solutions

50 mM ammonium chloride: 1.34g ammoniumchloride in 500 mL PBS.

2x BES-buffered saline (BBS), pH 6.96: 50 mM BES (N,N-bis[2-hydroxyethyl]-2-aminoethanesulfonic acid), 280 mM NaCl and 1.5 mM $Na_2HPO_4*2H_2O$ in H_2O at pH 6.96. Solution is sterile filtered and stored at -20°C.

Blocking Solution: 2% Fetal bovine serum, 2% BSA and 0.2% fish gelatine in H2O.

Borate Buffer: 1,24 g Boric acid (Merck, Germany) and 1,90 g Borax (Sodium borat) in 400 mL H_2O at pH 8.5.

0.1 M Calcium Chloride ($CaCl_2$): 1.11 g $CaCl_2$ in 100 mL H2O. Solution is sterile filtered.

HNE buffer: 40 mM HEPES, 138.5 mM NaCl, 0.1 mM EGTA; pH 7.4; osmol. 300-310

1 M Hepes: 23,8 g Hepes in 100 ml H2O at pH 7.25. Solution is autoclaved.

7 mM Hepes buffered Hank`s Balanced Salt Solution (HBSS): 3.5 ml 1M Hepes in 500 ml HBSS (Gibco, USA). Solution is sterile filtered.

5x Laemmli buffer: 250 mM Tris/HCl (pH 6.8), 1 M β-Mercaptoethanol, 10% (w/v) SDS, 30% (v/v) Glycerol in H_2O. If used as a sample buffer for SDS-PAGE, bromophenol blue was added.

Laminin Solution: 0.5mg/mL Laminin stock solution is diluted in warm N2-Medium just before coating.

LB(Luria-Bertani)-Medium: 10 g tryptone, 5 g yeast extract and 10 g NaCl in 1 L H_2O at pH 7.0. Medium is sterilized by autoclaving. If necessary, antibiotics were added after sterilizing (Kanamycin: 50mg/mL or Ampicilin: 100 mg/mL). For bacterial plates, 1.5% Bacto-Agar was added to the medium before autoclaving.

MEM-HS: 10 mL heat-inactivated horse serum in 90mL minimal essential medium (MEM).

5% Milk/PBS-Tween: 12.5 g dry milk in 250 mL PBS-Tween.

Neuronal Growth medium / N2 Medium: 50 mL 10x N2 Supplement and 100 mg ovalbumin in 450 ml N-MEM. Medium is sterile filtered.

10x N2 Supplement: 1 mL 5 mg/mL insulin, 1 mL 20 µM progesterone, 1 mL 100mM putrescine, 1 mL seleniumdioxide, 100 mg transferrin in 96 mL N-MEM. Medium is sterile filtered

N-MEM: 50 mL 10x MEM , 5 mL 1.1% pyruvic acid, 5mL 200 mM glutamine, 15 mL 20% glucose, 20 mL 5.5.% NaHCO3 in 405 mL H2O. Medium is sterile filtered.

Paraformaldehyde (16%): 16 g paraformaldehyde and 16 g Sucrose in 100 ml PBS at pH 7.4. Solution is sterile filtered. Dilutions are made from this stock in PBS.

PBS-Tween (0.1%): 0.5 mL Tween 20 in 500 mL PBS.

PHEM Buffer: 60mM PIPES, 25mM HEPES, 5mM EGTA and 1mM $MgCl_2$ in H_2O. For fixation 4% paraformaldehyde (from 16% stock), 0.25% glutaralaldehyde and 0.1% Triton X-100 is added.

Phosphate buffered saline (PBS): 0.2g KCl, 0.2g KH_2PO_4, 1.15g Na_2HPO_4 and 8g NaCl in 1L H_2O at pH 7.4.

Poly-L-lysine solution: 1 mg/mL Poly-L-lysine hydrobromide in borate buffer. Solution is sterile filtered. Glass cover slips are incubated with solution overnight and then washed three times with sterile H_2O.

SDS-PAGE Running Buffer: 1.5 g TrisHCl, 7.2 g Glycine and 0.1% SDS (w/v) in 1 L H2O.

Stripping buffer: 100 mM β-Mercaptoethanol, 2% (w/v) SDS , 62.5 mM TrisHcl (pH 6.7) in H_2O.

0.1% Triton X-100: 0.1% (v/v) Triton X-100 in PBS.

Trypsin: 1 mL 1M Hepes in 99mL Trysin-EDTA-Solution (Gibco, USA)

Transfer Buffer for western blotting: 3.2 g TrisHCl, 14,4 g Glycine and 100 mL Methanol in 900 mL H2O.

5.1.3 Commercial kits

Table 5-2: Commercial kits

Commercial Kit	Supplier
EndoFree Plasmid Maxi Kit	Quiagen
Neurite Outgrowth Assay Plus Kit (3 µm)	Millipore
Rat Neuron Nucleofector Kit	Amaxa

5.1.4 Equipment

Table 5-3: Equipment

Device	Model	Supplier
Primary Cell Culture		
Incubator (with CO_2)	HERAcell240	Kendro
Dissection stereomicroscope	Stemi SV6	Zeiss
Forceps	Straight forceps Dumon #5, 11cm, Biological tips	Fine Science Tools
	Curved forceps Dumont #7, 11.5cm, Biological tips	Fine Science Tools
Laminar air flow hoods	HERAguard HPH15	Kendro
(for dissection)	EdgeGARD Hood EG-3252	The Baker Company
Scissors	Vannas-Tübingen spring scissors, 8.5cm, straight tips	Fine Science Tools
	Hardened fine iris scissors, 11cm, straight tips	
	Extra fine scissors, model "Bonn", 8.5cm, straight tips	
Electroporation	Nucleofector II	Amaxa
Epifluorescence Microscope		
CCD Camera	4912-5000 or 4912-5100	Cohu
Camera control panel	C 2741	Hamamatsu
Image acquisition hardware for PC	LG3 image grabber	Scion Corp.
Inverted epifluorescence microscopes	Axiovert 135TV	Zeiss
	AxioObserver.D1	Zeiss
Confocal Microscope	SP2 confocal microscope	Leica
Spinning Disc Confocal Microscope		
	IX71 spinning disc confocal inverted microscope	Olympus
Scan head		Yokogawa
CCD Camera	CSU10	Andor
	iXon EM+ DU-897 BV back illuminated EMCCD	
Custom-Built Two Photon Laser Ablation Setup	Custom built setup (described in Maghelli and Tolic-Norrelykke, 2008)	
Laser	Single Ti:Sa femtosecond pulsed laser	Chameleon XR, Coherent
Total-Internal Reflection (TIRF) Microscope	Eclipse TE2000E	Nikon
CCD Cameras	Coolsnap and QuantEM EMCCD	Roper Scientific
Western blotting		
Western blot Electrophoresis Cell	XCell Surelock	Invitrogen
Spectrophotometer	Ultropspec 3000	Amersham Biosciences

5.1.5 Consumables

Table 5-4: Consumables

Device	Model	Supplier
Filtration Systems		
Bottle top filters	Steritop bottle top filter 250 ml/500 ml (0.22 µm)	Millipore
Filtration systems	Stericup filter unit 250 ml/500 ml (0.22 µm)	Millipore
	Filter System 250 ml/500 ml (0.22 µm)	Corning Inc.
Syringe driven filter units	Millex-GV, 0.22 µm (sterilization) or MillexR-HA, 0.45 µm (clarification)	Millipore
Microscopy and immunohisto-chemistry		
Cover glasses for microscopy	No. 1, ø 15 mm	Marienfeld
Cover glasses with relocation grid	Custom-made glass coverslips with 4x4 mm relocation grid	Laserzentrum Hannover
Glass bottom dishes (for live-cell imaging)	3 cm (#P35G-1.5-20-C; 20 mm hole size)	MatTek
Microscope slides	76x26 mm, with frosted end	Menzel-Gläser
Tissue culture		
Tissue culture flasks	Nunclon Delta surface, 75 cm^2	Nunc
Tissue culture plastic dishes	Nunclon, ø 3 cm or 6 cm	Nunc
	Falcon , ø 10 cm	Becton and Dickinson
Western blotting		
Western blot gel cassettes	Gel cassettes, 1.5 mm	Invitrogen
Semi-dry transfer system	Costum-made	Costum-made
Membrane for protein transfer	PVDF membrane, Hybond-P	GE Healthcare
Western blotting Detection System	ECL Plus Detection System	GE Healthcare
Molecular Weight Marker	Full range rainbow marker; range from 12K-225KDa	GE Healthcare

5.1.6 Antibodies

Table 5-5: Primary antibodies for immunofluorescence (IF) and western blotting (WB)

Antigen	Host	Dilution	Supplier
α-Tubulin (clone B-5-1-2)	mouse	IF: 1 : 20.000 WB: 1 : 50.000	Sigma
γ-Tubulin (clone GTU-88)	mouse	IF: 1 : 3000 WB: 1 : 10.000	Sigma
Centrin (clone 20H5)	mouse	IF: 1 : 10.000	gift of Dr. J. Salisbury
CPAP	rabbit	IF: 1 : 3000 WB: 1 : 10.000	gift of Dr. E. Nigg
GAPDH	mouse	WB: 1 : 3000	Abcam
GFP	mouse	IF: 1 : 2000	RDI
Histone H3	rabbit	WB: 1 : 2000	Cell Signaling
NEDD1	mouse	IF: 1 : 3000 WB: 1 : 10.000	Abnova
Pericentrin	rabbit	IF: 1 : 3000	Millipore

Table 5-6: Secondary antibodies

Antigen	Host	Conjugate
mouse IgG	donkey	Alexa Flour 555
	goat	Alexa Flour 555
	goat	Alexa Flour 568
	goat	Alexa Flour 488
	goat	HRP
rabbit IgG	goat	Alexa Flour 555
	goat	Alexa Flour 568
	donkey	Alexa Flour 488
	goat	HRP

All secondary antibodies for immunofluorescence were purchased from Invitrogen and diluted 1:400 in 10% blocking solution. Horseradish Peroxidase (HRP)-conjugated antibodies for western blotting were purchased from Sigma and diluted 1:5000 (mouse) and 1:10000 (rabbit) in 5% milk PBS-Tween.

5.1.7 Plasmids

Table 5-7: Plasmids

Construct	Plasmid	Resistance	Reference
GFP	pEGFP-N2	Kanamycin	Clontech
GFP-γ-tubulin	pCDNA3	Ampicilin	Khodjakov and Rieder., 1999
GFP-Centrin2	pEGFP-C1	Kanamycin	
GFP-EB3	pEGFP-N1	Kanamycin	Stepanova et al., 2003

pEGFP-C1 centrin2 was kindly provided by M. Distel and R. Köster (Helmholtz Center, Neuherberg, Germany). pcDNA3 γ-tubulin-GFP was a gift from A. Khodjakov (Wadsworth Center, Albany, NY, USA). pEGFP-N1-EB3 was generously provided by A. Akhmanova (Erasmus Medical Center, Rotterdam, Netherlands). Plasmids were propagated and amplified in DH5α E. coli bacteria.

5.2 Methods

5.2.1 Neuronal cell culture

5.2.1.1 Overview

The hippocampal culture system is based on coculturing astrocytes and neurons, although not on the same plane. The astrocytes secrete growth factors that are essential for the long-term survival of the neurons (Banker, 1980). First, the astrocytes are isolated from embryonic brain, plated and cultured until they reach around 20% confluency. Then the hippocampal neurons are isolated and plated onto coverslips. After the cells have attached, the coverslips are transferred to the dishes with astrocytes. With this coculture system, neurons can be cultured for at least four weeks.

5.2.1.2 Preparation of glass coverslips

Glass coverslips were incubated in nitric acid (≥65%) overnight, thoroughly washed in sterile, distilled water, baked at 220°C for 6 h. Paraffin dots were attached to the sterile coverlips and then coated with poly-L-lysine solution overnight at room temperature. After thorough washing with sterile, distilled water, the coverslips were incubated with MEM-HS overnight. For experiments in which it was necessary to relocate the same neuron, custom-made coverslips with a laser engraved grid (Laserzentrum Hannover) were used.

5.2.1.3 Preparation of rat hippocampal neurons

Primary hippocampal neurons were derived from rat embryos at embryonic day 17 or 18 (E17/18). The neurons were cultured following published protocols (de Hoop et al., 1997; Kaech and Banker, 2006). In brief, the hippocampi of E17/18 rats were dissected, trypsinized, and physically dissociated. The cells were then washed in Hepes buffered HBSS, and 100,000 cells were plated onto poly-L-lysine-treated glass coverslips in 6 cm petri dishes containing MEM-HS. The cells were kept in 5% CO_2

at 36.5 °C. After 12 h, the coverslips were transferred to a 6 cm dish containing astrocytes in N2-Medium. For protein extractions, 6 cm petri dishes were incubated with poly-L-lysine overnight and washed three times with H_2O. Then the dishes were incubated overnight with MEM-HS, and 300,000 cells were plated in N2-Medium.

5.2.1.4 Preparation of mouse hippocampal neurons with single GFP labelled neurons

To trace, axotomize and follow regeneration of single mature neurons integrated in complex neuronal networks, dissociated hippocampal neurons from wildtype (WT) mice were mixed with a very low proportion (1-3%) of GFP positive hippocampal neurons from genetically labeled mice. These neurons express enhanced green fluorescent protein (EGFP) under control of the ubiquitously active CAG promoter (Ikawa et al., 1995; Okabe et al., 1997), a hybrid promoter composed of the cytomegalovirus (CMV) enhancer, a fragment of the chicken β-actin promoter and rabbit β-globin exons (Niwa et al., 1991).

5.2.1.5 Preparation of glia cultures

Meninges was removed from cerebral hemispheres of E17/E18 rat or mouse embryos (~4-5 hemispheres for one culture flask or ~4 hemispheres for ~15 dishes for use during the next days). The hemispheres could be taken during the hippocampus dissection and stored in HBSS during the preparation of the hippocampal neurons. The hemispheres were then trypsinated and dissociated principally in the same way as the hippocampal neurons as described (de Hoop et al., 1997; Kaech and Banker, 2006). A volume corresponding to 4-5 hemispheres was then added to untreated tissue culture flasks containing 15-20 mL pre-warmed MEM-HS. The next day the medium was changed completely to remove cell debris. When the cells reached about 70-80% confluency (7-10 days), they were split in new flasks (1:3) or plated in 6 cm dishes (1 flask in 40 dishes). The astrocyte cultures could be passaged up to three times.

5.2.2 Transfection of hippocampal neurons

5.2.2.1 Nucleofection

Neurons were transfected before plating with the Amaxa Nucleofector system (Amaxa, USA). Directly after isolation, 3 μg of pEGFP-C1-centrin2 plasmid DNA was used for electroporation of 500,000 neurons according to the manufacturer's protocol. Subsequently cells were plated in MEM-HS and further cultured as described above.

5.2.2.2 Calcium-phosphate transfection

Differentiated neurons were transfected at 8 DIV using Calcium-phosphate transfection, as previously described (Goetze et al., 2004). Coverslips with differentiated neurons were transferred in the wells of a 12-well plate with 1 mL Glia-conditioned N2-medium in each well. 3 μg of Plasmid DNA were slowly added to freshly diluted 250 mM $CaCl_2$ to a total volume of 25 μL. 2XBBS (25 μL) was added to the DNA/$CaCl_2$ Mix and immediately vortexed for 5 seconds. After 15 minutes incubation, the mix was added dropwise to 1 mL of prewarmed N2-medium with constant vortexing. Then, the medium was removed form the coverslips in the 12-well dish and the transfection mix was added. After 1-1.5 hours, crystals form and the transfection mix was removed. Neurons were washed with HBSS and put back in the glia dish.

5.2.2.3 Semliki Forest virus (SFV)-mediated gene delivery

To express EB3-GFP in both young and differentiated neurons for TIRF microscopy, Semliki Forest virus (SFV)-mediated gene delivery was used as described (Jaworski et al., 2009). The EB3-GFP construct was cloned into the pSFV2 vector according to the manufacturer's instructions (Invitrogen). Constructs were packaged into SFV replicons, using coelectroporation of helper and vector RNA into baby hamster kidney-21 cells using DMRIEC reagent (Invitrogen, 2mg/ml). SFV-replicons were harvested 24 hours post-transfection, filter-sterilized, activated with α-chymotrypsin, and the

reaction was terminated with aprotinine. After concentrating the virus by ultracentrifugation, the pellet was dissolved in HNE buffer. Subsequently, the virus titer was determined by infection of BHK-21 cells with serial dilutions of concentrated virus, followed by fluorescence examination at 18-24 hrs post-infection. Cultured hippocampal neurons were infected at 2 DIV or 14 DIV by the addition of 1 µL (~107 replicons/ml) of SFV infectious replicons to the cultures 4 hours before life cell imaging.

5.2.2.4 Freezing and thawing of transfected neurons

To transfer cells for the ablation experiments in Dresden, neurons were frozen after transfection. Neuronal culture and transfection was performed as described above. Due to the cell death caused by freezing and thawing, the double amount of neurons was used (1 million neurons). Instead of plating, the transfected neurons were incubated in a final volume of ~900 µL (~100 µL cell suspension, 500 µL warm MEM-HS and additional 320 µL warm and equilibrated MEM-HS) in the incubator for 1.5 hours with sporadic shaking. After quickly adding 100 µL DMSO to the cell suspension and immediate mixing, cells were frozen to -80°C in a insulating container with an approximated cooling speed of 1°C per minute. The next day, cells were transferred to liquid nitrogen. The frozen cells were transported to Dresden in liquid nitrogen. Cells were quickly thawed in 37°C warm water and plated in two MEM-HS dishes with coverslips as usual. After two hours, coverslips were flipped into dishes with glia-conditioned N2-medium to remove the remaining DMSO.

5.2.3 Immunocytochemistry

Three different fixation methods were applied. Using paraformaldehyde as fixative, cells were fixed in warm 4% paraformaldehyde for 20 min and washed three times with PBS. After quenching free aldehyde groups in 50 mM ammonium chloride for

10 min and after extraction with 0.1% Triton X-100 for 5 min, cells were again washed three times with PBS. To visualize microtubules without unpolymerized tubulin subunits, cells were simultaneously fixed and permeabilized in PHEM Buffer containing 4% paraformaldehyde, 0.25% glutaraldehyde and 0.1% Triton X-100. After having washed three times with PBS, aldehyde groups were quenched in 50 mM ammonium chloride for 10 min. For the analysis of centrosome components, methanol fixation was used. Cells were fixed in -20 °C cold methanol for 3 min and then rehydrated three times for 5 min in 0.1% Triton X-100. Finally, cells were washed three times with PBS. All fixed neurons were incubated in blocking solution for 60 min at room temperature. Subsequently, cells were incubated with primary antibodies diluted in 10% blocking solution for 60 min. Following wahing with PBS, cells were incubated with secondary antibodies for 30 min. After the staining, the cells were washed with PBS and mounted on objective slides using Gelmount.

5.2.4 Protein extraction

For western blot analysis, three 6 cm Petri dishes with 300,000 cells were washed once with PBS and then lysed in 300 µL 1 x Laemmli buffer without dye. The cell lysate was boiled for 5 min at 95 °C, spun down and again boiled for 5 min at 95 °C. To increase the protein concentration, the proteins were precipitated by 20 °C acetone. Therefore, 1.8 mL 20 °C acetone was added to no more than 400µL of the extract. The sample was kept at least 60 min at 20 °C, spun down, and the pellet was resuspended in 30 µL of 1x Laemmli buffer without dye. The protein concentration was determined by the Bradford assay (Biorad, Germany). The concentrations were adjusted to the same value with 1x Laemmli Buffer.

5.2.5 Axonal and cell soma protein extraction

To prepare axon or cell body fractions, neurites were plated on filter inserts with 3 μm pore size membranes (Neurite growth assay, Milipore). Filters were coated with poly-L-Lysine solution overnight, washed with distilled water. 30 min before plating, the bottom side only of the filter was coated with laminin (50 μg/mL). Then, cells were plated and grown for 8 days according to the manufacturer's instructions. After 8 days, cells were fixed with ice cold methanol. To obtain only axonal extracts, cell bodies were removed by wiping the upper side of the filter with flattened cotton tips following the manufacturer's instructions. To obtain extracts only from cell bodies, axons were removed with a sharp razor blade and cotton tips at the bottom of the filter. Fractions were then lysed using hot SDS sample buffer.

5.2.6 Western blotting

The equivalent amount (around ~30 μg) whole cell lysate of each sample was loaded on a 12 % polyacrylamide gel (6 mL 30 % acrylamide/0.8 % bisacrylamid, 3.75 ml 4x Tris-Cl/SDS (pH 8.8), 5.25 ml H_2O, 50 μl 10 % ammonium persulfate, 10 μl TEMED). As a standard, 10 μL of Prestained Protein Marker, Broad Range (New England BioLabs, USA) was loaded. The gel was run at 200 V with 1 x running buffer. The gel was blotted onto Hybond-P membrane (Amersham, USA) with 150 mA current. Successful blotting was confirmed by Ponceau staining. Blots were then blocked with 5% milk/PBS-Tween for 60 min at room temperature. The primary antibody was applied overnight at 4 °C. Blots were washed 5 times for 10 min with PBS-T and incubated with the secondary antibody for 60 min at room temperature. Blots were washed 5 times for 10 min with PBS-Tween. ECL plus (Amersham, USA) was used according to the manufacturer's instructions. The blot was exposed to an X-ray film and the film was developed. If necessary, the blot was stripped three times for

15 min with stripping buffer at 55 °C and probed again. Antibodies were diluted in 5% milk/PBS-T.

5.2.7 Axotomy

Single mature GFP-expressing neurons from mixed cultures were axotomized as described previously (Gomis-Ruth et al., 2008). The neurons were grown on coverslips with a laser engraved grid (Laserzentrum Hannover). For axotomy, the coverslips were placed in glass-bottom dishes with prewarmed HBSS. The area around the microscope was heated to 35°C. Single labelled neurons were localized using a epifluorescence microscope with a plan-neofluar 25x oil objective. Neurons were imaged in phase contrast and fluorescent light to determine the position of the axon. The axon of the GFP positive neuron was identified by morphology. Pulled glass capillaries with a diameter of few micrometers were used for performing the cuts. The capillary was mounted in the needle holder of a manual micromanipulator and the axon was cut using the micromanipulator. To avoid reconnection of the sectioned axons, the distal part was removed with the capillary. After axotomy, cells were brought back to the incubator. 24 h after axotomy, the neuron was relocalized and axon regeneration was analyzed. Neurons were then either kept for additional 5 days in the incubator or immediately fixed with -20°C methanol to assess centrosomal γ-tubulin. Axotomy was performed with neurons at 8 to 17 DIV.

5.2.8 Centrosome ablation

Ablation of centrosomes was performed using a custom-built two-photon microscope capable of laser ablation (Maghelli and Tolic-Nørrelykke, 2008) with a 63x 1.0 N.A. water dipping objective (W Plan-Apochromat 63x/1.0 VIS-IR, Zeiss). Both two photon imaging and ablations were performed using a single Ti:Sa femtosecond pulsed

laser (Chameleon XR, Coherent), tuned to a wavelength of 880 nm. The laser power, measured at the sample plane, was 4 mW for imaging and around 100 mW during the ablation process. The ablations were performed on a user-defined region of interest (ROI), drawn around the centrosome on a selected plane. The ROI was defined while continuously acquiring a 10 planes stack (500 nm between planes, 50 µs/pixel, 5 s/stack) with a resolution of 40 nm/pixel. Ablation was achieved by scanning the laser at high power over the ROI, for a defined exposure time (typically between 20 ms and 100 ms). The temperature of the sample was kept constant at 35 °C using a Peltier element and controller. Neurons were plated on coverslips with a laser engraved grid (Laserzentrum Hannover) to relocate them for further analysis. Ablation was done in neurons 1.5 to 2DIV after plating. After ablation, cells were either analyzed for centrosome removal or put back in the incubator for subsequent analysis of axon growth. Successful ablation of the centrosome was then confirmed after measuring axon length.

5.2.9 Nocodazole wash-out

First, microtubules were completely depolymerized by nocodazole. A 6.67 mM nocodazole stock in DMSO was used for dilutions. To distribute the nocodazole homogenously, 1 mL of medium was taken from the Petri dish, mixed with the appropriate nocodazole amount, and put back into the dish, resulting in the desired concentration. 2 day old cells were treated with 3.3 µM nocodazole for 4 h, 11 day old cells with 33 µM nocodazole for 6 h. During the treatment, cells were kept in the incubator at 37 °C. After nocodazole treatment, coverslips were washed in warm Hepes-buffered HBSS and incubated in equilibrated N2-Medium at 37 °C for certain periods (from 30 s up to 15 min) to let the microtubules repolymerize. Cells were then fixed using the PHEM-Buffer. To assess microtubule regrowth in living cells after

laser ablation, neurons transfected with GFP-centrin2 and GFP-EB3 were incubated in nocdazole to depolymerize microtubules. After laser ablation, nocodazole was washed out and microtubules regrew in HBSS at 37°C on the microscope stage.

5.2.10   Electron microscopy

Cultured hippocampal neurons were fixed by adding glutaraldehyde to the medium to a final concentration of 2%. E18 hippocampi were dissected from brains and fixed with 4% paraformaldehyde (PFA) and 1% glutaraldehyde in phosphate buffer, pH 7.2. Postnatal day 6 (P6) rats were terminally anesthetized with 5% chloral hydrate solution (prepared in saline) and transcardially perfused with phosphate buffered saline (PBS; 0.1M, pH 7.4) followed by 4% PFA and 1% glutaraldehyde in phosphate buffer, pH 7.2. Hippocampi of E18 animals were dissected as for the hippocampal culture and the hippocampi directly put into fixative and postfixed as above. Vibratom sections were cut from hippocampi or the P6 brains (Leica VT1000S). Cultured hippocampal neurons and vibratomsections were postfixed with 1% osmium tetroxide. Cells and tissue were then dehydrated and embedded in Epon, cut by an ultramicrotome (Leica EM UC6) at 70 nm and poststained with lead citrate and uranyl acetate by an ultrastainer (LKB). Electron microscopy images of the sections were acquired using a Zeiss EM10 (Kodak 4489) and a JEOL JEM-1230 electron microscope with CCD-camera (Gatan Orius SC1000). The neuronal identity of the analyzed cells was confirmed by immunofluorescence (E18) or by morphology (P6).

To validate laser ablation of the centrosome, the cells were fixed in 2% PFA, 2% glutaraldehyde in 0.1 M phosphate buffer. After postfixation with 1% osmium tetroxide and dehydration, samples were embedded in LX 112 resin (Ladd Research) as a thin layer. The glass coverslip was removed with liquid nitrogen and selected regions remounted. Serial 70 nm-ultrathin sections were cut on a Leica UCT ultramicrotome

(Leica Microsystems), poststained with uranyl acetate and lead citrate and viewed in a Morgagni electron microscope (FEI company). Images were taken with a Morada camera (Olympus/SIS company).

5.2.11 Fluorescence microscopy

Cells were analyzed using a Zeiss Axiovert 135 equipped with Plan-Neofluar 25x and Plan-Apochromat 40x and 63x objectives. Images were captured using a camera from the 4912 series (Cohu, USA). The camera was connected to a Hamamatsu CCD camera C 2741 control panel. Pictures were recorded on the hard disc of a personal computer equipped with a LG3 image grabber and Scion Image software, version Beta 4.0.2 (both from Scion Corp.).

5.2.12 Confocal microscopy

Confocal laser scanning microscopy was done with a Leica SP2 confocal microscope. Images were taken with the Leica software as series of different focal planes, which were processed to obtain a view through the section scanned.

5.2.13 Spinning disc confocal microscopy

To record GFP-EB3 dynamics in living cells after laser ablation, an Olympus IX71 spinning disc confocal inverted microscope equipped with a Yokogawa CSU10 scan head and an Andor iXon EM+ DU-897 BV back illuminated EMCCD was used. A 100x 1.4 N.A. oil immersion objective (100x / 1.40 Oil UPlanSApo) was used, giving images with a pixel size of 166 nm/pixel. The laser line used was 488 nm. During imaging, the cells were kept at 37°C in Hepes-buffered HBSS.

5.2.14   Total-internal reflection (TIRF) microscopy

Time-lapse recordings of EB3-GFP after nocodazole washout in young and mature neurons were acquired using a total-internal reflection (TIRF) microscope as described in (Jaworski et al., 2009). The setup consisted of an inverted research microscope Nikon Eclipse TE2000E (Nikon) with a CFI Apo TIRF 100x 1.49 N.A. oil objective (Nikon), equipped with a Coolsnap and a QuantEM EMCCD cameras (Roper Scientific) controlled by MetaMorph 7.1 software (Molecular Devices). For excitation, the 488nm laserline of an argon laser (Spectra-Physics Lasers) and a Chroma ET-GFP filter cube were used. During imaging cells were maintained at 37°C in the standard culture medium in a closed chamber with 5% CO_2 (Tokai Hit). Images of live cells were processed and analyzed using MetaMorph, Adobe Photoshop and LabVIEW (National Instruments) software.

5.2.15   Image analysis and processing

Length, area and intensity measurements were performed using ImageJ analysis software (NIH). The intensity of centrosomal γ-tubulin antibody staining was analyzed was analyzed by measuring the intensity of a circle around the centrosome with a fixed area of 32 pixels. The centrosomal region was determined by the pericentrin costaining. To assess the cytoplasmic staining, the whole cell body without neurites was selected and the mean intensity of the soma was measured. Afterwards, the ratio of centrosomal staining to cytoplasmic staining was analyzed. Maximum projections in **Figure 2-2** were obtained using custom-written routines in LabVIEW 8.5 (National Instruments). Before projecting the maximum value of each pixel during acquisition onto a single image, each plane was low-pass filtered and convoluted with the top-hat filter described in (Mashanov and Molloy, 2007). These projections were used to draw arrows for all EB3 tracks that persisted for at least 3 frames and were

unambiguously identifiable. Maximum projections in **Figure 2-15** were obtained using ImageJ. These projections were used to draw arrows for EB3 tracks. All pictures were processed using Adobe Photoshop CS and Deneba Canvas 9.

5.2.16   CaCl$_2$ competent cells (E. coli, DH5α)

500 mL of LB medium were inoculated with 5 mL of an E. coli DH5α culture and grown until an optical density of A = 0.5 at λ = 600 nm was reached. Culture was spun down and resuspended in 10 mL of cold, sterile 0.1 M CaCl2. Suspension was kept for 15-30 min on ice, spun down and resuspended again in 10 mL of cold, sterile 0.1 M CaCl$_2$. Sterile glycerol was added to final concentration of 20%. 10 µl Aliquots were frozen and kept at -80 °C.

5.2.17   Transformation of E.Coli and propagation of plasmids

2 µL of DNA were added to 10 µL of competent cells and incubated for 5-10 minutes on ice. 100 µL LB Medium were added and the suspension was shaken for 1h at 37 °C. After that the plasmid was plated on a LB medium agar plate containing the respective antibiotic (for pEGFP-C1-centrin2 plasmid: 50 µg / mL Kanamycin). After incubation overnight at 37 °C, a single colony was picked and 3 mL of LB-medium containing antibiotic were inoculated. This culture was shaken at 37 °C for around 9 h. Then, 100 mL LB-Medium containing antibiotic were inoculated with 200 µL of the starting culture. After shaking at 37 °C overnight, the culture was spun down at 3000 rpm for 15 min. Supernatant was decanted and pellet was frozen at 20 °C. After thawing, plasmid DNA was extracted and purified with the EndoFree Maxi Prep Kit (Qiagen, Germany) according to the manufacturer's protocol.

5.2.18   Statistical analysis

All data are shown as mean ± s.e.m., except microtubule growth speed, which is shown as mean ± s.d. In the quantification of the electron microscope analysis, error bars were s.e.m. of a binominal distribution. Student's t-test was performed taking into account the two-tailed distribution and two-sample unequal variance of the data. Mean values, errors and t-test were computed using Microsoft Office Excel 2003.

6 <u>References</u>

Ahmad FJ, Echeverri CJ, Vallee RB, Baas PW. 1998. Cytoplasmic dynein and dynactin are required for the transport of microtubules into the axon. J Cell Biol 140:391-401.

Ahmad FJ, Joshi HC, Centonze VE, Baas PW. 1994. Inhibition of microtubule nucleation at the neuronal centrosome compromises axon growth. Neuron 12:271-280.

Akhmanova A, Steinmetz MO. 2008. Tracking the ends: a dynamic protein network controls the fate of microtubule tips. Nature Rev Mol Cell Biol 9:309-322.

Aldaz H, Rice LM, Stearns T, Agard DA. 2005. Insights into microtubule nucleation from the crystal structure of human gamma-tubulin. Nature 435:523-527.

Andersen JS, Wilkinson CJ, Mayor T, Mortensen P, Nigg EA, Mann M. 2003. Proteomic characterization of the human centrosome by protein correlation profiling. Nature 426:570-574.

Andersen SS, Bi GQ. 2000. Axon formation: a molecular model for the generation of neuronal polarity. Bioessays 22:172-179.

Arimura N, Kaibuchi K. 2007. Neuronal polarity: from extracellular signals to intracellular mechanisms. Nat Rev Neurosci 8:194-205.

Asada N, Sanada K, Fukada Y. 2007. LKB1 regulates neuronal migration and neuronal differentiation in the developing neocortex through centrosomal positioning. J Neurosci 27:11769-11775.

Baas PW. 1999. Microtubules and neuronal polarity: lessons from mitosis. Neuron 22:23-31.

Baas PW, Ahmad FJ. 1993. The transport properties of axonal microtubules establish their polarity orientation. J Cell Biol 120:1427-1437.

Baas PW, Deitch JS, Black MM, Banker GA. 1988. Polarity orientation of microtubules in hippocampal neurons: uniformity in the axon and nonuniformity in the dendrite. Proc Natl Acad Sci U S A 85:8335-8339.

Baas PW, Joshi HC. 1992. Gamma-tubulin distribution in the neuron: implications for the origins of neuritic microtubules. J Cell Biol 119:171-178.

Baas PW, Karabay A, Qiang L. 2005. Microtubules cut and run. Trends Cell Biol 15:518-524.

Bamburg JR, Bray D, Chapman K. 1986. Assembly of microtubules at the tip of growing axons. Nature 321:788-790.

Banker GA. 1980. Trophic interactions between astroglial cells and hippocampal neurons in culture. Science 209:809-810.

Barnes AP, Polleux F. 2009. Establishment of axon-dendrite polarity in developing neurons. Annu Rev Neurosci 32:347-381.

Bartolini F, Gundersen GG. 2006. Generation of noncentrosomal microtubule arrays. J Cell Sci 119:4155-4163.

Basto R, Lau J, Vinogradova T, Gardiol A, Woods CG, Khodjakov A, Raff JW. 2006. Flies without centrioles. Cell 125:1375-1386.

Becker EB, Bonni A. 2005. Beyond proliferation--cell cycle control of neuronal survival and differentiation in the developing mammalian brain. Semin Cell Dev Biol 16:439-448.

Berbari NF, Bishop GA, Askwith CC, Lewis JS, Mykytyn K. 2007. Hippocampal neurons possess primary cilia in culture. J Neurosci Res 85:1095-1100.

Bettencourt-Dias M, Glover DM. 2007. Centrosome biogenesis and function: centrosomics brings new understanding. Nat Rev Mol Cell Biol 8:451-463.

Bishop GA, Berbari NF, Lewis J, Mykytyn K. 2007. Type III adenylyl cyclase localizes to primary cilia throughout the adult mouse brain. J Comp Neurol 505:562-571.

Blagden SP, Glover DM. 2003. Polar expeditions--provisioning the centrosome for mitosis. Nat Cell Biol 5:505-511.

Bornens M. 2008. Organelle positioning and cell polarity. Nat Rev Mol Cell Biol 9:874-886.

Bradke F, Dotti CG. 1997. Neuronal polarity: vectorial cytoplasmic flow precedes axon formation. Neuron 19:1175-1186.

Bradke F, Dotti CG. 1999. The role of local actin instability in axon formation. Science 283:1931-1934.

Bradke F, Dotti CG. 2000. Differentiated neurons retain the capacity to generate axons from dendrites. Curr Biol 10:1467-1470.

Brown A. 2003. Axonal transport of membranous and nonmembranous cargoes: a unified perspective. J Cell Biol 160:817-821.

Buck KB, Zheng JQ. 2002. Growth cone turning induced by direct local modification of microtubule dynamics. J Neurosci 22:9358-9367.

Bugnard E, Zaal KJ, Ralston E. 2005. Reorganization of microtubule nucleation during muscle differentiation. Cell Motil Cytoskeleton 60:1-13.

Chilton JK. 2006. Molecular mechanisms of axon guidance. Dev Biol 292:13-24.

Conde C, Caceres A. 2009. Microtubule assembly, organization and dynamics in axons and dendrites. Nat Rev Neurosci 10:319-332.

Cowan CR, Hyman AA. 2004. Centrosomes direct cell polarity independently of microtubule assembly in C. elegans embryos. Nature 431:92-96.

Craig AM, Banker G. 1994. Neuronal polarity. Annu Rev Neurosci 17:267-310.

Dammermann A, Desai A, Oegema K. 2003. The minus end in sight. Curr Biol 13:R614-624.

de Anda FC, Pollarolo G, Da Silva JS, Camoletto PG, Feiguin F, Dotti CG. 2005. Centrosome localization determines neuronal polarity. Nature 436:704-708.

de Hoop M, Meyn L, Dotti CG. 1997. Culturing hippocampal neurons and astrocytes from fetal rodent brain. In: Celis JE, editor.Celis JEs. Cell Biology. A Laboratory Handbook. San Diego, CA: Academic Press.

Dehmelt L, Halpain S. 2004. Actin and microtubules in neurite initiation: are MAPs the missing link? J Neurobiol 58:18-33.

Dent EW, Gertler FB. 2003. Cytoskeletal dynamics and transport in growth cone motility and axon guidance. Neuron 40:209-227.

Desai A, Mitchison TJ. 1997. Microtubule polymerization dynamics. Annu Rev Cell Dev Biol 13:83-117.

Dictenberg JB, Zimmerman W, Sparks CA, Young A, Vidair C, Zheng Y, Carrington W, Fay FS, Doxsey SJ. 1998. Pericentrin and gamma-tubulin form a protein complex and are organized into a novel lattice at the centrosome. J Cell Biol 141:163-174.

Dotti CG, Banker G. 1991. Intracellular organization of hippocampal neurons during the development of neuronal polarity. J Cell Sci Suppl 15:75-84.

Dotti CG, Banker GA. 1987. Experimentally induced alteration in the polarity of developing neurons. Nature 330:254-256.

Dotti CG, Sullivan CA, Banker GA. 1988. The establishment of polarity by hippocampal neurons in culture. J Neurosci 8:1454-1468.

Doxsey S. 2001. Re-evaluating centrosome function. Nat Rev Mol Cell Biol 2:688-698.

Doxsey S, McCollum D, Theurkauf W. 2005. Centrosomes in cellular regulation. Annu Rev Cell Dev Biol 21:411-434.

Dumont J, Petri S, Pellegrin F, Terret ME, Bohnsack MT, Rassinier P, Georget V, Kalab P, Gruss OJ, Verlhac MH. 2007. A centriole- and RanGTP-independent spindle assembly pathway in meiosis I of vertebrate oocytes. J Cell Biol 176:295-305.

Efimov A, Kharitonov A, Efimova N, Loncarek J, Miller PM, Andreyeva N, Gleeson P, Galjart N, Maia AR, McLeod IX, Yates JR, 3rd, Maiato H, Khodjakov A, Akhmanova A, Kaverina I. 2007. Asymmetric CLASP-dependent nucleation of noncentrosomal microtubules at the trans-Golgi network. Dev Cell 12:917-930.

Ehrengruber MU, Lundstrom K, Schweitzer C, Heuss C, Schlesinger S, Gahwiler BH. 1999. Recombinant Semliki Forest virus and Sindbis virus efficiently infect neurons in hippocampal slice cultures. Proc Natl Acad Sci U S A 96:7041-7046.

Einstein EB, Patterson CA, Hon BJ, Regan KA, Reddi J, Melnikoff DE, Mateer MJ, Schulz S, Johnson BN, Tallent MK. 2010. Somatostatin signaling in neuronal cilia is critical for object recognition memory. J Neurosci 30:4306-4314.

Erturk A, Hellal F, Enes J, Bradke F. 2007. Disorganized microtubules underlie the formation of retraction bulbs and the failure of axonal regeneration. J Neurosci 27:9169-9180.

Etienne-Manneville S, Hall A. 2003. Cdc42 regulates GSK-3beta and adenomatous polyposis coli to control cell polarity. Nature 421:753-756.

Eyer J, Peterson A. 1994. Neurofilament-deficient axons and perikaryal aggregates in viable transgenic mice expressing a neurofilament-beta-galactosidase fusion protein. Neuron 12:389-405.

Ferhat L, Cook C, Chauviere M, Harper M, Kress M, Lyons GE, Baas PW. 1998. Expression of the mitotic motor protein Eg5 in postmitotic neurons: implications for neuronal development. J Neurosci 18:7822-7835.

Ferhat L, Cook C, Kuriyama R, Baas PW. 1998. The nuclear/mitotic apparatus protein NuMA is a component of the somatodendritic microtubule arrays of the neuron. J Neurocytol 27:887-899.

Ferhat L, Kuriyama R, Lyons GE, Micales B, Baas PW. 1998. Expression of the mitotic motor protein CHO1/MKLP1 in postmitotic neurons. Eur J Neurosci 10:1383-1393.

Ferreira A, Palazzo RE, Rebhun LI. 1993. Preferential dendritic localization of pericentriolar material in hippocampal pyramidal neurons in culture. Cell Motil Cytoskeleton 25:336-344.

Fliegauf M, Benzing T, Omran H. 2007. When cilia go bad: cilia defects and ciliopathies. Nat Rev Mol Cell Biol 8:880-893.

Fukata Y, Itoh TJ, Kimura T, Menager C, Nishimura T, Shiromizu T, Watanabe H, Inagaki N, Iwamatsu A, Hotani H, Kaibuchi K. 2002. CRMP-2 binds to tubulin heterodimers to promote microtubule assembly. Nat Cell Biol 4:583-591.

Gadde S, Heald R. 2004. Mechanisms and molecules of the mitotic spindle. Curr Biol 14:R797-805.

Garvalov BK, Flynn KC, Neukirchen D, Meyn L, Teusch N, Wu X, Brakebusch C, Bamburg JR, Bradke F. 2007. Cdc42 regulates cofilin during the establishment of neuronal polarity. J Neurosci 27:13117-13129.

Geraldo S, Gordon-Weeks PR. 2009. Cytoskeletal dynamics in growth-cone steering. J Cell Sci 122:3595-3604.

Goetz SC, Anderson KV. 2010. The primary cilium: a signalling centre during vertebrate development. Nat Rev Genet 11:331-344.

Goetze B, Grunewald B, Baldassa S, Kiebler M. 2004. Chemically controlled formation of a DNA/calcium phosphate coprecipitate: application for transfection of mature hippocampal neurons. J Neurobiol 60:517-525.

Goldberg DJ, Burmeister DW. 1986. Stages in axon formation: observations of growth of Aplysia axons in culture using video-enhanced contrast-differential interference contrast microscopy. J Cell Biol 103:1921-1931.

Gomis-Ruth S, Wierenga CJ, Bradke F. 2008. Plasticity of polarization: changing dendrites into axons in neurons integrated in neuronal circuits. Curr Biol 18:992-1000.

Gonzalez C. 2008. Centrosome function during stem cell division: the devil is in the details. Curr Opin Cell Biol 20:694-698.

Gordon-Weeks PR. 2004. Microtubules and growth cone function. J Neurobiol 58:70-83.

Goshima G, Kimura A. 2010. New look inside the spindle: microtubule-dependent microtubule generation within the spindle. Curr Opin Cell Biol 22:44-49.

Goslin K, Banker G. 1989. Experimental observations on the development of polarity by hippocampal neurons in culture. J Cell Biol 108:1507-1516.

Govek EE, Newey SE, Van Aelst L. 2005. The role of the Rho GTPases in neuronal development. Genes Dev 19:1-49.

Grabham PW, Seale GE, Bennecib M, Goldberg DJ, Vallee RB. 2007. Cytoplasmic dynein and LIS1 are required for microtubule advance during growth cone remodeling and fast axonal outgrowth. J Neurosci 27:5823-5834.

Grenningloh G, Soehrman S, Bondallaz P, Ruchti E, Cadas H. 2004. Role of the micro-tubule destabilizing proteins SCG10 and stathmin in neuronal growth. J Neurobiol 58:60-69.

Gupton SL, Salmon WC, Waterman-Storer CM. 2002. Converging populations of f-actin promote breakage of associated microtubules to spatially regulate microtubule turn-over in migrating cells. Curr Biol 12:1891-1899.

Harada A, Teng J, Takei Y, Oguchi K, Hirokawa N. 2002. MAP2 is required for dendrite elongation, PKA anchoring in dendrites, and proper PKA signal transduction. J Cell Biol 158:541-549.

Haren L, Remy MH, Bazin I, Callebaut I, Wright M, Merdes A. 2006. NEDD1-dependent recruitment of the gamma-tubulin ring complex to the centrosome is necessary for centriole duplication and spindle assembly. J Cell Biol 172:505-515.

Herrup K, Yang Y. 2007. Cell cycle regulation in the postmitotic neuron: oxymoron or new biology? Nat Rev Neurosci 8:368-378.

Higginbotham H, Tanaka T, Brinkman BC, Gleeson JG. 2006. GSK3beta and PKCzeta function in centrosome localization and process stabilization during Slit-mediated neuronal repolarization. Mol Cell Neurosci 32:118-132.

Higginbotham HR, Gleeson JG. 2007. The centrosome in neuronal development. Trends Neurosci 30:276-283.

Hirokawa N, Funakoshi ST, Takeda S. 1997. Slow axonal transport: the subunit transport model. Trends Cell Biol 7:384-388.

Hoenger A, McIntosh JR. 2009. Probing the macromolecular organization of cells by elec-tron tomography. Curr Opin Cell Biol 21:89-96.

Hoogenraad CC, Bradke F. 2009. Control of neuronal polarity and plasticity--a renaissance for microtubules? Trends Cell Biol 19:669-676.

Horton AC, Ehlers MD. 2003. Dual modes of endoplasmic reticulum-to-Golgi transport in dendrites revealed by live-cell imaging. J Neurosci 23:6188-6199.

Horton AC, Racz B, Monson EE, Lin AL, Weinberg RJ, Ehlers MD. 2005. Polarized secre-tory trafficking directs cargo for asymmetric dendrite growth and morphogenesis. Neuron 48:757-771.

Howard J, Hyman AA. 2003. Dynamics and mechanics of the microtubule plus end. Nature 422:753-758.

Hung LY, Tang CJ, Tang TK. 2000. Protein 4.1 R-135 interacts with a novel centrosomal protein (CPAP) which is associated with the gamma-tubulin complex. Mol Cell Biol 20:7813-7825.

Ikawa M, Kominami K, Yoshimura Y, Tanaka K, Nishimune Y, Okabe M. 1995. A rapid and non-invasive selection of transgenic embryos before implantation using green fluorescent protein (GFP). FEBS Lett 375:125-128.

Ishikawa R, Kohama K. 2007. Actin-binding proteins in nerve cell growth cones. J Pharma-col Sci 105:6-11.

Jacobson C, Schnapp B, Banker GA. 2006. A change in the selective translocation of the Kinesin-1 motor domain marks the initial specification of the axon. Neuron 49:797-804.

Janson ME, Loughlin R, Loiodice I, Fu C, Brunner D, Nedelec FJ, Tran PT. 2007. Crosslinkers and motors organize dynamic microtubules to form stable bipolar arrays in fission yeast. Cell 128:357-368.

Janson ME, Setty TG, Paoletti A, Tran PT. 2005. Efficient formation of bipolar microtubule bundles requires microtubule-bound gamma-tubulin complexes. J Cell Biol 169:297-308.

Jaworski J, Kapitein LC, Gouveia SM, Dortland BR, Wulf PS, Grigoriev I, Camera P, Spangler SA, Di Stefano P, Demmers J, Krugers H, Defilippi P, Akhmanova A, Hoogenraad CC. 2009. Dynamic microtubules regulate dendritic spine morphology and synaptic plasticity. Neuron 61:85-100.

Job D, Valiron O, Oakley B. 2003. Microtubule nucleation. Curr Opin Cell Biol 15:111-117.

Johnson KA, Borisy GG. 1977. Kinetic analysis of microtubule self-assembly in vitro. J Mol Biol 117:1-31.

Kaech S, Banker G. 2006. Culturing hippocampal neurons. Nat Protoc 1:2406-2415.

Kalil K, Szebenyi G, Dent EW. 2000. Common mechanisms underlying growth cone guidance and axon branching. J Neurobiol 44:145-158.

Kapitein LC, Schlager MA, Kuijpers M, Wulf PS, van Spronsen M, MacKintosh FC, Hoogenraad CC. 2010. Mixed microtubules steer dynein-driven cargo transport into dendrites. Curr Biol 20:290-299.

Karabay A, Yu W, Solowska JM, Baird DH, Baas PW. 2004. Axonal growth is sensitive to the levels of katanin, a protein that severs microtubules. J Neurosci 24:5778-5788.

Kawano Y, Yoshimura T, Tsuboi D, Kawabata S, Kaneko-Kawano T, Shirataki H, Takenawa T, Kaibuchi K. 2005. CRMP-2 is involved in kinesin-1-dependent transport of the Sra-1/WAVE1 complex and axon formation. Mol Cell Biol 25:9920-9935.

Khodjakov A, Cole RW, Oakley BR, Rieder CL. 2000. Centrosome-independent mitotic spindle formation in vertebrates. Curr Biol 10:59-67.

Khodjakov A, Rieder CL. 1999. The sudden recruitment of gamma-tubulin to the centrosome at the onset of mitosis and its dynamic exchange throughout the cell cycle, do not require microtubules. J Cell Biol 146:585-596.

Kim AH, Puram SV, Bilimoria PM, Ikeuchi Y, Keough S, Wong M, Rowitch D, Bonni A. 2009. A centrosomal Cdc20-APC pathway controls dendrite morphogenesis in postmitotic neurons. Cell 136:322-336.

Kim T, Chang S. 2006. Quantitative evaluation of the mode of microtubule transport in Xenopus neurons. Mol Cells 21:76-81.

Kimura T, Watanabe H, Iwamatsu A, Kaibuchi K. 2005. Tubulin and CRMP-2 complex is transported via Kinesin-1. J Neurochem 93:1371-1382.

Kirkham M, Muller-Reichert T, Oegema K, Grill S, Hyman AA. 2003. SAS-4 is a C. elegans centriolar protein that controls centrosome size. Cell 112:575-587.

Konishi Y, Setou M. 2009. Tubulin tyrosination navigates the kinesin-1 motor domain to axons. Nature Neurosci 12:559-567.

Kwiatkowski AV, Rubinson DA, Dent EW, Edward van Veen J, Leslie JD, Zhang J, Mebane LM, Philippar U, Pinheiro EM, Burds AA, Bronson RT, Mori S, Fassler R, Gertler FB. 2007. Ena/VASP Is Required for neuritogenesis in the developing cortex. Neuron 56:441-455.

Lancaster MA, Gleeson JG. 2009. The primary cilium as a cellular signaling center: lessons from disease. Curr Opin Genet Dev 19:220-229.

Lasek RJ. 1986. Polymer sliding in axons. J Cell Sci Suppl 5:161-179.

Leask A, Obrietan K, Stearns T. 1997. Synaptically coupled central nervous system neurons lack centrosomal gamma-tubulin. Neurosci Lett 229:17-20.

Lechler T, Fuchs E. 2007. Desmoplakin: an unexpected regulator of microtubule organization in the epidermis. J Cell Biol 176:147-154.

Lee JH, Gleeson JG. 2009. The role of primary cilia in neuronal function. Neurobiol Dis 38:167-172.

Li R, Gundersen GG. 2008. Beyond polymer polarity: how the cytoskeleton builds a polarized cell. Nat Rev Mol Cell Biol 9:860-873.

Loncarek J, Hergert P, Magidson V, Khodjakov A. 2008. Control of daughter centriole formation by the pericentriolar material. Nat Cell Biol 10:322-328.

Lowery LA, Van Vactor D. 2009. The trip of the tip: understanding the growth cone machinery. Nat Rev Mol Cell Biol 10:332-343.

Lu M, Witke W, Kwiatkowski DJ, Kosik KS. 1997. Delayed retraction of filopodia in gelsolin null mice. Journal of Cell Biology 138:1279-1287.

Luders J, Patel UK, Stearns T. 2006. GCP-WD is a gamma-tubulin targeting factor required for centrosomal and chromatin-mediated microtubule nucleation. Nat Cell Biol 8:137-147.

Luders J, Stearns T. 2007. Microtubule-organizing centres: a re-evaluation. Nat Rev Mol Cell Biol 8:161-167.

Ma Y, Shakiryanova D, Vardya I, Popov SV. 2004. Quantitative analysis of microtubule transport in growing nerve processes. Curr Biol 14:725-730.

Maghelli N, Tolic-Nørrelykke I. 2008. Versatile laser-based cell manipulator. J Biophotonics 1:299-309.

Malikov V, Kashina A, Rodionov V. 2004. Cytoplasmic dynein nucleates microtubules to organize them into radial arrays in vivo. Mol Biol Cell 15:2742-2749.

Marsh L, Letourneau PC. 1984. Growth of neurites without filopodial or lamellipodial activity in the presence of cytochalasin B. Journal of Cell Biology 99:2041-2047.

Mashanov GI, Molloy JE. 2007. Automatic detection of single fluorophores in live cells. Biophys J 92:2199-2211.

Meng W, Mushika Y, Ichii T, Takeichi M. 2008. Anchorage of microtubule minus ends to adherens junctions regulates epithelial cell-cell contacts. Cell 135:948-959.

Mimura F, Yamagishi S, Arimura N, Fujitani M, Kubo T, Kaibuchi K, Yamashita T. 2006. Myelin-associated glycoprotein inhibits microtubule assembly by a Rho-kinase-dependent mechanism. J Biol Chem 281:15970-15979.

Mitchison T, Kirschner M. 1984. Dynamic instability of microtubule growth. Nature 312:237-242.

Moritz M, Agard DA. 2001. Gamma-tubulin complexes and microtubule nucleation. Curr Opin Struct Biol 11:174-181.

Moskowitz PF, Oblinger MM. 1995. Sensory neurons selectively upregulate synthesis and transport of the beta III-tubulin protein during axonal regeneration. J Neurosci 15:1545-1555.

Moudjou M, Bordes N, Paintrand M, Bornens M. 1996. gamma-Tubulin in mammalian cells: the centrosomal and the cytosolic forms. J Cell Sci 109 (Pt 4):875-887.

Mulari MT, Patrikainen L, Kaisto T, Metsikko K, Salo JJ, Vaananen HK. 2003. The architecture of microtubular network and Golgi orientation in osteoclasts--major differences between avian and mammalian species. Exp Cell Res 285:221-235.

Murata T, Sonobe S, Baskin TI, Hyodo S, Hasezawa S, Nagata T, Horio T, Hasebe M. 2005. Microtubule-dependent microtubule nucleation based on recruitment of gamma-tubulin in higher plants. Nat Cell Biol 7:961-968.

Myers KA, He Y, Hasaka TP, Baas PW. 2006. Microtubule transport in the axon: Rethinking a potential role for the actin cytoskeleton. Neuroscientist 12:107-118.

Nakata T, Hirokawa N. 2003. Microtubules provide directional cues for polarized axonal transport through interaction with kinesin motor head. J Cell Biol 162:1045-1055.

Niwa H, Yamamura K, Miyazaki J. 1991. Efficient selection for high-expression transfectants with a novel eukaryotic vector. Gene 108:193-199.

Ohama Y, Hayashi K. 2009. Relocalization of a microtubule-anchoring protein, ninein, from the centrosome to dendrites during differentiation of mouse neurons. Histochem Cell Biol 132:515-524.

Okabe M, Ikawa M, Kominami K, Nakanishi T, Nishimune Y. 1997. 'Green mice' as a source of ubiquitous green cells. FEBS Lett 407:313-319.

Pak CW, Flynn KC, Bamburg JR. 2008. Actin-binding proteins take the reins in growth cones. Nat Rev Neurosci 9:136-147.

Pedersen LB, Veland IR, Schroder JM, Christensen ST. 2008. Assembly of primary cilia. Dev Dyn 237:1993-2006.

Pollard TD. 2007. Regulation of actin filament assembly by Arp2/3 complex and formins. Annu Rev Biophys Biomol Struct 36:451-477.

Pollard TD, Borisy GG. 2003. Cellular motility driven by assembly and disassembly of actin filaments. Cell 112:453-465.

Pugacheva EN, Jablonski SA, Hartman TR, Henske EP, Golemis EA. 2007. HEF1-dependent Aurora A activation induces disassembly of the primary cilium. Cell 129:1351-1363.

Purro SA, Ciani L, Hoyos-Flight M, Stamatakou E, Siomou E, Salinas PC. 2008. Wnt regulates axon behavior through changes in microtubule growth directionality: a new role for adenomatous polyposis coli. J Neurosci 28:8644-8654.

Ramon y Cajal S. 1890. À quelle époque apparaissent les expansions des cellules nerveuses de la moëlle épinière du poulet? Anatomomischer Anzeiger 21–22:609–639.

Raynaud-Messina B, Merdes A. 2007. Gamma-tubulin complexes and microtubule organization. Curr Opin Cell Biol 19:24-30.

Reed NA, Cai D, Blasius TL, Jih GT, Meyhofer E, Gaertig J, Verhey KJ. 2006. Microtubule acetylation promotes kinesin-1 binding and transport. Curr Biol 16:2166-2172.

Reilein A, Yamada S, Nelson WJ. 2005. Self-organization of an acentrosomal microtubule network at the basal cortex of polarized epithelial cells. J Cell Biol 171:845-855.

Roll-Mecak A, Vale RD. 2006. Making more microtubules by severing: a common theme of noncentrosomal microtubule arrays? J Cell Biol 175:849-851.

Salisbury JL, Suino KM, Busby R, Springett M. 2002. Centrin-2 is required for centriole duplication in mammalian cells. Curr Biol 12:1287-1292.

Schaefer AW, Kabir N, Forscher P. 2002. Filopodia and actin arcs guide the assembly and transport of two populations of microtubules with unique dynamic parameters in neuronal growth cones. J Cell Biol 158:139-152.

Sharp DJ, Kuriyama R, Baas PW. 1996. Expression of a kinesin-related motor protein induces Sf9 cells to form dendrite-like processes with nonuniform microtubule polarity orientation. J Neurosci 16:4370-4375.

Sharp GA, Weber K, Osborn M. 1982. Centriole number and process formation in established neuroblastoma cells and primary dorsal root ganglion neurones. Eur J Cell Biol 29:97-103.

Siegrist SE, Doe CQ. 2007. Microtubule-induced cortical cell polarity. Genes Dev 21:483-496.

Singla V, Reiter JF. 2006. The primary cilium as the cell's antenna: signaling at a sensory organelle. Science 313:629-633.

Stepanova T, Slemmer J, Hoogenraad CC, Lansbergen G, Dortland B, De Zeeuw CI, Grosveld F, van Cappellen G, Akhmanova A, Galjart N. 2003. Visualization of microtubule growth in cultured neurons via the use of EB3-GFP (end-binding protein 3-green fluorescent protein). J Neurosci 23:2655-2664.

Sullivan M, Morgan DO. 2007. Finishing mitosis, one step at a time. Nat Rev Mol Cell Biol 8:894-903.

Suter DM, Forscher P. 2000. Substrate-cytoskeletal coupling as a mechanism for the regulation of growth cone motility and guidance. J Neurobiol 44:97-113.

Sutterlin C, Colanzi A. 2010. The Golgi and the centrosome: building a functional partnership. J Cell Biol 188:621-628.

Szollosi D, Calarco P, Donahue RP. 1972. Absence of centrioles in the first and second meiotic spindles of mouse oocytes. J Cell Sci 11:521-541.

Tanaka E, Ho T, Kirschner MW. 1995. The role of microtubule dynamics in growth cone motility and axonal growth. J Cell Biol 128:139-155.

Tang CJ, Fu RH, Wu KS, Hsu WB, Tang TK. 2009. CPAP is a cell-cycle regulated protein that controls centriole length. Nat Cell Biol 11:825-831.

Terada S. 2003. Where does slow axonal transport go? Neurosci Res 47:367-372.

Terada S, Kinjo M, Hirokawa N. 2000. Oligomeric tubulin in large transporting complex is transported via kinesin in squid giant axons. Cell 103:141-155.

Uehara R, Nozawa RS, Tomioka A, Petry S, Vale RD, Obuse C, Goshima G. 2009. The augmin complex plays a critical role in spindle microtubule generation for mitotic progression and cytokinesis in human cells. Proc Natl Acad Sci U S A 106:6998-7003.

Verollet C, Colombie N, Daubon T, Bourbon HM, Wright M, Raynaud-Messina B. 2006. Drosophila melanogaster gamma-TuRC is dispensable for targeting gamma-tubulin to the centrosome and microtubule nucleation. J Cell Biol 172:517-528.

Vogl AW, Weis M, Pfeiffer DC. 1995. The perinuclear centriole-containing centrosome is not the major microtubule organizing center in Sertoli cells. Eur J Cell Biol 66:165-179.

Wang L, Brown A. 2002. Rapid movement of microtubules in axons. Curr Biol 12:1496-1501.

Wang X, Tsai JW, Imai JH, Lian WN, Vallee RB, Shi SH. 2009. Asymmetric centrosome inheritance maintains neural progenitors in the neocortex. Nature 461:947-955.

Wasteneys GO, Ambrose JC. 2009. Spatial organization of plant cortical microtubules: close encounters of the 2D kind. Trends Cell Biol 19:62-71.

Watabe-Uchida M, John KA, Janas JA, Newey SE, Van Aelst L. 2006. The Rac activator DOCK7 regulates neuronal polarity through local phosphorylation of stathmin/Op18. Neuron 51:727-739.

Waterman-Storer CM, Salmon ED. 1997. Actomyosin-based retrograde flow of microtubules in the lamella of migrating epithelial cells influences microtubule dynamic instability and turnover and is associated with microtubule breakage and treadmilling. J Cell Biol 139:417-434.

Wiese C, Zheng Y. 2006. Microtubule nucleation: gamma-tubulin and beyond. J Cell Sci 119:4143-4153.

Witte H, Bradke F. 2008. The role of the cytoskeleton during neuronal polarization. Curr Opin Neurobiol 18:479-487.

Witte H, Neukirchen D, Bradke F. 2008. Microtubule stabilization specifies initial neuronal polarization. J Cell Biol 180:619-632.

Yamada KM, Spooner BS, Wessells NK. 1970. Axon growth: roles of microfilaments and microtubules. Proc Natl Acad Sci U S A 66:1206-1212.

Yamada KM, Spooner BS, Wessells NK. 1971. Ultrastructure and function of growth cones and axons of cultured nerve cells. J Cell Biol 49:614-635.

Yang Y, Kim AH, Bonni A. 2010. The dynamic ubiquitin ligase duo: Cdh1-APC and Cdc20-APC regulate neuronal morphogenesis and connectivity. Curr Opin Neurobiol 20:92-99.

Ye B, Zhang Y, Song W, Younger SH, Jan LY, Jan YN. 2007. Growing dendrites and axons differ in their reliance on the secretory pathway. Cell 130:717-729.

Yu W, Baas PW. 1994. Changes in microtubule number and length during axon differentiation. J Neurosci 14:2818-2829.

Yu W, Centonze VE, Ahmad FJ, Baas PW. 1993. Microtubule nucleation and release from the neuronal centrosome. J Cell Biol 122:349-359.

Yu W, Cook C, Sauter C, Kuriyama R, Kaplan PL, Baas PW. 2000. Depletion of a microtubule-associated motor protein induces the loss of dendritic identity. J Neurosci 20:5782-5791.

Yu W, Qiang L, Solowska JM, Karabay A, Korulu S, Baas PW. 2008. The microtubule-severing proteins spastin and katanin participate differently in the formation of axonal branches. Mol Cell Biol 19:1485-1498.

Yu W, Solowska JM, Qiang L, Karabay A, Baird D, Baas PW. 2005. Regulation of microtubule severing by katanin subunits during neuronal development. J Neurosci 25:5573-5583.

Zheng Y, Wildonger J, Ye B, Zhang Y, Kita A, Younger SH, Zimmerman S, Jan LY, Jan YN. 2008. Dynein is required for polarized dendritic transport and uniform microtubule orientation in axons. Nat Cell Biol 10:1172-1180.

Zimmerman WC, Sillibourne J, Rosa J, Doxsey SJ. 2004. Mitosis-specific anchoring of gamma tubulin complexes by pericentrin controls spindle organization and mitotic entry. Mol Biol Cell 15:3642-3657.

Ziv NE, Spira ME. 1998. Induction of growth cone formation by transient and localized increases of intracellular proteolytic activity. Journal of Cell Biology 140:223-232.

Zmuda JF, Rivas RJ. 1998. The Golgi apparatus and the centrosome are localized to the sites of newly emerging axons in cerebellar granule neurons in vitro. Cell Motil Cytoskeleton 41:18-38.

Zolessi FR, Poggi L, Wilkinson CJ, Chien CB, Harris WA. 2006. Polarization and orientation of retinal ganglion cells in vivo. Neural Develop 1:2.

7 <u>Acknowledgements</u>

First, I would like to thank Frank for giving me this excellent project that turned out so well. I am very grateful for your constant support, the fruitful discussions, selecting such wonderful lab members and for being a fantastic boss.

I am also very grateful to the members of my thesis committee, Ruediger Klein and Olaf Stemmann for their time and helpful suggestions.

I am very thankful to Jonathan MacKinnon, Dorothee Neukirchen and Claudia Laskowski for carefully reading the manuscript and giving a lot of input. Thanks a lot!

Big credits go also to Sergio Cañada for his time and the help with figures.

I would also like to thank my collaborators: Special thanks go out to Nicola Maghelli and Iva Tolíc-Nørrelykke at the MPI of Cell Biology and Genetics in Dresden. Nicola, it was so much fun working with you. Although we had some much troubles and frustrations, you were always convinced of a positive outcome. I also would like to thank Iva and the whole Tolic-lab (Jana, Miguel, Bernhard, Isabell, Davide, Manuel and Stefan) for their great hospitality and the great atmosphere! Furthermore, I would like to thank Michaela Wilsch-Bräuninger for the great EM work and the unselfish support. I am also indebted to the Huttner Lab (Elena, Anne-Marie and Andreas), who allowed me to use their cell culture and gave me great support for my experiments.

I also would like to thank Lukas Kapitein and Casper Hoogenraad at the EMC Rotterdam for their spontaneous collaboration during the paper revision.

There are also many people at our institute and the MPI of Biochemistry to whom I want to express my gratitude: Liane Meyn, for the fantastic cultures, technical assistance and keeping the lab running. Susana Gomis-Rüth, for being the master of axotomy and giving me axotomized cells; Marianne Braun for her excellent EM work and the very successful search for centrosomes in neurons. I would also like to thank the former and present members of the Nigg-Lab (Julia, Thorsten, Jens, Ina, Gernot,

8 <u>Curriculum Vitae</u>

Personal data

Name   Michael Stieß

Education

Since 2007   PhD thesis with PD Dr. Bradke at the Max Planck Institute for Neurobiology, Martinsried, Germany

2006   Technical University of Munich
                        M.Sc. Biochemistry

2004   Technical University of Munich
                        B.Sc. Biochemistry

2000   Ludwigsgymnasium München
                        Abitur

9 <u>Publications</u>

Schmidt MV*, Schülke J-P*, Liebl C*, <u>Stiess M</u>, Avrabos C, Bock J, Wochnik
GM, Davies HA Zimmermann N, Scharf SH, Trümbach D, Wurst W, Turck C,
Holsboer F, Stewart MG, Bradke F, Eder M, Müller MB, Rein T.
Novel actin bundling factor links stress, synaptic function and behaviour.
submitted

<u>Stiess M,</u> Bradke F. 2010.
Neuronal Polarity: The cytoskeleton leads the way.
Developmental Neurobiology, in press

<u>Stiess M,</u> Maghelli N, Kapitein LC, Gomis-Ruth S, Wilsch-Brauninger M,
Hoogenraad CC, Tolic-Norrelykke IM, Bradke F. 2010.
Axon extension occurs independently of centrosomal microtubule nucleation.
Science 327:704-707.

<u>Stiess M</u>, Bradke F. 2009.
Cytoskeleton in axon growth.
In: *Encyclopedia of Life Sciences (ELS).* Chichester: John Wiley & Sons, Ltd.

Moosmang S., Haider N., Klugbauer N., Adelsberger H., Langwieser N., Müller J.,
<u>Stiess M.,</u> Marais E., Schulla V., Lacinova L., Goebbels S., Nave K.A., Storm D.,
Hofmann F., Kleppisch T.
**The Role of Hippocampal $Ca_v1.2$ Ca^{2+} Channels in NMDA Receptor-
Independent Synaptic Plasticity and Spatial Memory.**
Journal of Neuroscience, 2005, 25: 9883-92